



Proyecto de Sistemas Informáticos.
Curso 2009-2010.

**DSP-BASED IMPLEMENTATION OF A
DIGITAL RADIO DEMODULATOR
ON THE ULTRA-LOW POWER PROCESSOR
COOLFLUX BSP**

Authors:

Elena Pérez-Toril Gracia
Álvaro Martínez López

Project Supervisor:
Luis Piñuel Moreno

**Departamento de Arquitectura de Computadores y Automática.
Facultad de Informática.
Universidad Complutense de Madrid.**

Contents

1 Preliminary concepts in DAB	2
1.1 Signal Modulation	2
1.2 Multipath Propagation	5
1.3 QPSK (Quadrature Phase Shift Keying)	10
1.4 FDM (Frequency Division Multiplexing)	13
1.5 Orthogonal Frequency-Division Multiplexing (OFDM)	14
1.6 Fast Fourier Transform (FFT)	23
1.6.1 Overview	23
1.6.2 Digital Implementation	24
1.6.3 The Discrete Fourier Transform	24
1.6.4 Computation of the DFT	25
1.6.5 The Fast Fourier Transform	26
1.6.6 Applications to DAB	27
1.6.7 Complex Numbers	28
1.6.8 Negative Frequencies	29
1.6.9 Linearity of the transforms	30
1.6.10 Combination of I and Q	31
1.6.11 Addition of the Guard Interval	33
1.7 Finite Impulse Response Filters(FIR)	34
1.7.1 How to characterize digital FIR filters	34
1.8 Error Measures	36

1.8.1	Bit Error Rate	36
1.8.2	Modulation Error Rate	37
1.9	Errors Detection and Correction	38
1.9.1	Viterbi Decoder	38
1.9.2	De-puncturing	46
1.10	Digital Signals Processors (DSP)	47
2	CoolFlux BSP Architecture	49
2.1	Overview	49
2.2	Registers	50
2.3	The Data Path	50
2.3.1	Multipliers	53
2.3.2	Arithmetic and Logic Units (XALU and YALU)	54
2.4	Move Buses and RSS Units	55
2.4.1	Xbus and Ybus Move Buses	55
2.4.2	Moving to an Accumulator	56
2.4.3	Moving from an Accumulator	57
2.4.4	Round, Saturate and Select Units (RSS)	58
2.5	Memories and I/O	60
2.5.1	Individual Data Memory (X, Y)	60
2.5.2	Dual Precision Memory (XY)	60
2.5.3	I/O Memory Space	60
2.6	X and Y Addressing Units	61
2.6.1	Indexed Stack Pointer Addressing	62
2.6.2	Indexed Pointer Addressing	62
2.7	Program Control Unit	62
2.7.1	Hardware Loop Stack	63
2.8	Hardware Interface	63
2.8.1	I/O Memory	64
2.8.2	DMA	64

2.9	Multi-Cycle Instructions and Delay Slots	64
2.9.1	Multi-cycle Instructions	64
2.9.2	Delay Slots	65
2.10	Hardware Loops	66
2.11	Debug Mode	67
2.12	Interrupts	67
2.13	BSP C Compiler	67
2.13.1	Optimizations	70
3	DAB Implementation on the CoolFlux BSP	71
3.1	Automatic Gain Control	74
3.2	FFT	76
3.3	Differential Demodulation	77
3.4	Frecuency de-interleaving	78
3.5	Quantization	80
3.5.1	Hard Decision	80
3.5.2	Soft Decision	82
3.6	Time De-Interleaving	83
3.7	Errors Detection and Correction	87
3.8	Energy Dispersal Unscrambling	89
3.9	Synchronization channel	90
3.9.1	Null Symbol Detection	91
3.9.2	TFPR symbol	93
3.9.3	Coarse Frequency Correction	96
3.9.4	Fine Frequency Correction	98
3.9.5	Fine time synchronization	100
3.10	Transport mechanisms	102
3.10.1	Fast Information Channel (FIC)	105
3.10.1.1	Fast Information Block (FIB)	106
3.10.1.2	Fast Information Group (FIG)	106

3.10.1.3	Calculation of the CRC word	109
3.10.2	Main Service Channel (MSC)	110
3.11	Audio Coding	111
3.11.1	Formatting of the audio bit stream	112
3.11.2	CRC check for audio side information	114
4	Hardware implementation of the DAB demodulator	116
4.1	An overview to CoolFlux BSP	116
4.1.1	Baseband Signal Processor(BSP)	119
4.1.2	DAB as a Real Time Application	120
4.1.3	DAB hardware definition	120
4.1.4	Components Description	124
4.1.4.1	Maxim 2172 v1.0.25	124
4.1.4.2	Tektronix TDS210	125
4.1.4.3	FPGA Board Virtex XC4VLX100	126
4.1.4.4	PE 1542 DC Power Supply Philips	126
4.1.4.5	Hewlett Packard 8596E Oscilloscope	126
4.1.4.6	CoolFlux simulator, CoolFlux debugger, Chess compiler .	127
4.1.4.7	Reception Antenna	127
4.1.4.8	JTAG(Joint Test Action Group)	127
4.1.5	DAB demodulator datapath	129
4.1.6	Local memories	131
4.1.7	Debug interface	131
4.1.8	Interrupt interface	132
4.1.9	Shared Buffers	132
4.2	Description of the BSP instances	134
4.2.1	<i>BSP</i> ₀ : Synchronization, Time correction, Save OFDM symbols . .	134
4.2.2	<i>BSP</i> ₁ : FFT, Deinterleaving, Demapping	139
4.2.3	<i>BSP</i> ₂ : FIC and MSC Decoding. Audio decoding	140

5 Conclusions	141
5.0.4 Start point	142
5.0.5 Proposed and accomplished goals	142
5.0.6 Future aspects	142
5.0.7 Difficulties found within the development phase	143
Appendices	144
A The Fourier Transform	145
A.1 Motivation	145
A.2 Approximation by the minimum mean square error	149
A.3 Orthogonality	151
A.4 Fourier Transform in Periodic Complex Functions	154
A.5 Integral Fourier Transform	158
A.6 DFT	160
A.7 Spectral Analysis	163
A.8 Applications of the Fourier Transform	166
A.8.1 Noise Filter	166
A.8.2 Image Compression	168
B Resumen en español del proyecto	173
B.1 Implementación software de DAB sobre la arquitectura CoolFlux BSP . . .	173
B.2 Control Automático de Ganancia	174
B.3 FFT	175
B.4 Demodulación diferencial	176
B.5 Frecuency de-interleaving	176
B.6 Cuantización	177
B.6.1 Hard Decision	177
B.6.2 Soft Decision	178
B.7 Time De-Interleaving	178
B.8 Energy Dispersal Unscrambling	179

B.9	Canal de Sincronización	179
B.9.1	Símbolo Nulo	180
B.9.2	TFPR symbol	180
B.10	Implementación hardware del demodulador DAB	181
B.10.1	DAB datapath	184
B.10.2	Memorias locales	184
B.10.3	Interfaz de depuración	184
B.10.4	Interfaz de interrupciones	185
B.10.5	Buffers Compartidos	185
B.11	Descripción de los módulos BSP	186
B.11.1	BSP_0 : Sincronización y buffering de muestras	186
B.11.2	BSP_1 : FFT, Deinterleaving, Demapping	187
B.11.3	BSP_2 : FIC and CIF Decoding, Audio decoding	188
B.12	Conclusiones	188
B.12.1	Punto de partida	189
B.12.2	Objetivos propuestos y cumplidos	190
B.12.3	Aspectos futuros	190
B.12.4	Dificultades encontradas	191

El presente documento es la memoria del proyecto de fin de carrera realizado por Álvaro Martínez López y Elena Pérez-Toril Gracia en la compañía NXP Semiconductors en Lovaina (Bélgica) para la asignatura Sistemas Informáticos de la titulación de “Ingeniería en Informática” en la Universidad Complutense de Madrid. Los autores de este proyecto autorizan a la Universidad Complutense de Madrid a difundir esta memoria con fines académicos, no comerciales y mencionando expresamente a sus autores.

Álvaro Martínez López

Elena Pérez-Toril Gracia

Universidad Complutense de Madrid, June 2010

Acknowledgements

The realization of this project has been possible thanks to the contribution of many people. In the first place I want to thank Luis Piñuel Moreno, the director of this project, for giving me the wonderful opportunity of going to Belgium for working on this project. I want to thank Pancho, my mentor at NXP, for teaching me everything I know about signal modulation, embedded systems and digital signal processors. Thanks a lot for those marvelous 6 months in Leuven. I also want to mention my gratitude towards Ludo, Marleen and Sandrine from NXP for their help and support, specially during the month of august. Many thanks to Elena, my project colleague and friend, for her companionship.

For me, this is not only a final year project but a symbol that represents all my trajectory during the years I spent as an undergraduate student at university. As such I want to mention all that people that has contributed to this venture. First of all, thank to my family, specially my mother, sister and grandmother, for their love, dedication and support while raising me. Many thanks to my friends Emilio, Pedroche, Cavero, Blasco, Agus and Saul. Among other things, I will never forget those marvelous days during our summer holidays in La Marina. I also want to thank you Andrés, for your wisdom and special understanding towards me.

In Memoriam my father

A.M.L.

Abstract

The new digital radio system Digital Audio Broadcasting (DAB) is a digital radio technology for broadcasting radio stations, which will likely replace most existing methods for radio broadcasting in many parts of the world.

Mobile reception without disturbance was the basic requirement for the development of the DAB system. The special problems of mobile reception are caused by multipath propagation: the electromagnetic wave will be scattered, diffracted, reflected and reaches the antenna in various ways as an incoherent superposition of many signals with different travel times, which in classical radio systems like AM or FM meant a deficit in the quality of sound, or even complete cancellation.

This document will present the software development of a DAB demodulator for the CoolFlux BSP and its subsequent implementation on the ultra-low power architecture CoolFlux BSP, developed by NXP Semiconductors.

For the implementation of the DAB system, a hard work in signal processing and code optimization techniques has been carried out aimed to get the smallest power and memory storage. Important correction codes and measures have also been applied to the data for ensuring a good quality reception.

Once all the algorithms have been introduced, we describe their implementation on a FPGA in order to perform real time processing of the signal. Although one CoolFlux BSP is capable of running the whole demodulator in real time on its own, the FPGA is constrained to 50 MHz (against 300 MHz of an actual BSP). Thus, the demodulation chain had to be pipelined into three BSP cores, all of which were mapped on one FPGA.

Resumen

Digital Audio Broadcasting (DAB) es un estándar de emisión de radio digital desarrollado por EUREKA como un proyecto de investigación para la Unión Europea (Eureka 147). Este sistema pronto reemplazará a la mayoría de los métodos existentes de transmisión de radio en muchas partes del mundo.

El principal motivo para el desarrollo del sistema DAB era conseguir un sistema para la recepción móvil sin alteraciones de la señal. Los principales problemas de la recepción móvil provienen de la propagación multipath: la onda electromagnética está sujeta a fenómenos de reflexión, dispersión y difracción y llega al receptor como una superposición incoherente de señales, lo que en sistemas clásicos de radio tales como FM o AM se traduce en una recepción pobre o incluso en la pérdida total de los datos.

El presente documento mostrará el desarrollo del software de un demodulador de DAB y su posterior implementación hardware en la arquitectura CoolFlux BSP, el sistema para aplicaciones de bajo consumo desarrollado por NXP Semiconductors, destinado a dispositivos móviles de consumo energético limitado.

Para la implementación del sistema DAB, se ha realizado un gran trabajo en cuanto a procesamiento de señales y se han aplicado técnicas de optimización destinadas a conseguir el menor consumo de potencia posible con el mínimo almacenamiento de memoria y ciclos de computación. También se han aplicado numerosos códigos de corrección de errores a los datos, para asegurar una alta calidad del audio emitido.

Anteriormente a este trabajo se realizaron estudios de viabilidad en los que se concluyó que tan sólo sería necesario un BSP para demodular la señal en tiempo real. Sin embargo, el prototipado del sistema en una FPGA (cuya frecuencia de reloj es considerablemente más limitada que un sistema real) exigía la necesidad de utilizar 3 instancias del BSP conectadas en cascada.

Keywords

- DSP
- BSP
- CoolFlux
- Digital Radio
- DAB
- Demodulator
- FFT
- Digital Signal
- Error correction
- Real Time
- Processor

Chapter 1

Preliminary concepts in DAB

Before we introduce the actual implementation of the DAB demodulator on the CoolFlux BSP we present some theoretical concepts in radio communications. The problem at hand is that of transmitting information in an efficient manner using the electromagnetic spectrum. In this scenario we have the broadcaster -that is the agent that transmits the information- and the receiver. The space between them is known as the channel and, as we shall see, a great effort is devoted in DAB to transmit a clean signal through it (figure 1.1).

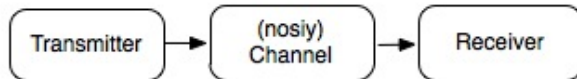


Figure 1.1: Elements in radio communications

1.1 Signal Modulation

The main concept behind radio communications is that of modulation. An electromagnetic wave has three main attributes that can be varied in time to convey information: amplitude (A), frequency (ω) and phase (ψ) (figure 1.2).

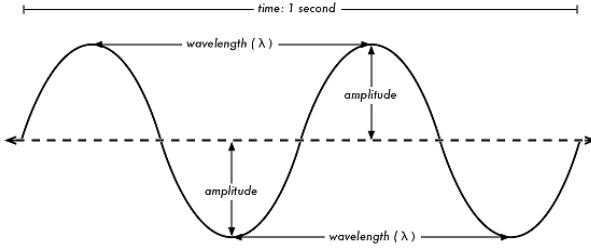


Figure 1.2: Wave attributes.

Figure(1.3) shows three waves with the same frequency and amplitude, but different phases:

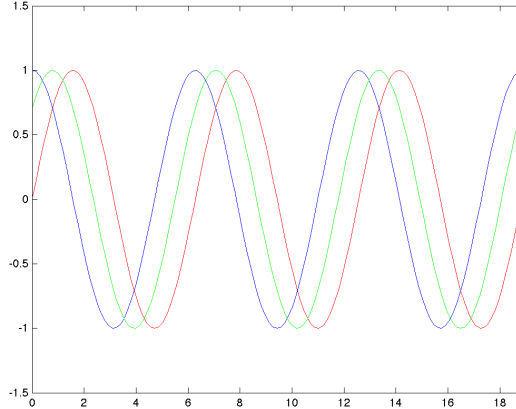


Figure 1.3: Three waves with different phase.

In radio communications two waves are used to transport the message, the base signal and the carrier signal. We can multiply the former by the later to form the modulated signal. The device used to carry out this process is known as a modulator. In the same way, a demodulator is a device that takes as its input the modulated signal to extract the base signal, hence recovering the information.

Classically, information was sent in an analog fashion by varying the amplitude, frequency or phase within a continuous range. As an example let's mention the well known FM and AM radio systems (picture 1.4), in which the amplitude and frequency are changed over time respectively^[2].

By contrast, digital information is made up of discrete symbols, also called bauds, chosen

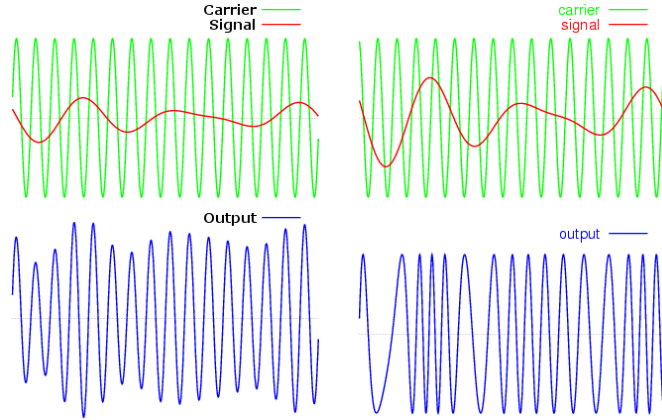


Figure 1.4: Amplitude Modulation and Frequency Modulation.

from a finite alphabet. If the alphabet has 2^N symbols then, each symbol carries N bits of information. The equivalent digital modulation schemes to those presented so far are known as PSK, FSK (figure 1.5) and ASK for which, in turn, finite values of phase, frequency and amplitude are employed. A variation of the first one, called DQPSK will be our main concern later, since it is the standard used in DAB^[3].

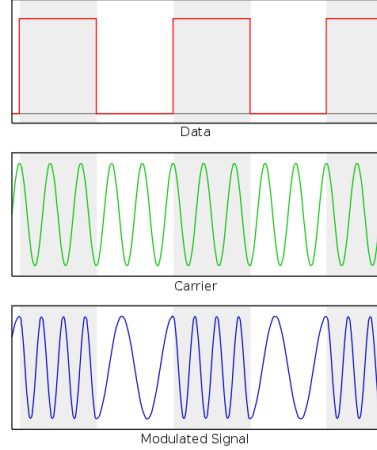


Figure 1.5: Frequency-shift keying.

Strictly speaking, even though the information is digitally modulated, the actual signal that goes out the transmitter is analog since nature does not allow a physical magnitude to change from one state to another in a finite amount of time without passing through all intermediate values. An Analog to Digital Convertor (ADC) is a device that takes an

analog signal as its input and converts it to a digital representation in a process known as sampling^[4]. .

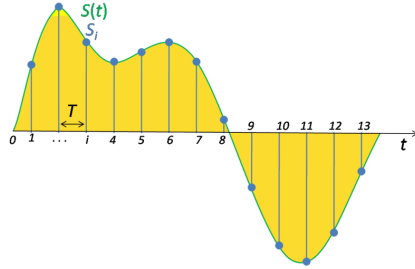


Figure 1.6: Sampling of an analog signal.

1.2 Multipath Propagation

Most existing means for radio communication which can use simple omni-directional receiving antennas are affected adversely by multipath propagation, particularly in a changing environment such as when the receiver is located in a moving vehicle. The effect on broadcast FM radio is well known where, in built-up areas, even if there is sufficient mean field strength, mobile reception can be severely impaired by bursts of noise and audio distortion, and sometimes a fluttering effect on the audio signal.

In addition to a direct signal from the transmitter, the receiver is often presented with signals reflected and diffracted by buildings and the terrain. These can combine constructively or destructively in the receiving antenna as the relative lengths of the propagation paths change, or as the wavelength changes. Indeed, the sensitivity to the wavelength, or frequency, is the main reason for the audio distortion with FM signals.

Constructive addition can give up to 6 dB enhancement, for two signals of equal magnitude, but subtraction can cause complete cancellation. This phenomenon is known as fading, and multipath propagation is one of two mechanisms by which it can be caused; the other is blocking of the propagation path by obstacles. In the latter case, the problem can often be overcome simply by increasing transmitter powers, but this is not always true for multipath fading; destructive combination of two signals of equal magnitude causes complete cancellation regardless of the transmitter power. When an FM receiver is pre-

sented with insufficient signal power its own front-end noise is demodulated giving a burst of audio noise. In most common environments, reflected and diffracted signals usually have smaller magnitudes than a direct signal, but a direct line-of-sight path might not always be available. Most reflections occur by lossy mechanisms (i.e. not large sheets of metal), and reflected signals often have further to travel so they are subject to greater spreading losses. On the other hand the phenomenon by which fading affects only a fixed range frequencies within the signal is called selective fading.

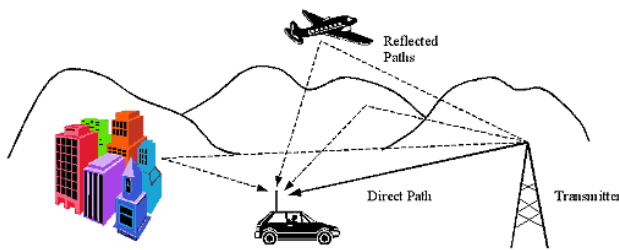


Figure 1.7: Multipath propagation in the environment.

The receiver performance can be enhanced by using a directional antenna, which is only appropriate to fixed reception, or a diversity system using more than one antenna, which may be applicable to a more-expensive vehicular installation. Indeed, the audio quality available from fixed FM receivers with rooftop directional antennas is very good, but the market for radio consumption has changed from what was anticipated at the start of BBC FM services. The widespread use of portable and mobile receivers now demands a means for delivery which offers the highest audio quality, in most environments within a service area, without the need for a complicated antenna system or one that may need adjustment.

On this basis, there is little that can be done to rescue an FM signal, or any other analogue signal, in the presence of severe fading or interference. Much of the damage is done in the receiving antenna, and there is little scope for ‘post-processing’ to rectify the situation. However, in broadcasting and many other fields of communication, a solution is being sought in the application of digital techniques, implying a radical departure from the classical methods of broadcasting. This introduces numerous problems for the broadcasters and the receiver manufacturers (none of which is technically insurmountable, nowadays), but it offers the great advantage of ‘post-processing’ in the form of error correction.

The effect of fading and interference on a digital system is to introduce errors into the received signal, but improvements are possible by virtue of the numerical nature of the bit-stream. Error detection can be achieved in the receiver by sending a small amount of additional data derived from the original data, such as checksums. By sending further additional data, it becomes possible to correct errors. Such additional data are often referred to as ‘redundant’ data, but this does not imply that they are not needed; only that they carry no new information. The trivial case would be simply to transmit all of the original data twice with independent checksums, so with the benefit of error detection a complete set of good data could be reconstructed. However, this would make relatively inefficient use of the available bit-rate, as there still remains a probability that some of the same bits could be in error in both of the received versions. Many more-complicated, and ingenious methods have been developed for such Forward Error Correction (FEC; ‘forward’ implies that action is taken at the transmitter), which make more efficient use of a given amount of redundancy.

Powerful FEC, by whatever method, requires the transmission of substantial amounts of redundant data which increases the demand for radio frequency spectrum. However, the Eureka DAB system achieves greatly improved ruggedness without sacrificing efficiency in its use of radio spectrum by applying in addition what could be called ‘advanced’ digital techniques. To explain how the DAB system works, we should first look more closely at the effects of multipath propagation, in both the time and frequency domains.

Incidentally, the word ‘coding’ is used widely in the context of error correction, and digital communications generally. Sometimes the intended meaning is the whole principle of encoding and decoding data, and sometimes it is used instead of ‘encoding’. The former meaning will be applied here, and in order to avoid ambiguity, the terms ‘encoding’ and ‘decoding’ will be used where they are meant.

The time and frequency domains provide different viewpoints for the same effects, a principle well known to anyone who has used an oscilloscope and a spectrum analyzer to inspect the same signal. The oscilloscope allows inspection of the way that a signal voltage changes as time progresses, almost irrespective of the rate at which it is changing, whereas the spectrum analyzer allows inspection of the content of the signal at different frequencies

(i.e. rates of change), almost irrespective of time. Often, different aspects of a phenomenon being investigated can be visualized more clearly in one or other of the two domains. For example, the vestigial sideband in a conventional AM television signal can be inspected using a spectrum analyzer, but an oscilloscope gives no obvious hint to its existence.

If the effects of a phenomenon are described mathematically in each of the domains, the two descriptions are related by the Fourier transform. For example, the frequency response of a filter is related to its time impulse response by the Fourier transform.

One effect of multipath propagation is to generate inter-symbol interference. When a direct signal and delayed ‘echoes’ arrive at the receiving antenna, there will be occasions when their modulation represents data from different symbols, previous as well as present. This is illustrated in figure 1.8 for the case of a single delayed signal, although there may be many in practice.

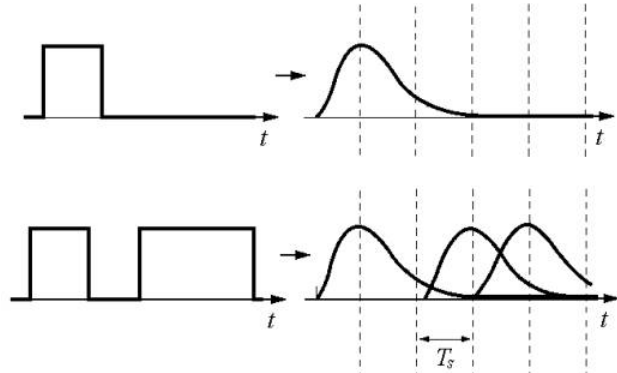


Figure 1.8: inter-symbol interference

Returning to figure 1.8, when the combined signal is demodulated and the modulation state is detected, the effect of the overlapping different symbols is to cause corruption of the data; that is, inter-symbol interference. For example, figure 1.8 shows a symbol generated in the transmitter (first row). Let’s suppose the transmitter is sending the binary string “01000”. As we pointed out before, the actual signal that travels through the air is not like a perfect step function, but slightly smoother. The symbol is echoed three times and arrives at the receiver as shown in the second row. The receiver shall not receive “01000” but “01110” instead. However, rather than making a ‘snap’ decision at one point in time during each symbol, as implied in the figure, in some cases it can be more efficient for the

detector to integrate the demodulator output signal over the whole of each symbol, with respect to some timing reference (which may be the direct signal). This makes use of all of the received signal power.

In that case, as long as the delay is less than the symbol duration, the echo will carry the same modulation as the direct signal for some portion of integration period. Undoubtedly this will have some effect because the demodulator output signal represents the phase of whatever is input; in this case the ‘vector’ sum of the direct and delayed signals. However, a method is available to prevent this from upsetting the operation of the detector; that is, differential modulation which will be described later. Entirely different symbols overlap for the remainder of the integration, so the degree to which the result is corrupted depends on the magnitudes of the echo signals and on their delays.

When a mobile receiver is traveling in a dense urban environment, which imposes one of the most difficult multipath conditions, short-delay echoes are often received in greater numbers than long-delay ones owing to multiple reflections (of a relatively direct signal) from local buildings and terrain. Very long delay echo signals tend to have smaller magnitudes because they have travelled greater distances. Therefore, the majority of the collective echo power arises from short delay echoes, so modulation schemes which use long symbols (or low symbol rates) provide the greatest tolerance to this effect because the proportion of each symbol that is corrupted is minimized.

We could measure the collective echo power received with different delays in time. An idealized result is illustrated in figure 1.9 where the transmitted (i.e. direct) signal is shown as a single impulse; in practice, more-complicated signals are used in such measurements to overcome the infinite bandwidth requirement of true impulses, but the results can be presented in a similar fashion.

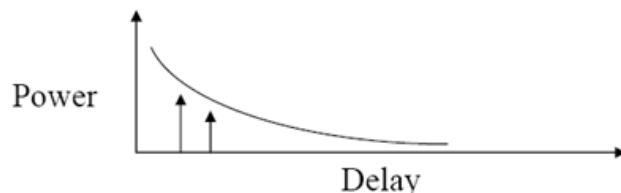


Figure 1.9: Delay spread

By taking a large number of measurements in a particular type of environment, the statistical distribution can be built up, and in many cases this is found to approximate to an exponential curve (see figure 1.9). The distribution is characterized by a single parameter known as the ‘delay spread’, which can be interpreted as either the mean or the standard deviation in the case of an exponential distribution. The next equation expresses the statistical distribution of the echo power as a function of the delay ξ . The parameter T is the delay spread.

$$P(\xi) = \frac{1}{T} e^{-\frac{\xi}{T}}$$

The incremental effects of greater delay or greater echo power are similar, they both increase the potential for inter-symbol interference, so the delay spread (interpreted as the mean) is a guide to the interference potential of a given type of environment. The average degree of data corruption is proportional to the ratio of the symbol duration to the delay-spread. For the case of outdoor reception from a single terrestrial transmitter, the delay spread can range from less than 0.5s to 5 μs , or more; a typical median value (for 50% of locations) is around 1 μs . Echoes with delays outside this range can be encountered, but the percentage of locations for which they contribute significantly to the delay spread is small (less than 1%). Direct reception from a satellite yields values of 0.5 μs , or less.

Thus, it was a pre-requisite for the DAB system that the symbol duration should be much greater than the values of delay-spread encountered in common broadcasting environments. In other words, the symbol duration should have a minimum value of at least 50 μs for terrestrial broadcasting^{[6][5]}.

1.3 QPSK (Quadrature Phase Shift Keying)

So far, we pointed out that PSK uses a finite set of phases to represent the symbols that compose the message. QPSK uses four points on the constellation diagram, equispaced around a circle. With four phases, QPSK can encode two bits per symbol, shown in the diagram with Gray coding to minimize the Bit Error Ratio (BER).

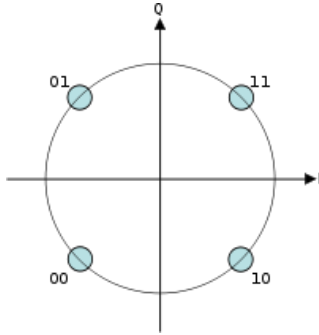


Figure 1.10: Constellation diagram.

Let T_s be the duration of one symbol. The mathematical expression for each symbol ($i = 1, 2, 3, 4$) is:

$$S_i(t) = \sqrt{\frac{2E_s}{T_s}} \cos(2\pi f_c t + (2i - 1)\frac{\pi}{4}) \quad i = 1, 2, 3, 4$$

where E_s is the energy employed to send the signal. The last equation also shows that the less the energy employed for the transmission the closer the symbols will be in the constellation diagram, thus the chance of one symbol becoming another is higher. The signal constellation consists of the signal-space 4 points:

$$(\pm \sqrt{\frac{E_s}{2}}, \pm \sqrt{\frac{E_s}{2}})$$

The factors of $1/2$ indicate that the total power is split equally between the two carriers. A QPSK signal is actually a composition of two orthogonal basis functions,

$$\begin{aligned} \phi_1(t) &= \sqrt{\frac{2}{T_s}} \cos(2\pi f_c t) \\ \phi_2(t) &= \sqrt{\frac{2}{T_s}} \sin(2\pi f_c t) \end{aligned}$$

where f_c is the carrier frequency.

The first and second bases are called the in-phase (I) and quadrature (Q) components of the signal respectively. From the orthogonality of the I and Q components, it follows

that we can send both signals through a single channel -that is, a single frequency- without having them interfering with each other.

The following picture shows some random bits mapped in the I and Q components of a QPSK signal. Both the I and Q components are added together to form the actual QPSK signal.

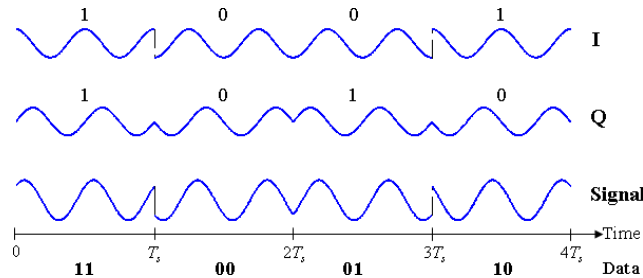


Figure 1.11: I and Q components mapped into QPSK signal.

The next picture shows a conceptual transmitter structure for QPSK. The binary data stream is split into the in-phase and quadrature-phase components. These are then separately modulated onto two orthogonal basis functions. In this implementation, two sinusoids are used. Afterwards, the two signals are superimposed, and the resulting signal is the QPSK signal. Note the use of polar non-return-to-zero encoding. These encoders can be placed before or after the binary data source, but have been placed after to illustrate the conceptual difference between digital and analog signals involved with digital modulation.

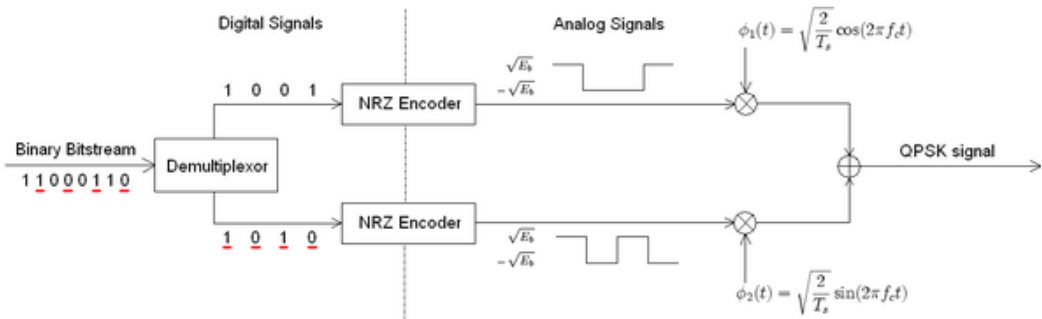


Figure 1.12: QPSK modulator

On the other hand, a receiver might be implemented as follows. The matched filters can be replaced with correlators. Each detection device uses a reference threshold value to determine whether a 1 or 0 is detected.

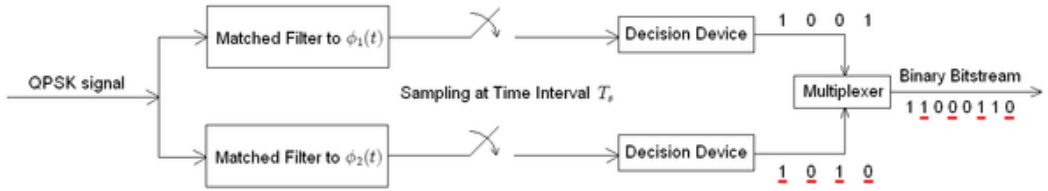


Figure 1.13: QPSK demodulator

Despite its apparent simplicity, QPSK has a major drawback. QPSK uses absolute phases (e.g $0^\circ, 90^\circ, 180^\circ, 270^\circ$) to determine whether the current symbol is '00', '01', '11' or '10'. There can happen that due to noise in the channel, the current and future QPSK symbols suffer a phase shift of say 90° , thus rotating the constellation diagram. Of course, the conveyed digital information would be erroneous.

A better approach would be to differentially encode the phases of two consecutive QPSK symbols. This scheme is called DQPSK, and it is the standard in DAB. The actual phase is not that of the current symbol but the difference between the last symbol and the current one. In this case, all the symbols that pass through the channel will be shifted in time (thus in phase) by the same offset. Therefore operating with the difference of phases between two subsequent symbols will cancel out that offset^[7].

1.4 FDM (Frequency Division Multiplexing)

The process by which multiple broadcasters share the radio spectrum is called multiplexing. If two or more broadcasters want to emit at the same frequency there has to be an agreement between both to send their signals at different times. Otherwise, their signal would interfere with each other, destroying the information. This turning on the use of the channel is what is called in telecommunications TDM (Time Division Multiplexing)^[8].

A more common way of sharing the spectrum is to allow each transmitter to emit at a different frequency. We avoid interference among different frequency carriers by introducing an additional guard space between them. This process is called FDM (Frequency Division Multiplexing). As an example, the next picture illustrates the spectra of a signal composed of 8 subcarriers^[9].

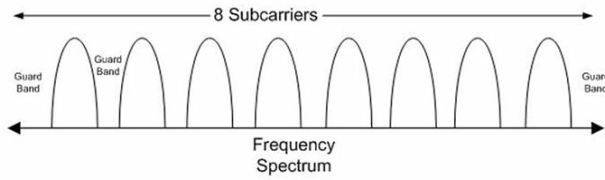


Figure 1.14: Frequency Spectrum

1.5 Orthogonal Frequency-Division Multiplexing (OFDM)

The bandwidth of a digitally modulated signal is proportional to the symbol-rate. The exact relationship depends on the modulation scheme and factors such as filtering, but generally for a given modulation scheme, doubling the symbol rate doubles the bandwidth. The simple way to increase the bandwidth of the DAB signal without compromising its spectral efficiency would be to make it carry several radio programs at the same time, by bringing together data representing a number of audio signals and multiplexing them before transmission.

However, this gives rise to a dilemma: if the DAB signal were to use a single carrier, then in order to achieve a wide bandwidth, the symbol rate would need to be high, but this conflicts with the requirement for long symbols.

A solution is to use not one, but a multiplicity of carriers each at a different radio frequency. By modulating each carrier independently at a low symbol rate by a small fraction of the data to be transmitted, individually the carriers will then be relatively resistant to multipath echoes because of their long symbols.

The requirement for mobile reception imposes an upper limit on the symbol duration. The changing characteristics of the transmission channel can have adverse effects on whatever modulation system is used, and generally, the maximum symbol duration is related to

the required maximum vehicle speed. Thus, the maximum symbol duration chosen for the DAB system is 1 ms. In isolation, this allows good reception at vehicle speeds of at least 100 km/hr.

On the other hand, it is found that the resistance to multipath effects improves as the bandwidth is increased, accommodating more extreme multipath conditions which could otherwise cause flat fading. Hence, the actual bandwidth chosen for the DAB signal is 1.537 MHz

Clearly, the greater the number of individually modulated carriers that can be packed into the given bandwidth, the greater the potential data capacity of the signal, but the upper limit is set by the requirement for independent demodulation without mutual interference. The significant bandwidth occupied by each modulated carrier is determined by the chosen symbol rate and the modulation scheme, and a simple way to avoid mutual interference would be to separate adjacent carriers by frequency guard bands. However, such a simple Frequency-Division Multiplexing (FDM) approach would be wasteful of RF spectrum. Without guard bands, the spectra of adjacent modulated carriers are likely to overlap, and the allowable degree of overlap depends on the method of demodulation, so this establishes a maximum packing density, or a minimum separation between the carrier frequencies. In either case, some form of spectrum analysis technique is needed in the receiver.

The DAB system uses a technique known as Orthogonal Frequency-Division Multiplexing (OFDM) which allows the greatest possible packing density consistent with the use of practicable (mainly digital) processing techniques. This requires the minimum separation of the carrier frequencies to be equal to the reciprocal of the symbol duration, 1 kHz, so the spectra of adjacent modulated carriers will certainly overlap. In that case, the maximum number of modulated carriers would be 1537, but in practice one carrier is not used. Therefore, the maximum number of modulated carriers in the DAB signal is 1536. (See the appendix about the Fourier Transform for a mathematical explanation of orthogonality)

In this scheme, the possibility arises that data conveyed by some of the individual carriers will not be received successfully because of selective fading, but in this case the application of FEC is most efficient (and necessary) because the loss of a small number of carriers represents the loss of only a small fraction of the total data. Thus, for the same

degree of protection, the amount of redundant data that needs to be transmitted is much smaller than would be required for scheme using a single-carrier. For the DAB system, the abbreviation OFDM is prefixed with a ‘C’, for coded, to indicate the application of FEC, giving ‘COFDM’.

With all that at hand, we can deduce the total bit rate of a DAB ensemble:

$$1536 \text{ subcarriers} * 2 \text{ bits per symbol (DQPSK)} * 1000 \text{ symbols/sec} = 3.072 \text{ Mbits/sec}$$

Generation of an OFDM signal is easily visualized because, in principle, it could be carried out by partly-analogue means using a large bank of synthesized oscillators followed by modulators (i.e. multipliers). This principle is illustrated in picture 1.15 where three, of many, oscillators are shown although it should not be inferred that such a cumbersome arrangement is used in practice.

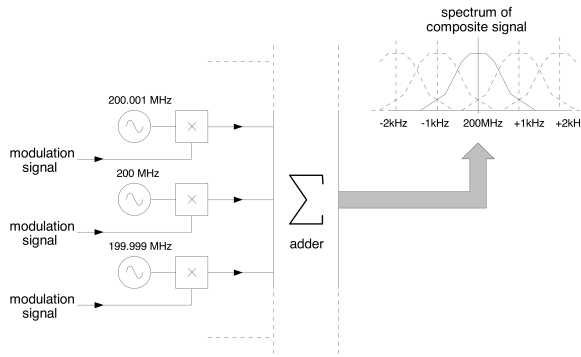


Figure 1.15: generation of an OFDM signal

Each oscillator provides one of the carriers, and the modulation is applied by each multiplier. All of the modulated carrier signals are then added together to make up the composite signal. The addition (or summation) can be considered as taking effect in the frequency domain; all of the frequency components produced by the multiplications are combined without affecting the time-waveform of any component. If the modulation signals are composed of symbols, such that changes only occur at the symbol boundaries then, during each symbol, each modulated carrier is temporarily a sinusoidal wave with a particular phase and/or amplitude representing the modulation.

However 1536 such oscillators could occupy a large room. The key to compact digital implementation lies in the recognition that this process parallels the operation of a mathematical process known as the inverse Discrete Fourier Transform (iDFT). The iDFT is a method of calculating the waveform of a signal for which the spectrum is known. The iDFT operates with time-domain and frequency-domain variables which must be expressed as series of discrete samples.

In this case, the array of modulation signals which are to be applied to the carriers during a single symbol provide a specification of the spectrum of the required composite signal for that symbol. The modulation of the carriers is intended to remain static during each symbol, so each modulation signal contains one sampled value per symbol. The array of modulation signals can then be thought of as a series of samples which make up a ‘function of frequency’.

The composite OFDM signal will be produced by the iDFT as a series of samples which follow one another in time, so it can be thought of as a ‘function of time’.

The array of oscillator signals can be thought of as a function of both frequency and time; the array of different frequencies forms a series with respect to frequency (as with the modulating signals), and if each oscillator provides a sine wave, a sampled version of this forms a series with respect to time.

With this nomenclature, the iDFT (and the contents of figure Fig 1.15) can be expressed as:

$$f(t) = \sum_{\text{lowest frequency}}^{\text{highest frequency}} \text{function of frequency} \times \text{oscillator signal}$$

To produce the first sample of the ‘function of time’, each of the modulation ‘samples’ is multiplied by the first time sample of its corresponding oscillator signal, and all of the products are added together. For the second sample, the second time samples of the oscillator signals are used, and so on. In this way, any number of samples of the ‘function of time’ can be produced which represent the composite OFDM signal for one symbol. In practice, this number is minimized in order to constrain the demand for processing, and the fundamental limit is set by the so-called Nyquist criterion; the time-sampling rate must be

at least twice the frequency of the highest frequency component represented in the function of time to avoid ‘aliasing’ distortion.

The period of time over which the whole calculation is performed can be called the ‘processing time-window’, and it is a requirement for correct operation of the iDFT that the duration of this window and the interval between the oscillator frequencies should have a reciprocal relationship. In this case, the required time-window (i.e. symbol) duration is 1 ms, so the oscillator frequencies are separated by 1 kHz. The required number of carriers, 1536, defines the highest frequency represented in the function of time, so the minimum time-sampling rate is then defined. The iDFT process is repeated for subsequent symbols, in each case with a new set of values in the array of modulation signals.

It is relatively straightforward to implement this transform in a computer program, or by means of digital hardware of some other form, where all of the sample values are represented by digital numbers. Furthermore, the availability of fast ADCs and DACs means that, nowadays, it is entirely practicable to carry out symbol-by-symbol processing in real time. With modern VLSI technology, the complexity (i.e. the number of carriers) is of relatively minor importance.

The recovery of the modulation signals from an OFDM signal (i.e. ‘decomposition’ of the OFDM signal) is rather less straightforward, but essentially this follows from the generation process by interchanging time and frequency. It was mentioned earlier that integrating over each symbol is an efficient way to determine the modulation state of a carrier, and an extension of this principle provides a useful starting point.

To simplify the explanation, the receiver should initially be visualized as containing a large bank of local-oscillators, mixers (i.e. multipliers) and integrators although, as before, such an arrangement is not used in practice. Each oscillator/mixer combination acts as a demodulator, in the manner of a direct-conversion radio receiver. The incoming signal is fed equally to all of the demodulators, and each of these is followed by an integrator. Each integrator operates over a limited period of time before yielding a result. This is illustrated in Fig. 1.16.

Each modulated carrier is demodulated by the mixer which is fed with a local-oscillator signal of the corresponding frequency but, since the spectra of adjacent modulated carriers

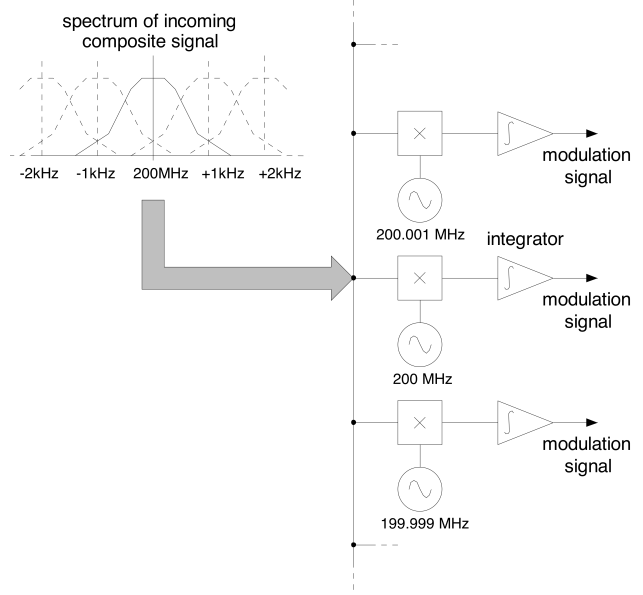


Figure 1.16: generation of an OFDM signal

are allowed to overlap, each integrator will be presented with interference (or crosstalk) contributions as well as the wanted demodulated signal. However, if the radio frequencies could be chosen so that over the period of integration, the symbol duration, the integrals of all the interference signals amounted to zero, then mutual interference would be cancelled.

This condition is known as ‘orthogonality’, and is achieved when the carrier frequencies and the local-oscillator frequencies are located on a regular comb where the frequency interval is equal to the reciprocal of the symbol duration.

With reference to Fig. 1.17, take for example the modulated carrier at 200MHz, with neighbors at ± 1 kHz, ± 2 kHz, etc. either side. The modulation state of each carrier is held constant over each symbol, so each carrier is temporarily a sinusoidal wave with a particular phase and/or amplitude representing the modulation. When the incoming signal is acted upon by the mixer with the 200 MHz local-oscillator, the 200 MHz wave will produce a DC output signal, and contributions from the neighbors will produce 1 kHz, 2 kHz, etc. AC components (the 400 MHz products will be neglected). When the composite signal output by this mixer is integrated over 1 ms, all of the AC components will cancel because

they contain whole cycles, but the DC signal will accumulate to produce an output signal representing the modulation state of the 200 MHz carrier alone.

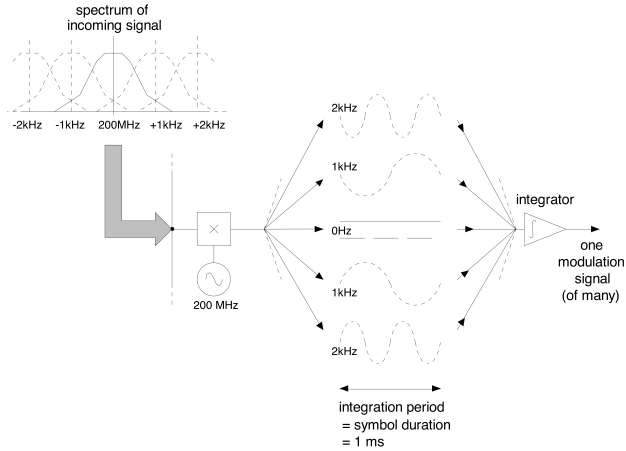


Figure 1.17: demodulation without mutual interference

A similar argument applies for each of the other carriers, with input frequencies and local-oscillator frequencies separated by the reciprocal of the symbol duration. The overall effect of this process is to analyze the spectrum of the incoming signal, and to output numerous signals each representing the modulation of one of the carriers.

If analogue processing were relied upon, the acceptable complexity of a domestic receiver would probably limit the maximum number of carriers to as few as 16 but, once again, the solution is to represent the process digitally. It is probably not surprising that the decomposition process has a direct counterpart in mathematics known as the forward DFT, or simply the 'DFT'. The DFT is the digital counterpart of the well-known Fourier Transform which relates the time and frequency domains, but the input and output functions of the DFT are series of discrete samples rather than continuous signals. The DFT is related to the iDFT essentially by interchanging time and frequency.

The incoming OFDM signal can be sampled in time and the series of samples can be thought of as a 'function of time'. As before, each of the modulation signals contains one sample per symbol, so the array of modulation signals can be thought of as a series of samples which make up a 'function of frequency'; that is, a description of the spectrum

of the incoming composite signal. The array of oscillator signals can be thought of as a function of both time and frequency, as before.

The action of integrating each output signal corresponds, in discrete terms, to the summation of numerous consecutive discrete samples in time, so the decomposition process (and the contents of 1.16.) is modeled by the DFT which can be written as:

$$f(\text{frequency}) = \sum_{\text{first time sample}}^{\text{last time sample}} \text{function of time } x \text{ oscillator signal}$$

To produce the first sample of the ‘function of frequency’, that is, the modulation signal from the first (e.g. the lowest-frequency) carrier, each sample of the incoming ‘function of time’ is multiplied by the first frequency sample of the array of oscillator signals (e.g. the lowest-frequency one), and all of the products are added together. To recover the second modulation signal, the second frequency samples of the oscillator signals are used, and so on.

As before, the minimum time-sampling rate is set by the Nyquist criterion and the processing window duration (1 ms) must be equal to the reciprocal of the carrier frequency separation (1 kHz). Thus, a fixed number of samples of the ‘function of frequency’ can be produced which represent the modulation signals recovered from the individual carriers. The process is then repeated for subsequent symbols to yield the subsequent sets of modulation signals.

It is within the scope of modern VLSI technology to perform this decomposition process within one integrated circuit and, of course, in such a ‘fully-digital’ system as DAB, it is unnecessary to provide additional ADCs and DACs purely for these tasks.

In practice, an algorithm (i.e. a means for performing a computation which yields the same result) is used to perform the DFT in the receiver, and this is known as the Fast Fourier Transform, or FFT. An inverse FFT is used to generate the OFDM signal in the transmitter. The advantage of the FFT is increased processing speed for a given level of complexity. An FFT operates with complex numbers, in digital form, which represent the amplitudes and phases of its sampled input and output signals; the multiplications to which the last two sections have referred are actually complex multiplications.

A principal difference from the DFT is that the number of time samples must be equal to the number of frequency samples. This means that if all of the available samples are used, then the time-sampling rate can only just satisfy the Nyquist criterion. In most practical implementations of an FFT, the number of time or frequency samples is made equal to 2 raised to some power, so a 2048-sample FFT is used to process the 1536-carrier DAB signal. In that case, some ‘headroom’ is provided against aliasing.

When an FFT processor is presented with a digital representation of a time-domain signal (i.e. of a voltage varying with time), it has the effect of analyzing the spectrum of the signal and it outputs numerous baseband signals, each corresponding to a particular range of input frequencies. Each baseband signal represents the amplitude and phase of whatever component of the signal is present in that particular frequency range. Thus, the function of the FFT can also be visualized as that of a bank of band-pass filters, followed by frequency down-converters. The effective filter bandwidths are contiguous and are each equal to the reciprocal of the duration of the processing time-window. The centre frequencies of the pass-bands are integer multiples of this reciprocal. The frequency response of each filter has a $\sin f/f$ shape, where f represents the relative frequency with appropriate scaling. By making the window 1 ms long, each bandwidth becomes 1 kHz and the centre-frequencies fall on a regular 1 kHz comb. The frequency response of each filter exhibits nulls at ± 1 kHz, ± 2 kHz, etc., and this accounts for the cancellation of inter-carrier interference noted earlier.

Therefore, it should be clear that the absolute frequencies of the carriers presented to the FFT processor, and their frequency separation, are intimately related to the symbol duration, and that any divergence from this relationship will cause some loss of orthogonality (i.e. crosstalk between carriers).

All of these features apply equally, but in a reversed sense, to the inverse FFT used in the transmitter. The absolute carrier frequencies and their separation are automatically related to the reciprocal of the symbol duration. Of course, it is possible to specify the spectrum of the OFDM signal such that certain carriers are suppressed (i.e. their amplitudes are set to zero), and this is done for the remainder of the 2048 frequency samples beyond the 1536 that are used for the DAB signal. The spectrum could also be configured such that every

other carrier was suppressed, so the relationship between the frequency separation and the reciprocal of the symbol duration need not be 1:1, it could be 2:1 or some other integer ratio. However, a 1:1 relationship provides the greatest possible packing density consistent with the facility for independent demodulation and makes the greatest use of the available processing power^[6].

1.6 Fast Fourier Transform (FFT)

Please, for a better understanding of this section, refer to the appendix in which a mathematical view of the Fourier Transform is given.

1.6.1 Overview

In developing DAB to combat multipath propagation, attention has been paid to the effects of radio propagation in both the time domain and the frequency domain. As noted in the first chapter these two domains provide different viewpoints for the same effects. Equally, when generating or receiving a signal, certain aspects of the processing can be carried out more easily in one or other of the domains. This is particularly true in the case of DAB, where the multiple-carrier RF signal is more easily synthesized and analyzed in the frequency domain, but the symbol-by-symbol modulation is more easily treated in the time domain. Indeed, if a DAB signal is displayed on an oscilloscope, it appears similar to band-limited white noise punctuated by the null symbols (every 96 ms in Mode 1), which gives little clue to the existence of multiple discrete carriers.

Successive stages of a DAB transmitter, or receiver, operate on constituents of the DAB signal in both of these domains. In the channel encoder, the spectrum of the signal is constructed essentially as an array of numbers, each representing the instantaneous amplitude and phase of one of the QPSK carriers. From this frequency-domain spectrum, the equivalent time-domain signal is produced, which can be up-converted to the final frequency and transmitted. The changes of modulation states from symbol to symbol are effected by changing the numbers input to the array. In the receiver, from the incoming time-domain

signal, the spectrum is re-constructed as an array of numbers representing the individual modulated carriers, from which their modulation states can be determined.

The link between the time and frequency domains is process of transformation. Bearing in mind the number of carriers, 1536 in Mode 1, it would be out of the question to perform this process in a domestic receiver using analogue circuitry (e.g. banks of oscillators and filters).

The solution is to implement the transformation digitally, and there are several possible approaches, of which one of the most rapid is the FFT algorithm. The treatment in the section 1.5, in practical terms, show how the discrete Fourier transform (DFT) can be developed from a block diagram of the OFDM decomposition process^[6].

1.6.2 Digital Implementation

It is important to impose time limits in order to limit the extent of the summation. In practice, the number of input samples which are available to be transformed may already be defined (e.g. by the symbol duration, in the case of DAB), and this automatically imposes time limits. It is convenient to think of this as the application of a ‘time window’; processing is only carried out on those samples which appear when the window is ‘open’. This action also imposes a limit on the range of frequency values which need to be considered in the summation, which will be explained later.

As is often the case in sampled systems, a compromise has to be made between accuracy and an acceptable amount of processing. Generally, the sampling frequency must be greater than twice that of the highest frequency component in the input signal, and this, so-called, Nyquist criterion is applicable in most cases of time-domain sampling. Frequency components above half the sampling frequency are not represented accurately and may need to be removed from the input signal by filtering. A frequency component at exactly half the sampling frequency can be considered to be at the Nyquist limit^[6].

1.6.3 The Discrete Fourier Transform

The result of the DFT provides a series of samples of the spectrum, for negative and positive frequencies. The time-domain sampling of the input signal gives rise to repetitions

of this two-sided spectrum at higher frequencies, centered on multiples of the sampling frequency (i.e. the spectrum is periodic in terms of frequency). If the sampling frequency is sufficiently great, these can be removed by filtering. Insufficient sampling frequency gives rise to overlapping spectra, so-called ‘aliasing’, which cannot easily be removed. A spectral component at the Nyquist limit must, by definition, contain an unwanted alias.

If the Nyquist criterion is just satisfied in the time-domain sampling, then the resulting sampled spectrum cannot contain useful information at frequencies above half the time-sampling frequency. If the time-sampling frequency is f_s and the time-window duration is T , then the number of samples processed $N = Tf_s$. The interval between the frequency-domain samples is $1/T$ and the useful range lies between $\pm f_s/2$, so the number of useful samples is $\pm(f_s/2)/(1/T) = \pm N/2$; that is, $N/2$ samples at positive frequencies and $N/2$ at negative frequencies. Thus, the total number of useful samples in the result is equal to the number of samples input. With N time-domain and N frequency-domain samples, a total of N^2 coefficients are needed in the summation.

The frequency-domain sampling of the result has a similar, although reciprocal, effect in the time domain; that is, the result of the DFT applies to the time-windowed input signal as if it were periodic with a period equal to the time-window duration. If the input signal really is periodic (i.e. it is composed of the same ‘waveform’ during consecutive and contiguous time windows), the results of consecutive DFT calculations will be the same. If it is not, subsequent DFT calculations will yield different results^[6].

1.6.4 Computation of the DFT

If a computer program was set up to implement a 16-sample DFT, it would take as its input 16 complex numbers representing consecutive samples of the time-domain signal to be transformed. For each sample in turn, the program would perform the complex multiplication of that sample and the appropriate coefficient for the first output frequency; the results would be added together and stored. This would then be repeated for the remaining 15 output frequencies, giving the result: 16 stored complex numbers representing samples of the spectrum at different frequencies. It is important to note that each output sample has contributions from every one of the input samples.

This would require 162 (i.e. 256) multiplication operations and 16 additions. Multiplications are more time-consuming operations for a computer, and generally the relationship between the number of multiplications and the number of input or output samples is a square law. This can lead to excessive computing time for large numbers of samples, which is a fundamental shortcoming of the DFT when implemented on a computer. However, there is a significant amount of redundancy in this ‘long-hand’ computation, and algorithms have been developed to exploit this. Notwithstanding this, in some cases, multiplication speed is less of a problem than other processes, such as memory access, and specialized integrated circuits are available which are designed to implement DFTs.

It was noted earlier that the inverse Fourier transform uses an integral which is very similar to that of the (forward) Fourier transform, so it follows that the inverse DFT uses a summation which is very similar to that of the (forward) DFT. Also, if the input frequency-domain array, remains static for consecutive inverse DFT calculations, the time-domain result will be periodic over consecutive time windows. If the window duration is equal to, or an integer multiple of, the period of this result, then the result will be a sampled waveform free from discontinuities (i.e. glitches). For example, with a 1 ms window, sinusoidal waves at 1 kHz and harmonics (within the Nyquist limit) can be portrayed without discontinuities^[6].

1.6.5 The Fast Fourier Transform

The FFT is a particularly efficient algorithm for implementing the DFT. It increases the speed of processing by cutting down the number of multiplications from n^2 to $(n/2)\log_2(n)$, where n is the number of input or output samples, in cases where n is a power of 2. Thus, representing a 1536-carrier DAB signal by means of 2048 samples, an FFT would require 11264 multiplications, whereas a DFT would require more than 4 million. The number $\log_2(n)$ has a value of 11 for DAB, and can be called the index of the FFT (i.e. $2^{11} = 2048$).

The FFT can be derived from the DFT by expressing the summation using matrix arithmetic. All of the computations relating the values of the output samples to the input samples can be expressed in a two-dimensional matrix. Individual elements of this matrix can be broken down into consecutive stages of simpler arithmetic; that is, they can be

factorized, just as $x^2 + 3x + 2$ can be factorized into $(x + 1)(x + 2)$. The matrix, as a whole, can be factorized into a number of matrices containing simpler expressions, and when this process is taken as far as possible, the number of factored matrices is equal to the index.

This factorization process, sometimes referred to as ‘decimation’, introduces several simplifications; some expressions always return zeros or ones, so they need not be calculated, and some others have counterparts in the same matrix which yield the same result but with the opposite sign. The overall benefit is the reduction in the number of multiplications required. There are different approaches to decimation which yield the same overall result but with greater internal complexity towards either the time-domain or frequency-domain end of the chain of matrices; these are known as ‘decimation in time’ and ‘decimation in frequency’, respectively. ‘FFT’ is really a generic name for this type of algorithm and there are many variants, the main differences being in the paths taken through the factored matrices.

The FFT algorithm is commonly based on a radix of 2; that is, the numbers of input and output samples are equal to 2 raised to some power. A larger radix (e.g. 4, 8, etc.) is sometimes used for very large arrays of samples. In the simplest form of FFT, the frequency-domain samples appearing in its output array cover the same frequency range as the ‘parent’ DFT, but their arrangement is rather different. It was noted earlier that the useful samples output by a DFT cover the range $\pm f_s/2$, and it was implied that they are symmetrically disposed about 0 Hz. However, it was also noted that the spectrum is repeated, centered about harmonics of f_s , so the negative-frequency samples re-appear between $f_s/2$ and f_s ; the sample at exactly f_s is a replica of the sample at 0 Hz. By convention, it is the range 0 Hz to one sample below f_s which is represented in the output array of the FFT.

The inverse FFT can be derived from the inverse DFT in a similar way, and these comments apply equally to its input array of frequency-domain samples^[6].

1.6.6 Applications to DAB

The DAB system uses 1536 carriers in Mode 1. This requires a 2048-sample inverse FFT in the transmitter and a 2048-sample FFT in the receiver.

The way that an FFT is implemented in hardware depends on the required balance of

speed versus hardware complexity. Clearly, parallel processing should yield the greatest speed, whilst using several processes consecutively should reduce the amount of arithmetic hardware, although it may increase the requirement for temporary storage. For DAB, there are options which are more economical of hardware than using 2048 arithmetic devices in parallel, and more economical of processing speed than using one arithmetic device for all computations.

In the DAB channel encoder, the array of complex numbers representing the spectrum of the signal during each 1 ms symbol is applied to the inverse FFT which produces samples of the time-domain signal, for that symbol. These can be converted to analogue form, up-converted and transmitted. In this case, full parallel processing is not necessary because the time-domain samples need to be output consecutively, and not simultaneously, although all of the frequency-domain samples must be available for each computation.

In the DAB receiver, the frequency-domain spectrum is derived from the incoming time-domain signal, symbol by symbol, using the forward FFT. However, this signal appears via an ADC as a series of consecutive samples, so a mirror-image of this approach can be used. This will produce the spectrum for each symbol when all of the samples have been received, but computations can start when only a small number of time-domain samples are available; two, for example.

It might seem wasteful to have to use 2048 samples to represent the 1536 carriers, apparently wasting 512, but these can be put to good use by purposely setting their amplitudes to zero. This can be used in the encoder and the receiver to simulate a band-pass filter with an amplitude frequency response much steeper at the band edges than can be achieved using an analogue filter^[6].

1.6.7 Complex Numbers

The Fourier transform operates with complex numbers in both domains, and this applies to the DFT and FFT derived from it, and their inverses. Whilst it is usually necessary to consider components of a spectrum as complex, having amplitudes and phases, the waveform of a radio signal is purely real; simply the variation of a voltage with the passage of time. This is not to say that such a waveform could not be specified using complex quantities,

only that division of its specification into real and imaginary parts would require that they be combined in some way before the final waveform could be generated.

Essentially, the input and output arrays of the FFT can be divided into real and imaginary parts. When complex numbers are represented, each real sample has an imaginary sample associated with it. Conventionally in this field of engineering, the real and imaginary parts of the time-domain array (i.e. the input array of an FFT, or the output array of an inverse FFT) are referred to as the ‘I’ and ‘Q’ ports, for ‘In-phase’ and ‘Quadrature’, respectively^[6].

1.6.8 Negative Frequencies

It was noted earlier that, up to the Nyquist limit, the DFT and the FFT produce as many output samples as are input, but in each case, half of the frequency-domain samples represent negative frequencies. Real radio signals are usually thought of as using only positive frequencies, but the mathematically rigorous definitions of their spectra should include components at negative, as well as positive, frequencies. All of the transforms being discussed require these full definitions.

For example, the spectrum of a cosine wave with frequency f contains two positive impulse functions (i.e. lines in the spectrum) at plus and minus f , each multiplied by half the amplitude of the wave. Of course, by trigonometry $\cos(-x) = \cos(x)$, so this is no different from the simplified view of a single positive impulse function at plus f , having both halves of the amplitude. In this simplified view, the negative frequencies are effectively ‘folded’ about 0 Hz, over into the positive frequency range. The spectrum is slightly more complicated for a sine wave of frequency f , because $\sin(-x) = -\sin(x)$; the two impulse functions at $\pm f$ are each multiplied by half the amplitude but with opposite signs, the positive-frequency one having negative sign.

When such spectra are calculated using the FFT or DFT, where the input waveform is expressed as a purely real function of time (i.e. it is presented to the I port, and zero is presented to the Q port), the transform of the cosine wave is purely real whilst that of the sine wave is purely imaginary. This might be expected in view of the orthogonal relationships of cosine and sine waves, or real and imaginary numbers. It can be shown that

if a sine wave is expressed as a purely imaginary function (i.e. it is presented to the Q port, and zero is presented to the I port), the resulting transform is purely real.

It follows that for an inverse FFT to output a single sine or cosine wave, it must be presented with frequency-domain data for the negative-frequency component as well as for its positive-frequency counterpart, and the relationship between these data and their real/imaginary status must follow certain rules^[6].

1.6.9 Linearity of the transforms

At first sight, this would appear to imply that an N-sample FFT could only provide N/2 useful frequency-domain samples, so the 1536 carriers used by the DAB system would require the use of a 4096-sample FFT, and inverse. However, there is a simple way to halve this requirement by exploiting a useful property of the FFT and its forebears, that of linearity.

If two time-domain waveforms are added and the sum is transformed, the result is the sum of the two corresponding spectra. By reversing the sign of one of the input waveforms, the result is the difference between the two spectra. This property also applies, in reverse, to the inverse transforms.

Therefore, if a real cosine wave and an imaginary sine wave, of equal amplitudes and the same frequency f , are (complex) added and applied to an FFT, the result is one positive impulse function at minus f , at the real output port, multiplied by the amplitude of either wave; the positive-frequency component is cancelled. Since the two input waves are purely real and imaginary, respectively, the complex addition consists of no more than applying them simultaneously to the appropriate I and Q input ports. If the sign of the imaginary sine wave is reversed, the result is one positive-real impulse function at plus f , and the negative-frequency component is cancelled.

Combinations of two sine waves, or two cosine waves, do not cause cancellation of the second impulse function. An FFT would output a single impulse function as one sample, amongst many, having a non-zero value.

By the reverse argument, if a single positive-frequency sample is applied to the real input port of an inverse FFT, with a positive value, the time-domain result is a cosine wave at the I output port and a negative sine wave at the Q output port. The amplitudes of these

sampled time waveforms are equal and are proportional to the input sample value, and their frequencies correspond to the position of the sample in the input array. With a negative-value input sample, the result is a negative-real cosine wave and a positive-imaginary sine wave. These, and other permutations can be derived from the above table by reading right to left.

Thus, it is possible to use the negative-frequency samples of an inverse FFT, independently of their positive-frequency counterparts, to produce combinations of sine and cosine waves. What is then needed is a method for combining the sampled waves appearing at the I and Q output ports to produce the required single output signal, and this can be achieved using a quadrature modulation system^[6].

1.6.10 Combination of I and Q

The I and Q data are applied separately to a pair of DACs (or one, with time multiplexing) to produce a pair of sampled baseband signals, which are then applied to low-pass filters to construct analogue signals (i.e. to remove the artifacts of sampling). Note that these filters are not used to implement matched filtering (e.g. cosine roll-off), as is used in some other digital modulation systems; that function is effectively carried out by the inverse FFT and the FFT in the receiver.

The filtered baseband signals are applied to a pair of mixers (i.e. multipliers), which are also fed with synchronous local-oscillator signals having 90 degrees (i.e. $\pi/2$) phase difference; that is, cosine and sine waves. The local-oscillator frequency is equal to the desired centre-frequency of the final signal. The outputs of the two mixers are then added to give the final signal which, after band-pass filtering to remove harmonics and other imperfections, can be transmitted. This quadrature modulation system is illustrated in Fig 1.18.

Taking, again, the example of a single positive-frequency sample applied to the real input port of the inverse FFT, with a positive value, the baseband cosine wave in the I channel is multiplied by the cosine local-oscillator signal and the baseband negative sine wave in the Q channel is multiplied by the sine local-oscillator signal. Each multiplication produces sum and difference-frequency cosine components (i.e. double-sideband suppressed-carrier AM),

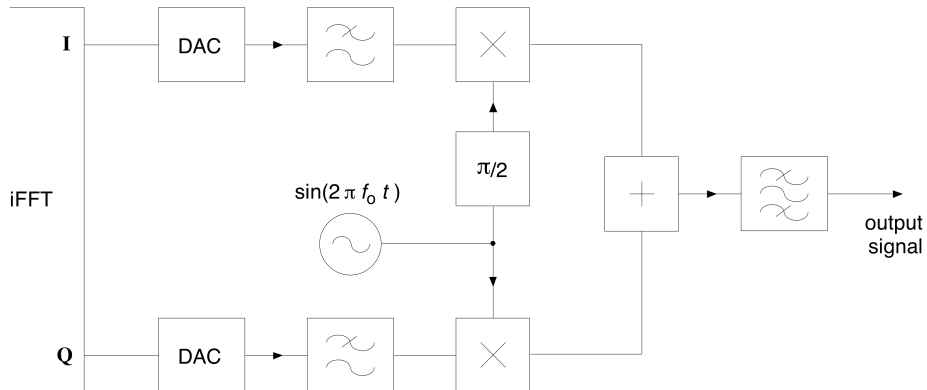


Figure 1.18: the quadrature modulation system

but in this case the difference-frequency components cancel when the mixer outputs are added. Thus, the final signal contains a single cosine wave at the local-oscillator frequency plus the baseband frequency.

In the channel encoder protocol, a 2048-sample inverse FFT is, indeed, used to produce the 1536-carrier Mode 1 signal. The computations are processed with a time- window duration of 1 ms, the symbol duration. Therefore, the frequency-domain sampling has an interval of 1 kHz, so adjacent input samples correspond to sinusoidal output waves separated by 1 kHz. Assuming conventional ordering of the input array, the first 1024 samples represent positive frequencies, from 0 Hz to 1023 kHz in the baseband signals. The 1024th sample represents ± 1024 kHz, which is at the Nyquist limit and is probably unusable. The remaining samples represent negative frequencies, from -1023 kHz to -1 kHz.

Of these, active data are applied to the 1536 surrounding 0 Hz; that is, those representing 1 kHz to 768 kHz and -1 kHz to -768 kHz, and static zeros are applied to the remainder. The inverse FFT then produces 2048 time-domain samples which are output to the DACs within 1 ms. Following up-conversion by the quadrature modulation system, carriers appear at frequencies from $f_0 - 768$ kHz to $f_0 + 768$ kHz.

The input data are changed from symbol to symbol giving the effect of QPSK modulated carriers. Of course, discontinuities occur when the signal is re-configured abruptly at the symbol boundaries, and this changes the fine detail of the spectrum. If the modulation data

are random, then over many symbols the power spectrum of each modulated carrier takes on a $(\sin f/f)^2$ distribution, as described in the main text.

In this approach, the sample which represents 0 Hz in the baseband signals is not used. If data were input to this sample, the corresponding I and Q output signals would be static (DC) voltages, and if the mixers in the quadrature modulation system could handle such signals, the output signal would be a wave at the local-oscillator frequency. However, the accuracy with which the phase of this wave could be controlled could be compromised by drifts in the DACs, and the mixers themselves, so this ‘zero carrier’ is not used to carry modulation.

The mirror image of this approach is used in the experimental DAB receivers, where the incoming signal is converted to an IF and band-pass filtered, and then applied to a similar quadrature modulation system. In this case, the local-oscillator frequency is the centre-frequency of the IF band and, of course, ADCs are substituted for the DACs.

What has been described is the approach that has been taken, so far, in all successive generations of experimental DAB transmitter equipment. However, it is worth noting that the FFT can be applied to multi-carrier signal generation and reception in other ways, some of which do not require the quadrature modulation system. Also, it is possible to implement a quadrature modulation system in the digital domain, rather than the analogue domain^[6].

1.6.11 Addition of the Guard Interval

It was noted earlier that if the frequency-domain data input to an inverse DFT remain static for consecutive time windows, then the time-domain result will be periodic over the consecutive windows, and this applies equally to the inverse FFT. In the DAB channel encoder, the window duration is equal to the active symbol duration, 1 ms in Mode 1, and the signals output by the transform are all sinusoidal waves at harmonics of 1 kHz, so they are periodic over whole multiples of the active symbol duration. Therefore, consecutive inverse FFT operations with the same input data would yield continuous waves in the baseband signals. For example, if the data were held static for two consecutive symbols, the waves would be continuous over 2 ms.

In the DAB receiver, in order to accomplish a single FFT operation, it would not matter

at what instant the time-window began as long as the input waves were continuous over 1 ms. A time displacement would only change the apparent phase of each of the waves, which would alter the absolute values of the data output by the FFT, but since the phase modulation is coded differentially, a slow change would not corrupt the decoded data. Thus, this example of an ‘oversized’ guard interval would permit time-agility in the receiver and the simultaneous reception of delayed signals as long as the limit of temporal coherence was not exceeded (i.e. the maximum vehicle speed would be limited further in this case).

Of course, there is no need to repeat the inverse FFT operation when the output samples can simply be stored, and read out to the DACs directly after the active symbol. Also, as noted in the main text, the DAB system actually uses the more-economical compromise of a $246 \mu\text{s}$ guard interval, so only about one quarter of the output samples need to be stored. According to available information, the samples making up the guard-interval appear to be applied to the DACs before each active symbol, so they are repetitions of the last quarter of those produced during the active symbol. This alternative arrangement does not imply additional storage, merely a re-ordering of the inverse FFT; either method is equally valid^[6].

1.7 Finite Impulse Response Filters(FIR)

These filters deserve attention since they are used several times during the implementation of the demodulator.

In signal processing, there are many instances in which an input signal to a system contains extra unnecessary content or additional noise which can degrade the quality of the desired portion. In such cases we may remove or filter out the useless samples.

1.7.1 How to characterize digital FIR filters

There are a few terms used to describe the behavior and performance of FIR filter including the following:

- Filter Coefficients : The set of constants, also called tap weights, used to multiply against delayed sample values. For an FIR filter, the filter coefficients are, by definition, the impulse response of the filter.

- Impulse Response : A filter's time domain output sequence when the input is an impulse. An impulse is a single unity-valued sample followed and preceded by zero-valued samples. For an FIR filter the impulse response of a FIR filter is the set of filter coefficients.
- Tap : The number of FIR taps, typically N, tells us a couple things about the filter. Most importantly it tells us the amount of memory needed, the number of calculations required, and the amount of "filtering" that it can do. Basically, the more taps in a filter results in better stopband attenuation (less of the part we want filtered out), less rippling (less variations in the passband), and steeper rolloff (a shorter transition between the passband and the stopband).
- Multiply-Accumulate (MAC) : In the context of FIR Filters, a "MAC" is the operation of multiplying a coefficient by the corresponding delayed data sample and accumulating the result. There is usually one MAC per tap.

There are a couple different basic filter responses. Each will have a unique frequency response based on its cut-off frequency, the number of taps used, its roll off, and amount of ripple. The various attributes describing a filter may be seen in the following diagram:

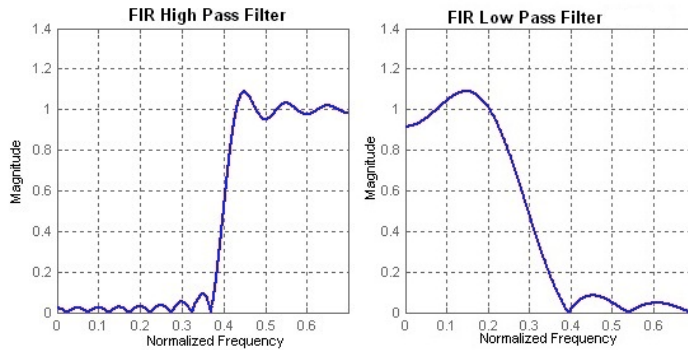


Figure 1.19: FIR filters

While high pass filters remove low frequency contents, low pass filters remove high frequency values. This kind of filters are used for synchronization and also for null symbol detection and automatic gain control. As we have seen before, these filters could be developed in software just updating properly the values for the filter coefficients^[13].

1.8 Error Measures

Some error detection measures were implemented for testing how precise was the system, such as BER and MER. These two measures are commonly used in digital modulation systems.

1.8.1 Bit Error Rate

This algorithm was implemented for measuring the accuracy of Viterbi decoding. Since the Viterbi algorithm has to recover the missing information during the transmission, it might be useful to know whether or not this information is reliable.

In digital transmission, the bit error rate or bit error ratio (BER) is the number of received bits that have been altered due to noise, interference and distortion, divided by the total number of transferred bits during the studied time interval. BER is a unitless performance measure, often expressed as a percentage number.

As an example, assume this transmitted bit sequence:

0 1 1 0 0 0 1 0 1 1,

and the following received bit sequence:

0 0 1 0 1 0 1 0 0 1,

The BER is in this case 3 incorrect bits divided by 10 transferred bits, resulting in a BER of 0.3 or 30%.

The bit error probability ρ_e is the expectation value of the BER. The BER can be considered as an approximate estimate of the bit error probability. This estimate is accurate for a long studied time interval and a high number of bit errors.

In a communication system, the receiver side BER may be affected by transmission channel noise, interference, distortion, bit synchronization problems, attenuation, wireless multipath fading, etc.

The BER may be improved by choosing a strong signal strength (unless this causes cross-talk and more bit errors), by choosing a slow and robust modulation scheme or line coding scheme, and by applying channel coding schemes such as redundant forward error correction codes.

The transmission BER is the number of detected bits that are incorrect before error correction, divided by the total number of transferred bits (including redundant error codes). The main problem of this algorithm is that the signal has to be decoded before^[14].

The implementation of this error measure algorithm was carried out in the following way:

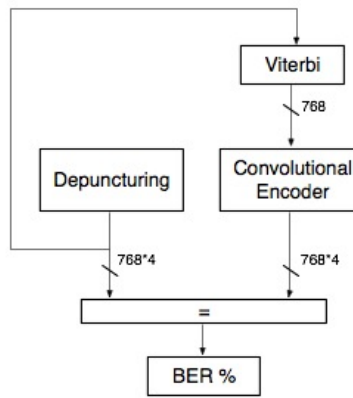


Figure 1.20: BER calculation

1.8.2 Modulation Error Rate

The aim of this algorithm is to check if the received data is good enough for ensure a good reception. The modulation error ratio or MER is a measure used to quantify the performance of a digital radio transmitter or receiver in a communications system using digital modulation. A signal sent by an ideal transmitter or received by a receiver would have all the constellation points precisely at the ideal locations, however various imperfections in the implementation (such as noise, low image rejection ratio, phase noise, carrier suppression, distortion, etc.) or signal path cause the actual constellation points to deviate from the ideal locations. Transmitter MER can be measured by specialized equipment, which demodulates the received signal in a similar way to how a real radio demodulator does it. Demodulated and detected signal can be used as a reasonably reliable estimate for the ideal

transmitted signal in MER calculation. It is defined in dB as:

$$MER(dB) = 10 * \log_{10} * \sqrt{P_{signal}/P_{error}}$$

where P_{signal} is the power of ideal transmitted signal, and P_{error} is the RMS power of the error vector. This value was around 29dB, and it is the typical MER figure quoted for digital radio systems, such as DAB^[?].

1.9 Errors Detection and Correction

1.9.1 Viterbi Decoder

In telecommunication, a convolutional code is a type of error-correcting code in which each m -bit information symbol (each m -bit string) to be encoded is transformed into an n -bit symbol, where m/n is the code rate ($n \geq m$) and the transformation is a function of the last k information symbols, where k is the constraint length of the code.

Convolutional codes are used extensively in numerous applications in order to achieve reliable data transfer, including digital video, radio, mobile communication, and satellite communication.

To convolutionally encode data, start with k memory registers, each holding 1 input bit. Unless otherwise specified, all memory registers start with a value of 0. The encoder has n modulo-2 adders and n generator polynomials - one for each adder (see figure 1.21 below). An input bit m_1 is fed into the leftmost register. Using the generator polynomials and the existing values in the remaining registers, the encoder outputs n bits. Now bit shift all register values to the right (m_1 moves to m_0 , m_0 moves to m_{-1}) and wait for the next input bit. If there are no remaining input bits, the encoder continues output until all registers have returned to the zero state.

The figure 1.21 below is an example of a convolutional encoder. $x(n)$ is the input and $G_0(n)$ and $G_1(n)$ are the encoded outputs. The rate of the convolution coder is defined as the number of input bits to output bits. This system has 1 input and 2 outputs thereby resulting in a coding rate of 1/2. The number of states of a convolution coder is determined

by its number of delay units. There are 2 delay units in this system and therefore, there are $2^2 = 4$ states. For a system with k delay units, there are 2^k states.

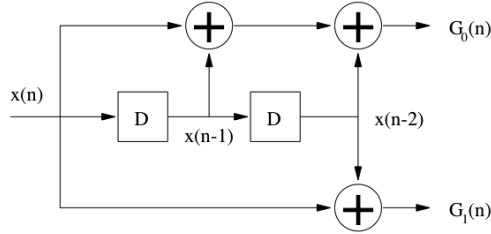


Figure 1.21: Convolutional Decoder

The system block diagram can be expressed with the following equations.

$$G_0(n) = x(n) + x(n - 1) + x(n - 2)$$

$$G_1(n) = x(n) + x(n - 2)$$

The state diagram of this system is depicted in Figure 1.22. The states are defined as $x(n - 1), x(n - 2)$ pairs and the state transitions are defined as $G_0(n), G_1(n)/x(n)$. The states are indicative of system memory. The state transitions gives you the path and the outputs associated with a given input. Since a state transition is associated with each possible input, the number of state transitions depends on the number of possible inputs. If there are m inputs, then there will be 2^m state transitions. The total number of state transitions at a point in time is the product of the number of state transitions and the number of states, 2^{m+k} .

The state diagram offers a complete description of the system. However, it shows only the instantaneous transitions. It does not illustrate how the states change in time. To include time in state transitions, a trellis diagram is used (Figure 1.23). Each node in the trellis diagram denotes a state at a point in time. The branches connecting the nodes denote the state transitions. Notice that the inputs are not labeled on the state transitions. They are implied since the input, $x(n)$, is included in the destination states, $x(n), x(n - 1)$. Another thing to note is that the state transitions are fixed by the definition of the source, $x(n - 1), x(n - 2)$, and the destination states. The state transitions are independent of the

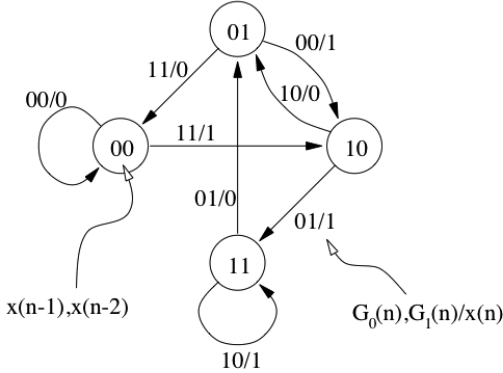


Figure 1.22: State Diagram

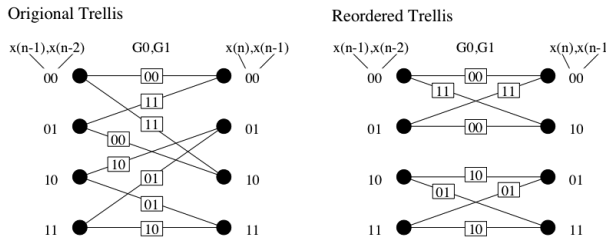


Figure 1.23: Trellis diagram

system equations. This a consequence of including the input, $x(n)$, in the state definition. In certain systems, definition of the states may be more complicated and may require special considerations. Explanation of such systems (such as the radix 4 trellis) is outside the scope of this example.

There are two trellis diagrams shown in Figure 1.23. They differ only in the way the destination states are ordered. The purpose for reordering is to obtain higher computational efficiency. The reordered trellis is partitioned into groups of states and state transitions that are isolated from other such groups. This allows realizable, specialized hardware to be designed that is dedicated to compute parameters associated with the particular group. The structure of the groups shown in Figure 1.23 is called the “butterfly” due to the physical resemblance. It is also referred to as the radix-2 trellis structure since each group contains 2 source and 2 destination states. Note, again, that the structure of the reordered trellis is fixed depending on how the states are defined. Not all trellis diagrams can be reordered

into butterflies. Fortunately, a number of commonly used convolution coders have this nice property.

An important feature of this convolution code is that in each butterfly, there are only two (out of four possible) distinct outputs: 00 and 11; or 01 and 10. Notice that the hamming distance of each output pairs is 2. This feature is available to a very small subset of all possible convolution codes. The usefulness of the this feature will be apparent later on when Viterbi decoding is described.

Figure 1.24 illustrates the entire process of encoding an input pattern to quantizing the received signal to decoding the quantized signal. The sample input pattern used is 1011010100. For the purpose of this example, this input pattern is sufficiently long. In practice, for proper error correction, the input pattern need to be longer than approximately 10 times the number of delay units plus 1, i.e. length of input pattern = $10(k + 1)$. ($k + 1$) is often referred to as the constraint length. For this example, $k = 2$ which implies 30 input symbols need to be received before decoding to improve the bit error rate.

The first trellis diagram in Figure 1.24 illustrates the state transitions associated with each input. This trellis diagram is used here to illustrate how the decoder operates. Use Figure 1.23 to verify the state transitions and the encoder outputs. The encoder outputs do not have to be generated using the trellis diagram. They can be generated using the system equations directly.

The encoded outputs are transmitted as signed antipodal analog signals (i.e. 0 is transmitted with a positive voltage and 1 is transmitted with a negative voltage). They are received at the decoder and quantized with a 3-bit quantizer. The quantized number is represented in 2's complement giving it a range of -4 to 3. Soft decision offers better performance results since it provides a better estimate of the noise (i.e. less quantization noise is introduced). In most circumstances, the noise is strong enough just to tip the signal over the decision boundary. If hard decision is used, a significant amount of quantization noise will be introduced. The quantized soft decision values are used to calculate the parameters for the Viterbi decoder.

Up to this point, no Viterbi decoding has been performed. Viterbi decoding begins after a certain number of encoded symbols have been received. This length, again, is usually

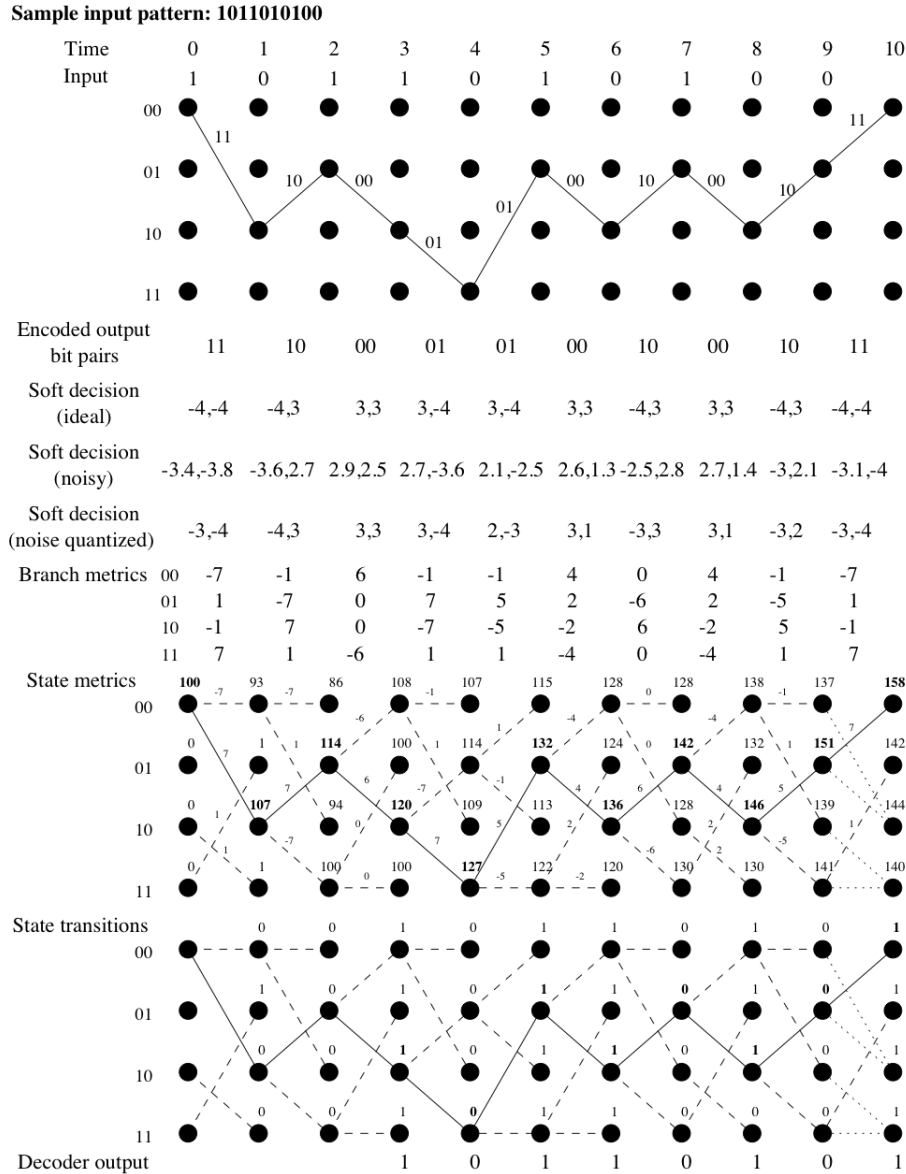


Figure 1.24: Trellis diagram states

longer than $10(k + 1)$ and is application dependent. In this example, 20 encoded symbols are received before being decoded. In some applications, Viterbi decoding is operated on a frame of received symbols and is independent of the neighboring frames. It is also possible to perform Viterbi decoding on a sliding window in which a block of decoded bits at the beginning of the window is error free, and the windows will have to overlap. With frame by frame decoding, a number of trailing zeros equalling to the number of states is added. This forces the last state of the frame to be zero providing a starting point for traceback. With sliding window decoding, the starting point for traceback is the state with the optimal accumulated metric. This starting state may be erroneous. However, the traceback path will converge to the correct states before reaching the block of error free bits.

Viterbi decoding can be broken down into two major operations, metric update and traceback. In metric update, two things are done in every symbol interval (1 symbol = 1 input bit = 2 encoded bits): the accumulated (state) metric is calculated for each state and the optimal incoming path associated with each state is determined. Traceback uses this information to derive an optimal path through the trellis. Referring to the second trellis in Figure 1.24, notice that a state at any time instance has exactly one incoming path but the number of outgoing paths may vary. This results in a unique path tracing backward.

What are state metrics and how are the optimal incoming paths determined? To understand the metrics used in Viterbi decoding, consider the received encoded bit pairs, $(G0(n), G1(n))$. Suppose 11 is transmitted, we would expect 11 to be received with a soft decision pair of (-4,-4). However, channel noise may corrupt the transmitted signal such that the soft decision pair may be (-0.4,-3.3) resulting in a quantized value of (0,-3) (see Figure 1.25). Without knowing anything about the encoded bit stream, the detector would decide that (3,-4) or 01 is transmitted which results in a bit error.

The Viterbi algorithm, on the other hand, exploits the structure of the convolution code and makes its decision based on previously received data (i.e. this is kept track of using the “states”). Referring back to Figure 1.23, observe that an encoded bit pair is associated with only 2 possible originating states, $x(n-1), x(n-2)$. For example, if 11 is transmitted, then the originating state must be either state 00 or state 01 (see Figure 1.23). Suppose that the original state is known to be 00, then it would be impossible for the detected encoded bit

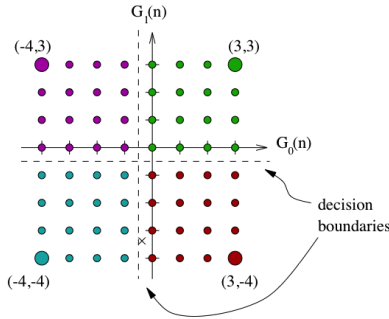


Figure 1.25: Decision boundaries.

pairs to be 01. The Viterbi decoder would then have to decide between the two possible encoded bit pairs, 00 or 11. This decision depends on how far away the received bit pairs are from the two possible transmitted bit pairs (Figure 1.26). The metric used to measure this is the Euclidean distance. It is also referred to as the local distance calculation.

$$\text{local distance}(n, i) = \sum_j [S_j(n) - G_j(n)]^2, j \in \text{encoded bits associated with a given input}$$

where n denotes the time instance and i denotes the path calculated for. The above equation can be further simplified by observing the expansion:

$$\text{local distance}(n, i) = \sum_j [S_j^2(n) - 2S_j(n)G_j(n) + G_j^2(n)]$$

and noting that $S_j^2(n)$ and $G_j^2(n)$ are constants in a given symbol period. These terms can be ignored since we are concerned with finding the minimum local distance path. The following measure will suffice for determining the local distance: Note that the -2 is taken out which implies

$$\text{local distance}_1(n, i) = \sum_j [S_j(n) - G_j(n)]$$

that instead of finding the path with the minimum local distance, we would look for the path with the maximum $\text{local distance}_1(n, i)$.

Going back to Figure 1.24, the branch metrics can now be calculated using the above

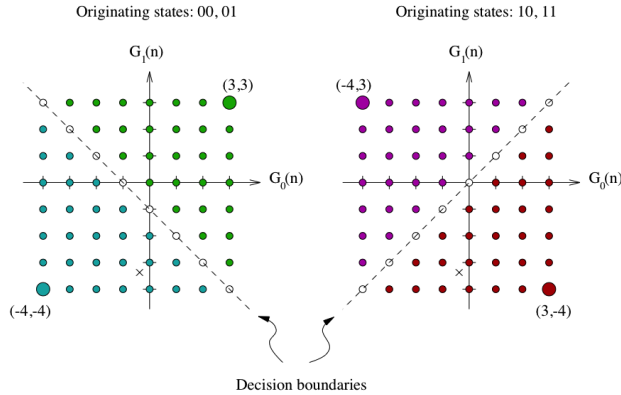


Figure 1.26: Decision boundaries for different states.

local distance equation. As an example, the branch metrics for time 0 and 1 is calculated here. The received quantized soft decision pair is $(-3, -4)$. The branch metric corresponding to $(G_0(n), G_1(n)) = (0, 0)$ is equal to $-3(1) - 4(1) = -7$. For $(G_0(n), G_1(n)) = (0, 1)$, it is $-3(1) - 4(-1) = 1$. For $(G_0(n), G_1(n)) = (1, 0)$, it is $-3(-1) - 4(1) = -1$. And for $(G_0(n), G_1(n)) = (1, 1)$, it is $-3(-1) - 4(-1) = 7$. Notice that the $G_j(n)$'s used in the local distance calculation are +1 and -1, rather than +3 and -4 respectively. There are three reasons. First, using unities makes computation very simple. The branch metrics can be calculated by adding and subtracting the soft decision values. Second, 3 and -4 can be scaled to approximately 1 and -1 respectively. As mentioned in the derivation of local distance 1, constant scaling can be ignored in determining the maxima and the minima. Finally, note that there are only two unique metric magnitudes, 1 and 7. Therefore, to compute the branch metric, you only need to do 1 add, 1 subtract, and 2 negation.

Once the branch metrics are calculated, the state metrics and the best incoming paths for each destination states can be determined. The state metrics at time 0 are initialized to 0 except for state 00, which takes on the value of 100. This value is arbitrarily chosen and is large enough so that the other initial states cannot contribute to the best path. This basically forces the traceback to converge on state 00 at time 0.

The state metrics are updated in two steps. First, for each of the two incoming paths, the corresponding branch metric is added to the state metric of the originating state. The two sums are compared and the larger one is stored as the new state metric and the cor-

responding path is stored as the best path. Take state 10 at time instance 2 for example Figure 1.24. The two paths coming in to this state originates from states 00 and 01 figure 1.23 Looking at the second trellis, we see that state 00 has a value of 93 and state 01 has a value of 1. The branch metric of the top path (connecting state 00 at time 1 and state 10 at time 2) is 1. The branch metric of the bottom path (between states 01 and 10) is -1. The top path gives a sum of $93 + 1 = 94$ and the bottom path give a sum of $1 + (-1) = 0$. As a result, 94 is stored as the state metric for state 10 at time 2 and the top path is stored as the best path in the transition buffer.

The transition buffer stores the best incoming path for each state. For a radix 2 trellis, only 1 bit is needed to indicate the chosen path. A value of 0 indicates that the top incoming path of the given state is chosen as the best path whereas a value of 1 indicates that the bottom path is chosen. The transition bits for our example is illustrated in Figure 1.24 in the third trellis.

Traceback begins after completing the metric update of the last symbol in the frame. For frame by frame Viterbi decoding, all that is needed by the traceback algorithm are the state transitions. The starting state is state 00. For sliding window decoding, the starting state is the state with the largest state metric. In our example, the starting state for both types of decoding is 00 since it has the largest state metric, 158. Looking at the state transition for state 00, we see that the bottom path is optimal (state transition = 1 implies bottom path). Two things now happen. First, the transition bit, 1, is sent to the decoder output. Second, the originating state, state 01, of this optimal path is determined. This process is repeated until time 2, which corresponds to the first input bit transmitted.

The decoded output is shown in Figure 1.24 in the last row. Notice that the order with which the decoded output is generated is reversed, i.e. decoded output = 10101101 whereas the sample input pattern is 10110101. Additional code need to be added to reverse the ordering of the decoded output to exactly reconstruct the sample input^[11].

1.9.2 De-puncturing

The addition of redundancy to the signal increments the data bandwidth in a 400%. To palliate this effect some bits of the outgoing signal are removed. Puncturing is the process

of removing some of the parity bits after encoding with an error correction-code. This has the same effect as encoding with an error-correction code with a higher rate, or less redundancy. However, with puncturing the same decoder can be used regardless of how many bits have been punctured, thus puncturing considerably increases the flexibility of the system without significantly increasing its complexity. In DAB, a pre-defined pattern of puncturing is used in the encoder. The inverse operation, known as depuncturing, is implemented by the decoder^[10].

If the code-word which results from puncturing is identical to that produced by a dedicated non-punctured encoder of the same rate, there is no loss of error correction performance. However, if a large range of different rates are required in practice, puncturing can cause a slight loss of performance relative to a non-punctured code of the same rate; this depends on the choice of generator polynomials and which bits are punctured.

1.10 Digital Signals Processors (DSP)

Traditionally, during the analog era, the common way to design a radio receptor was to design a very specific circuit with analog electronic components like operational amplifiers, resistances, capacitances, inductances, and so on. Everything was done in hardware. Due to advances in both computer and semiconductor technology, today we can replace that old-fashioned complicated circuitry by an embedded computer which is much cheaper and more reliable. The aim of these computers is to achieve the required performance while maintaining costs at a minimum price. Often, as in the case of this project, the energy consumption and heat dissipation must be taken into account very carefully, since the final demodulator will work with batteries and typically, no fan is available on a portable device.

In the context of telecommunications, these embedded processor are used to operate on digital signals, hence the acronym of DSP (Digital Signal Processors). Typically, algorithms for signal processing share a lot of features among them, and a specific algorithm will be used massively during the demodulation process. For example, for sure any algorithm for audio or video processing will perform the Fast Fourier Transform (FFT) on the input signal. Another common algorithm is the Viterbi decoder for the detection and correction of

errors. Another typical requirement for a DSP is that it cannot spend more than a certain amount of time to manipulate the input signal, that is, they must run in real time. As we shall see more deeply below, in DAB, the broadcaster transmits an audio frame each 96ms, therefore our DSP must be capable of processing the signal (that is, extract the audio) in less than this time. Otherwise, part of the audio will be missed. For this reason, a DSP has specialized hardware not available in a general purpose computer to perform such common tasks. All these constraints is what makes Digital Signal Processing a very motivating and interesting field of study. Figure 1.27 illustrates the abstract architecture used for any digital signal application^[12].



Figure 1.27: Electromagnetic signal to audio.

Chapter 2

CoolFlux BSP Architecture

2.1 Overview

The CoolFlux BSP is a general-purpose high precision, ultra low power, low cost dual Harvard, dual MAC BSP that has extensive support for fractional arithmetic as well as highly efficient support for the data types and operations encountered within ANSI C. In addition, CoolFlux BSP supports complex arithmetic, sub-word parallelism and larger addressing space.

The CoolFlux BSP is capable of sustaining two MACs, two memory operations and two pointer updates per cycle, making it highly cycle- efficient for computationally intensive applications. Many of the arithmetic operations ,Ãì such as the multiplication, additions, division etc - can be done in scalar mode or in packed mode. Packed mode can either be a complex operation or an SIMD operation. This makes it possible for instance to do four 12-bit multiplications in parallel.

The CoolFlux BSP architecture is a load/store architecture, that is:

- All memory operands have to be explicitly moved to the registers.
- All execution units take their input values from registers and write their results back into a register.
- All results produced in the registers have to be explicitly moved to memory.

Because of its Instruction Set Architecture design the CoolFlux BSP is also highly efficient at supporting control code as well, making it very well balanced for complete embedded applications in which 20/80 (80% of the time is spent for 20% of instructions) code mix is typical. When designing the CoolFlux BSP at the level of its micro-architecture, much attention has been paid to efficiently support the operations needed by ANSI C, making the CoolFlux BSP an excellent compiler target whilst maintaining very low power consumption^[18].

2.2 Registers

The CoolFlux BSP is a load/store architecture, making registers important. All execution units take their inputs from registers and write their results back to registers. Memory accesses are considered to be operations. A store operation takes the data from a register and writes it to memory, while a load operation reads a value from memory and stores it in a register.

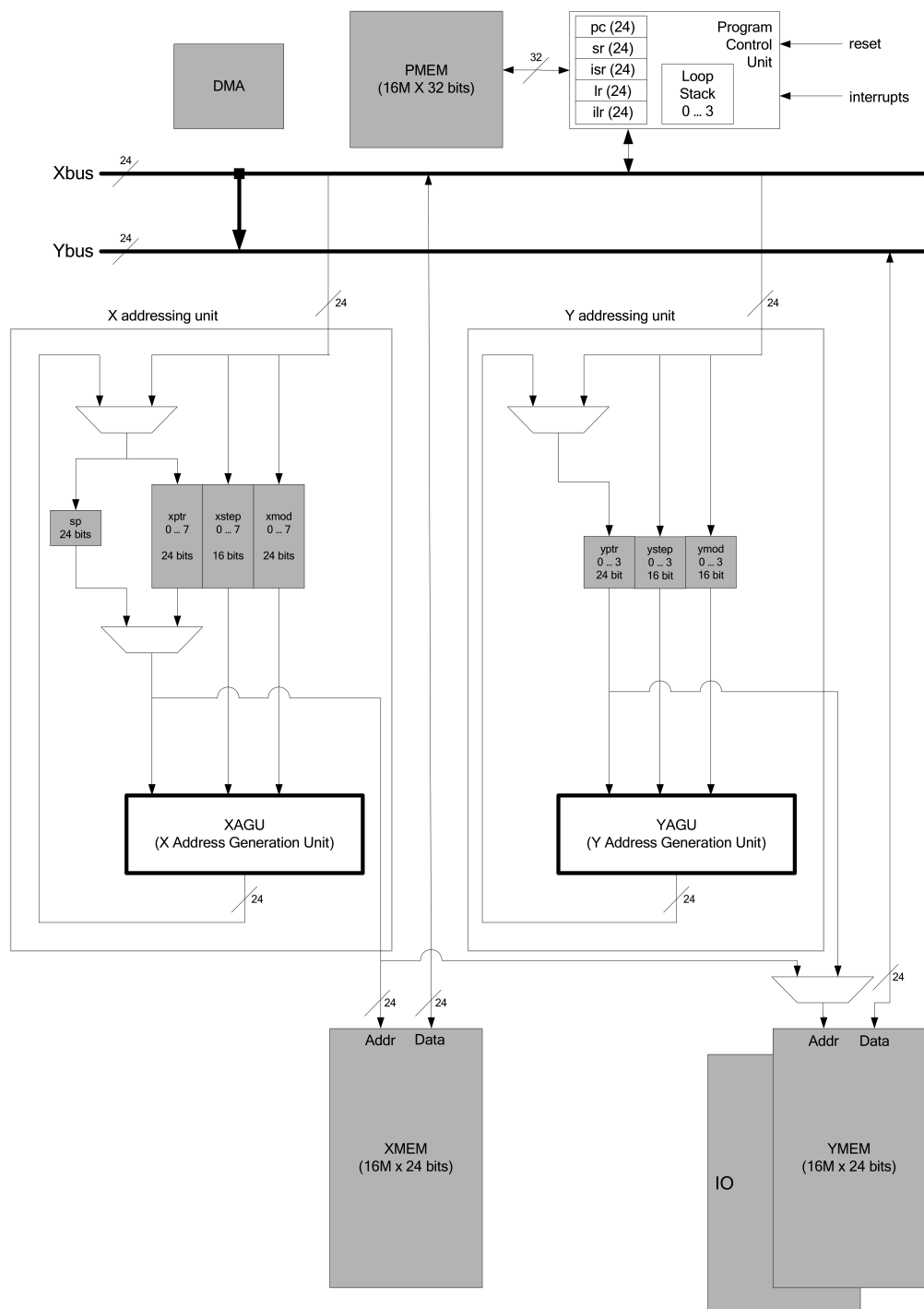
The registers of the CoolFlux BSP are organized in register files. All registers in a register file have the same name but a different index. Operations work on individual registers, but in their syntax description register file names are used. The reason is that all registers in a register file can be used equally in an operation. Individual registers must be used as source and destination registers in real operations.

The registers have different data widths. The architecture figures presented above show the data widths of the registers. They also show how the register files are connected to the different execution units^[18].

2.3 The Data Path

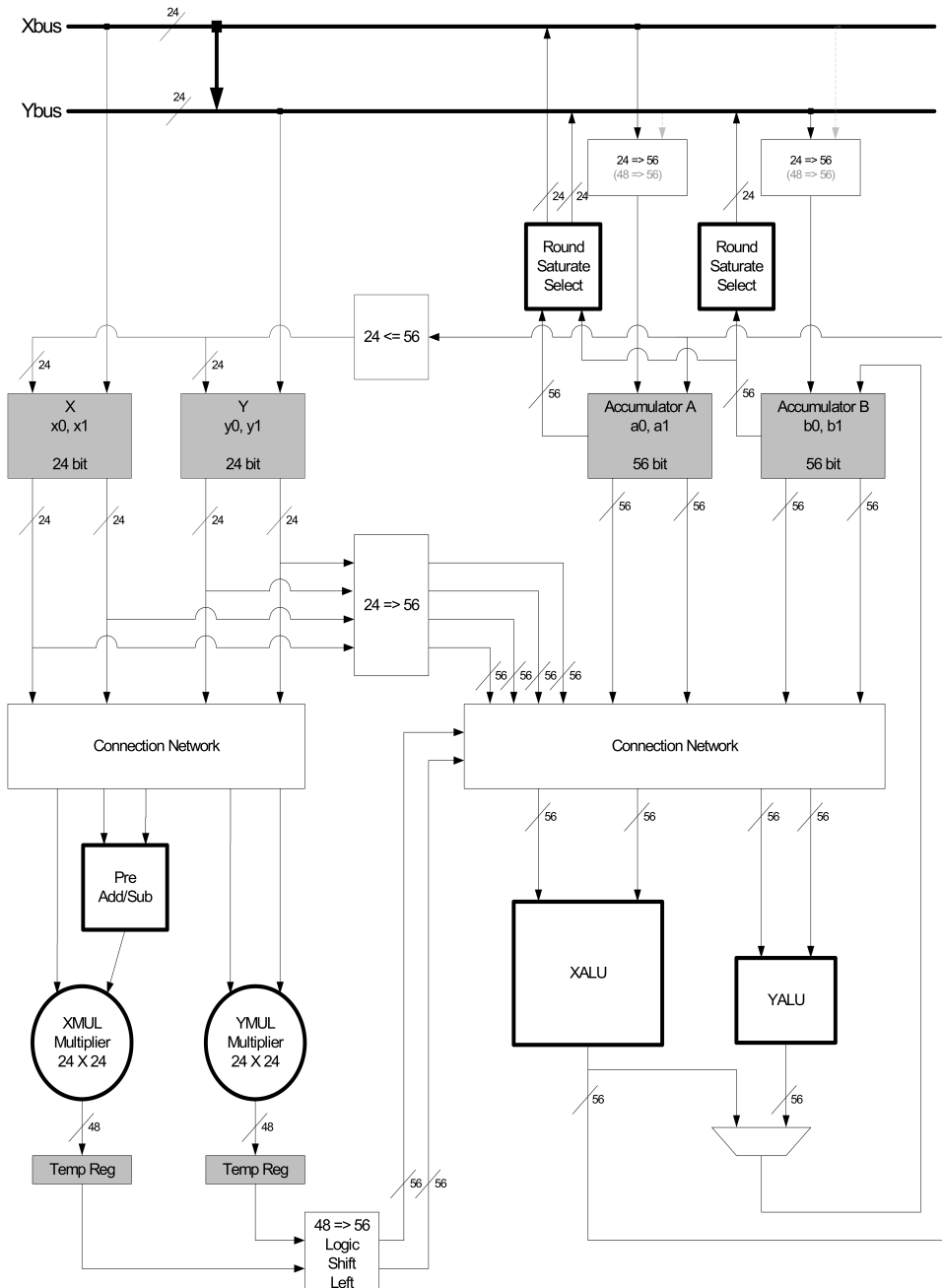
The data path consists of:

- Four register files A, B, X and Y connected to the arithmetic units
- Two multiplier units XMUL and YMUL (24x24 bits), which can be used in different



Addressing units, Xbus and Ybus move buses, memories, DMA and program control unit

Figure 2.1: Addressing Units. Xbus and Ybus move buses, DMA and program control units



Data path, RSS units and Xbus and Ybus move buses

Figure 2.2: step function

ways (signed, unsigned, complex, SIMD multiplication) with a pre-add/subtract unit before the XMUL multiplier

- Two ALU units XALU and YALU: The XALU executes single arithmetic and XMAC operations and the YALU executes parallel arithmetic and YMAC operations

2.3.1 Multipliers

The CoolFlux BSP contains 2 multiply units, XMUL and YMUL. The both have two inputs of 24 bits. They read their operands from the X and Y register files. The XMUL can be used for signed/signed, unsigned/signed, unsigned/unsigned, complex and SIMD multiplications. The YMUL supports signed/signed, complex and SIMD multiplications.

When doing a complex multiplication, the inputs are considered to contain an imaginary part and a real part, both 12 bits. A complex multiplication does the following actions:

$$\begin{aligned} \text{output_imag} &= \text{input_a_real} * \text{input_b_imag} + \text{input_a_imag} * \text{input_b_real} \\ \text{output_real} &= \text{input_a_real} * \text{input_b_real} - \text{input_a_imag} * \text{input_b_imag} \end{aligned}$$

It is also possible to get the following different intermediate results.

$$\begin{aligned} \text{output_imag} &= r \text{ input_a_real} * \text{input_b_imag} \\ \text{output_real} &= r \text{ input_a_real} * \text{input_b_real} \\ \text{output_imag} &= \text{input_a_imag} * \text{input_b_real} \\ \text{output_real} &= -\text{input_a_imag} * \text{input_b_imag} \end{aligned}$$

When doing an SIMD multiplication, the inputs are considered to contain two subparts of 12 bits each. A SIMD multiplication does the following actions:

$$\begin{aligned} \text{output_SIMD0} &= \text{input_a_SIMD0} * \text{input_b_SIMD0} \\ \text{output_SIMD1} &= \text{input_a_SIMD1} * \text{input_b_SIMD1} \end{aligned}$$

The XMUL unit is preceded by a pre-adder/subtraction unit. This unit can be used in 3 modes: pass, add and subtract. For simple multiplications it is used in pass mode where it just transfers one of its inputs to the output without doing any operation, this output is then multiplied in the XMUL unit to another XY register. In case it is used in add (or subtract) mode, it adds (subtracts) two XY registers and this output is then multiplied

with a third XY register. This pre-adder/subtraction unit is not used in complex or SIMD mode.

In all cases, the result of a multiplication is a full 48-bit number. Before being used in the ALUs it is converted to a 56-bit number. This 56-bit value is stored in a temporary register and in the next processor cycle used as an operand for accumulation through one of the ALU units (XALU for results of XMUL, YALU for results of YMUL).

The multipliers are always accessed via MAC operations (multiply accumulate), which take 2 processor cycles to complete. In the first cycle the multiplication is performed on XMUL or YMUL. In the second cycle the result is accumulated through the XALU or YALU units. Each processor cycle a new MAC operation can be started for which the multiplication runs in parallel with the accumulation of the previous MAC operation. This means that n consecutive MAC operations only take $n+1$ processor cycles to complete^[18].

2.3.2 Arithmetic and Logic Units (XALU and YALU)

The XALU and the YALU always operate on 56-bit operands, and generate 56-bit results. They take their inputs from the A, B, X and Y register files or from the temporary registers at the outputs of the multipliers. All these inputs are converted to 56 bits. The result of the XALU can be stored in the A, B, X and Y registers; the result of the YALU can be stored in a B register. The result is converted to 24 bits when it is written to an X or Y register.

The possible operations in scalar mode for XALU are:

- Add, subtract, (add and divide by 2), (subtract and divide by 2), reduced add, reduced subtract
- Logic and, logic or, logic xor
- Divide step
- Min, max
- Negate, exponent, absolute value, sign extend
- Logic and arithmetic shift, reduced shift

- Compare operations
- Load immediate value

Additionally, some of these operations can be made conditional. The YALU supports: add, subtract, (add and divide by 2), (subtract and divide by 2).

- In packed operation, the XALU can perform the following operations:
 - Add, subtract, (add and divide by 2), (subtract and divide by 2)
 - Divide step Absolute value
 - Compare operation
 - Logic and arithmetic shift
 - Conjugate operation
 - Packing operation
 - Unpacking operation
 - Conditional negate operation

Note that for all these operations, the result is the same, regardless of whether the operation SIMD or a complex operation^[18].

2.4 Move Buses and RSS Units

2.4.1 Xbus and Ybus Move Buses

Moves between the registers, and also between the memories and the registers are essential because of the load/store architecture of the CoolFlux BSP.

Two central buses are provided to move the data, in parallel with the operations in the data path. These buses provide a connection between all registers, and between all registers and the memories and support the move of data:

- from a source register to a destination register

- from a source register to a memory (store)
- from the memories to a destination register (load)

The buses support single and parallel moves. In a single move operation a single 24-bit data item is moved in a single processor cycle. With a parallel move operation two 24-bit data items are moved in a single processor cycle by using the two buses at the same time. In each move the source value is converted from its data width to a 24-bit value. This 24-bit value is transferred to the destination register, via the move buses, where it is converted to the destination data width. The way the conversions are done, depends whether the move is a scalar or packed move. The 24-bit buses are wide enough to make all 8-bit, 15-bit, 16-bit and 24-bit register and memory moves straightforward, but transferring from and to a 56-bit accumulator requires special attention^[18].

2.4.2 Moving to an Accumulator

The accumulator can be the destination of a move operation in 2 ways:

The full accumulator is the destination (a0, a1, b0, b1) An accumulator sub-register is the destination (ao0, ao1, ah0, ah1, al0, al1, bo0, bo1, bh0, bh1, bl0, bl1)

In case a sub-register is the target, its data width is either 8 or 24. So the conversion from 24 bits to the target data width is straightforward (the 8 LSBs are used, or no conversion is needed).

The full accumulator can be the destination in 4 ways:

- a 24 bit scalar move
- a 48 bit scalar move a 24 bit packed move
- a 48 bit packed move

In a 24-bit scalar move ('=' assignment), the 24 bit value is converted to 56 bits by sign extending the upper 8 bits and padding with 24 zeros at the LSB side. In a 48-bit scalar move ('=l' assignment), the Xbus and Ybus move buses are combined to move a 48-bit value. This 48-bit value is converted to 56 bits by sign-extending it with 8 bits. A 48-bit

move operation is only possible between two accumulators, or from the XY- memory to one of the accumulators.

In a 24-bit packed move ('=.c' assignment), the 24 bit value is split into two 12-bit sub-words. When converting to 56 bits, each 12 bit sub-word is converted to a 28-bit accumulator sub-word. This is done by sign extending the upper 4 bits and padding with 12 zeros at the LSB side. The 56-bit accumulator is then made by concatenating both sub-words.

$$\text{accumulator}(55 - 52) = \text{input}(23) \& \text{input}(23) \& \text{input}(23) \& \text{input}(23)$$

$$\text{accumulator}(51 - 40) = \text{input}(23 - 12)$$

$$\text{accumulator}(39 - 28) = 0$$

$$\text{accumulator}(27 - 24) = \text{input}(11) \& \text{input}(11) \& \text{input}(11) \& \text{input}(11)$$

$$\text{accumulator}(23 - 12) = \text{input}(11 - 0)$$

$$\text{accumulator}(11 - 0) = 0$$

In a 48-bit packed move ('=.cl' assignment), the Xbus and Ybus move buses are combined to move a 48-bit value. This 48-bit value is converted to 56 bits by sign-extending each of the 24-bit sub-words with 4 bits. A 48-bit move operation is only possible between two accumulators, or from the XY-memory to one of the accumulators^[18].

$$\text{accumulator}(55 - 52) = \text{input}(47) \& \text{input}(47) \& \text{input}(47) \& \text{input}(47)$$

$$\text{accumulator}(51 - 28) = \text{input}(47 - 24)$$

$$\text{accumulator}(27 - 24) = \text{input}(23) \& \text{input}(23) \& \text{input}(23) \& \text{input}(23)$$

$$\text{accumulator}(23 - 0) = \text{input}(23 - 0)$$

2.4.3 Moving from an Accumulator

The accumulator can be the source of a move operation in 2 ways: as a full accumulator (a0, a1, b0, b1) through one of its sub-registers (ao0, ao1, ah0, ah1, al0, al1, bo0, bo1, bh0, bh1, bl0, bl1)

In the case a sub-register is the source of a move operation, the data width is either 8 or 24. So the conversion to 24 bits is straightforward (sign-extension with 16 bits, or

no conversion). The selection of the correct sub-register (with eventual sign extension) is performed by the select part of an RSS unit.

A full accumulator can be the source of a move operation in 4 ways:

- a 24-bit scalar move
- a 48-bit scalar move
- a 24-bit packed move
- a 48-bit packed move

In 24-bit scalar move ('=' assignment), the 56-bit value is converted to 24 bits through the round and saturate part of the RSS unit and transferred to the destination register via one of the two move buses.

In a 48-bit scalar move ('=.l' assignment), the Xbus and Ybus move buses are combined to move a 48-bit value in a single processor cycle. The 56-bit source value is converted to 48 bits through the saturation logic of the RSS unit. A 48-bit scalar move operation is only possible between two accumulators, or from one of the accumulators to the XY- memory.

In a 24-bit packed move ('=.c' assignment), the 56-bit value is converted to 24 bits through the round and saturate part of the RSS unit and transferred to the destination register via one of the two move buses. In this packed move, both 28-bit sub-words will go through the round and saturate part of the RSS unit and become two 12-bit sub- words.

In a 48-bit packed move ('=.cl' assignment), the Xbus and Ybus move buses are combined to move a 48-bit value in a single processor cycle. The 56-bit source value is converted to 48 bits through the saturation logic of the RSS unit. In this packed move, both 28-bit sub-words will go through the saturation logic of the RSS unit and become two 24-bit sub-words. A 48-bit packed move operation is only possible between two accumulators, or from one of the accumulators to the XY-memory^[18].

2.4.4 Round, Saturate and Select Units (RSS)

The CoolFlux BSP has two round, saturate and select units (RSS), one for the A accumulators and one for the B accumulators. They convert between values held in 56- bit precision

in the accumulators and the precision of a particular move operation (24-bit or 48-bit) and are used when a 56-bit accumulator is the source of a move operation (scalar or packed), as described above. In case a sub-register is used as source, the RSS unit will select the correct part (overflow, high, low) of the accumulator and no actual conversion is done. In case the full accumulator is the source, its value needs to be converted from 56 bits to 24 or 48 bits which requires saturation and rounding. Both are handled by the RSS units which can operate in different modes.

The modes for the rounding are:

- truncation, simple biased
- truncation, sign-magnitude
- rounding, simple biased
- balanced-bias rounding

The modes for the saturation are:

- saturation
- wrapping

The rounding and saturation is done on the entire word or on the two sub-words, depending on the type of move (scalar or packed). The way the rounding and saturation works, however, is exactly the same^[18].

The mode of operation is equal for both RSS units and is controlled by setting and clearing the sr.b, sr.r and sr.s bits in the sr status register. The assignment operator determines which conversion (24 or 48 bit, scalar or packed) must be executed:

- = 24-bit scalar move
- =.l 48-bit scalar move
- =.c 24-bit packed move
- =.cl 48-bit packed move

2.5 Memories and I/O

The CoolFlux BSP is a dual Harvard architecture and has separate X and Y data memories. Each memory has 16 Mword of 24 bits. In a single processor cycle each memory can be accessed separately so that up to 2 data items can be read or written in a single cycle. There is a special mode in which the X and Y memories are combined logically into a single XY memory that stores and loads 48-bit data items.

Next to the data memories the I/O of the CoolFlux BSP is memory mapped. Also the I/O-space has 16 Mword of 24 bits. From a software point of view, I/O behaves as a memory to which data can be written and from which data can be read^[18].

2.5.1 Individual Data Memory (X, Y)

The CoolFlux BSP has 2 separate 16 Mword, 24 bit X and Y data memories. Typically accesses to both memories are used in parallel for intense BSP code so as to provide sufficient memory bandwidth for the computations being performed^[18].

2.5.2 Dual Precision Memory (XY)

There are dual precision load and store instructions, which can move a single 48-bit data item (long) to and from the memory sub-system. For these instructions both X and Y memories, and both Xbus and Ybus move buses are combined (used in parallel). In the memory the corresponding locations in both X and Y memory need to be reserved since, in this mode, both memories get the same address. This memory is referenced as XY-memory. It uses the X addressing unit for addressing and has the same addressing possibilities as the X-memory^[18].

2.5.3 I/O Memory Space

The I/O for the CoolFlux BSP is memory mapped. I/O-space is 16 Mwords, 24-bit wide. The I/O memory space can be addressed as the Y-memory space, using the Y addressing unit to generate its addresses^[18].

2.6 X and Y Addressing Units

The X and Y addressing units generate the addresses for the memory accesses. The following addressing modes are supported:

- direct addressing
- indirect addressing with post-modification
- indexed stack pointer addressing

Indirect addressing is supported by means of 2 pointer register files: XPTR, YPTR. These are located in the addressing units. The XPTR register file contains 8 pointers (xptr0 ... xptr7); the YPTR register file contains 4 pointers (yptr0 ... yptr3). When the memories are accessed indirectly via one of these pointers, the pointer value can be updated (post-modified) in parallel with the access. The calculations for this update are executed on the XAGU and YAGU, the address generation units. The post-modification operation is specified as part of the memory access. These operations use the registers in the other register files: XSTEP, YSTEP, XMOD and YMOD. The possible post-modification operations are:

- nop
- increment
- indexed stack pointer addressing
- decrement
- increment by 2
- decrement by 2
- add the step register
- subtract the step register
- and a special mode which is used for cyclic buffer addressing and bit-reverse addressing.

Besides the update operations that are part of the indirect addressing syntax, there are a number of specific pointer operations that are executed on the XAGU and YAGU. The operations that execute on the XAGU and YAGU are executed in parallel with the move operations on the Xbus and Ybus move buses, the accesses to memory, and the operations on the data path (XMUL, YMUL, XALU and YALU)^[18].

2.6.1 Indexed Stack Pointer Addressing

The X addressing unit contains a stack-pointer sp. This stack-pointer gives full stack support for the X-memory. The indexed stack pointer addressing mode implements indexed indirect addressing using the stack pointer as the base pointer, meaning that the address is calculated using an offset with respect to the stack pointer. In this operation the stack pointer is not automatically updated. A full range of operations is provided for updating the stack pointer.

A number of operations allow moving all registers efficiently from and to the stack^[18].

2.6.2 Indexed Pointer Addressing

The indexed pointer addressing mode implements indexed indirect addressing using the a pointer as the base pointer, meaning that the address is calculated using an offset with respect to this pointer. In this operation the pointer is not automatically updated. A full range of operations is provided for updating the pointers^[18].

2.7 Program Control Unit

This unit controls the program counter, the status register and the registers used for interrupt and subroutine linking. It controls the flow of the program and implements branches, subroutine calls, hardware loops and it handles interrupts. It also keeps track of the status register. It implements 4 registers that are directly accessible in the code:

The status register contains three flags (zero, negative and overflow), which are set by the XALU. There are a number of control bits that control the operation of the CoolFlux BSP. Three bits control the action of both RSS units (sr.b, sr.r, sr.s). The sr.ie bit is the

Name	Long name	Width	Description
sr	Status Register	24 bits	Contains the machine control and status word
lr	Link Register	24 bits	Contains the return address after a call instruction
ilr	Interrupt Link Register	24 bits	Contains the return address after an interrupt.
Isr	Interrupt Status Register	24 bits	It is used to save the value of the status register sr during an interrupt

interrupt enable/disable bit. Two bits are used for the packed division operation (sr.div0, sr.div1). Four bits keep track whether an overflow could occur in a packed move. There are two bits for the imaginary part (or the first word) and two bits for the real part (or the second word) (sr.ov_i, sr.ov_r, sr.ov_i2, sr.ov_r2). A last bit differentiates between an SIMD operation and a complex operation (srsimd). When this bit is set and a packed operation is executed, it will always be an SIMD operation. Note that the only difference between an SIMD operation and a complex operation is in the multiply operation. All other arithmetic operations and all moves are identical^[18].

2.7.1 Hardware Loop Stack

Hardware loops are implemented through a hardware loop stack. The stack is 4 levels deep, so that up to 4 nested loops are supported by hardware. When a loop is initiated, the start-and end address of the loop, and the number of times the loop must be executed is pushed onto the loop stack. When a loop finishes, the loop information is popped from the stack. The stack consists of^[18]:

- Four 24-bit start addresses
- Four 24-bit end addresses
- Four 24-bit loop counts (1 ... 16777215)

2.8 Hardware Interface

The CoolFlux BSP has extensive I/O facilities. These include a 16 Mword I/O memory for mapping peripherals, three hardware interrupts, a data DMA interface to access the data

memories and a program DMA interface to access the program memory. The CoolFlux BSP Interface Manual (See bibliography) outlines the hardware interfaces of the CoolFlux BSP in more detail including signals and timing^[18].

2.8.1 I/O Memory

There is a 16 Mword (24-bit) I/O memory that can be addressed in the same way as the Y-memory^[18].

2.8.2 DMA

The CoolFlux BSP has an arbitrated memory access scheme to all memories which is supported by a fully hand shaken DMA access mechanism. The data DMA port has a unified address space that can map onto X-memory or Y-memory. The program DMA port has access to the P-memory. Access to the X-memory, Y-memory and P-memory is possible when the CoolFlux BSP is running a program. The CoolFlux BSP can support program and data caches through the usage of core hold signals. Refer to the CoolFlux BSP Interface Reference Manual for more details of this interface^[18].

2.9 Multi-Cycle Instructions and Delay Slots

The CoolFlux BSP is a pipelined processor using 3 pipeline stages: fetch, decode and execute. As a consequence all flow control instructions, i.e. instructions that possibly change the pc (program counter), need to execute in multiple cycles, because the pipeline needs to be flushed and re-filled on a change in the pc program counter value^[18].

2.9.1 Multi-cycle Instructions

The following figures show the working of the pipeline stages for non flow-control instructions: the address of the next instruction is the address of the current instruction + 1, and the pipeline works perfect^[18].

When instruction i is a flow-control instruction, i.e. a branch, a call, a return from subroutine, a conditional branch ... the next instruction to be executed after this instruction

Cycle n	Cycle n+1	Cycle n+2	Cycle n+3	Cycle n+4
fetch instruction i+1	fetch instruction i+2	fetch instruction i+3	fetch instruction i+4	fetch instruction i+5
decode instruction i	decode instruction i+1	decode instruction i+2	decode instruction i+3	decode instruction i+4
execute i-1	execute i	execute i+1	execute i+2	execute i+3

is not instruction $i+1$, the pre-fetch scheme fails: the instruction that is already fetched and decoded is not the instruction that must be executed next. Another instruction (at address location k , the target of the branch) has to be fetched and decoded, which takes additional cycles:

Cycle n	Cycle n+1	Cycle n+2	Cycle n+3	Cycle n+4
fetch instruction i+1	fetch instruction i+2	fetch instruction k	fetch instruction k+1	fetch instruction k+2
decode instruction i	decode instruction i+1		decode instruction k	decode instruction k+1
execute i-1	execute i			execute k

The processor has to wait for the correct instruction to be fetched and decoded, it is idle for a few cycles; it stalls. In the figure above, it is as if instruction i takes three cycles to execute. Because of pre-decoding in the fetch stage not all flow control instructions take 3 cycles to execute, because the fetching of the correct instruction k can be started a cycle earlier. Also when a branch is not taken (no jump) the pre-fetching scheme will work, which means that the number of cycles for a conditional branch is 1 if not taken (when the condition code evaluates to false) and 3 if the branch is made (when the condition-code evaluates to true)^[18].

2.9.2 Delay Slots

There is an alternative to stalling the processor in case of flow-control instructions. This is called executing delay-slots. What happens is that the instructions that have already been fetched are not flushed but decoded and executed. In cases that useful instructions can

be inserted into these delay- slots, there is a benefit. The following diagram shows what happens:

Cycle n	Cycle n+1	Cycle n+2	Cycle n+3	Cycle n+4
fetch instruction i+1	fetch instruction i+2	fetch instruction k	fetch instruction k+1	fetch instruction k+2
decode instruction i	decode instruction i+1	decode instruction i+2	decode instruction k	decode instruction k+1
execute instruction i-1	execute instruction i	execute instruction i+1	execute instruction i+2	execute k

Some instructions of the CoolFlux BSP have two variants, the first is multi-cycle (no delay-slots), the other has a number of delay-slots (i.e. the number of cycles , ≥ 1). The option with the delay slots takes as many cycles to execute as the first variant but instead of stalling, the instructions in the delay-slots are executed^[18].

2.10 Hardware Loops

The CoolFlux BSP supports up to 4 nested hardware loops. When a loop instruction is executed the start address, the end address and the number of times the loop must be executed (the loopcount value) are pushed onto the hardware loop stack. This loop stack is four positions deep. When it is full and the program tries to initiate another loop, the instruction is ignored. When the address of the instruction that has been fetched last equals the end address of the loop at the top of the stack, the loopcount value of this loop is decremented. When this new loopcount value equals 0, the loop is popped from the stack. When it is not equal to zero, the new loopcount value is saved and the program counter is set to the start address of the loop and the instruction at the start address is the next instruction being fetched. Note that the loopcount value at the end of the loop is always 1, since the new loopcount value is only written if the loop has not ended.

The loop instruction has 2 initial delay slots, which means that the actual start address of the loop (the program counter value to which the loop jumps back at the end) is the value of the program counter after 2 processor cycles.

The loop end address is relative and thus calculated. The loop end address is calculated in the same way as done for the relative branches.

$$\text{Loop end address} = \text{PC value do instruction} + 2 + \text{offset}$$

$$\text{Loop end address} = \text{PC value do instruction} + 1 + \text{offset}$$

The first one is taken when there are two single cycle instructions in the two delay slots, while the second one is taken when there is a two cycle instruction in the two delay slots^[18].

2.11 Debug Mode

It is possible to enter debug mode using a software instruction. Whenever the debug instruction is executed, the program stops and goes into debug mode. This can be useful when debugging the design on an actual target, for instance on an FPGA. The debug instruction is a multi-cycle instruction that takes 3 cycles to execute. There are no delay slots^[18].

2.12 Interrupts

The CoolFlux BSP supports 3 vectored hardware interrupts as well as 4 software interrupts. On top, a hardware reset is treated as an interrupt located at interrupt vector table location 0. When an hardware or software interrupt occurs, the status register sr is saved into the isr register, the interrupts are disabled, the return address of the interrupt is stored in the interrupt link ilr register and then the processor jumps to an address in the interrupt vector table. This address is dependent of the source of the interrupt:

2.13 BSP C Compiler

To ease the development of applications on this processor, a very efficient optimizing C compiler is available, which is based on a retargetable tool called IP Designer TM patented by the company Target Compiler Technologies.

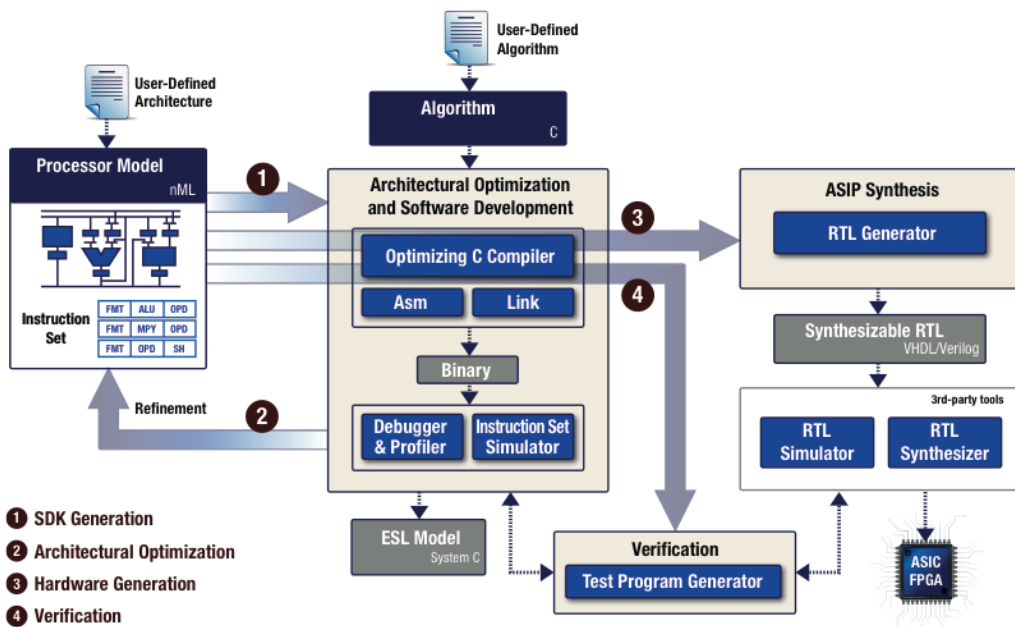
IP DesignerTM is a retargetable tool-suite for ASIP(Application-Specific Processors Design) application-specific processors design. The designer can easily describe each ASIP

Interrupt Vector Table		
Address	Interrupt Source	Remark
0	RESET	Hardware reset
1	INT0	Hardware interrupt
2	INT1	Hardware interrupt
3	INT2	Hardware interrupt
4	SW4	Software interrupt
5	SW5	Software interrupt
6	SW6	Software interrupt
7	SW7	Software interrupt

core in nML, the world's first commercially available high-level processor description language, that offers an unprecedented architectural breadth. From nML, an efficient SDK is generated instantaneously, containing:

- An optimizing c compiler that maps algorithm descriptions into highly optimized machine code for the target ASIP. The unique and patented graph-based modeling and optimization technology in the C compiler enables full exploitation of instruction-level parallelism and pipelining, and of the heterogeneous aspects of the ASIP architecture. The C compiler produces machine code in the Elf/Dwarf (Debug With Arbitrary Record Format) object file format. The C compiler is complemented with an assembler, disassembler, and linker.Executable and Linkable Format
- An instruction-set simulator (ISS) that can execute the compiled machine code both in an instruction- accurate and a cycle-accurate way. The ISS supports cosimulation, and can automatically be encapsulated in SystemC ESL models. The ISS comes with a graphical C source-level debugger, that can connect both to the ISS and to the hardware target for on- chip debugging. Profiling capabilities are provided, as a basis for architectural or algorithmic refinement.
- A hardware generator that creates a synthesizable RTL implementation of the ASIP core, in VHDL and Verilog, for implementation in an ASIC or FPGA. Optionally, the generated RTL model can contain support for on-chip debugging.

- A test generator that produces a large number of processor-specific assembly test programs, with high fault coverage.



Under Target's IP Programmer™ service, ASIP-specific versions of all software development tools, including C compiler, instruction-set simulator, and debugger, can be created instantaneously from the IP Designer retargetable tool-suite. This ASIP-specific SDK can then be distributed to the community of system integrators who want to implement their application software on the newly designed ASIP core. The SDK is identical to the one in IP Designer, except that the processor model is read from a shared library or DLL rather than from nML source code^[20].

Two applications included within the tool suite provided by Target Compiler Technologies have been extensively used during the development of the DAB demodulator:

- Chess: The C compiler. It directly produces an executable in machine code. Directives added to the C code allow optimization.
- Checkers: The simulator, which simulates the machine code and produces diagnostics, profiling info,...

A library of building blocks for complex arithmetic, SIMD acceleration, FFT and modem functions is available.

To allow bit-true simulation on the host machine of the C code intended for the CoolFlux BSP, a library has been developed which supports the CoolFlux BSP types, operations and intrinsic functions (that is, functions that have a direct efficient hardware implementation). When this library is included, the C code for the CoolFlux BSP can be compiled with a standard C++ compiler under Windows or linux. This allows you to simulate and functionally debug the C code very fast before it is compiled and optimized for the CoolFlux BSP using the Chess compiler. The compilation using your standard C compiler is called “native compilation”^[19].

2.13.1 Optimizations

The directives for the C compiler allow code optimizations and steering, whilst remaining completely within the unified C language environment. You are advised to write the majority of the code for the CoolFlux BSP in ANSI C, resorting to assembly language programming only when absolutely necessary^[19].

Chapter 3

DAB Implementation on the CoolFlux BSP

In this chapter we explain the demodulation process of DAB together with its actual implementation under the CoolFlux BSP. The modulation techniques explained in chapter 2 should be fairly enough to understand this chapter.

From an abstract point of view, the input to the DAB demodulator consists of an OFDM-DQPSK modulated signal, represented numerically by a set of complex numbers. The output is the actual sound (other kind of data might be also present in the signal, like textual information).

The DAB demodulation is divided up in a chain of modules, each one performing a transformation on its data input, thus providing partial results to the following module. The aim of this chapter is to explain the functionality of each module, together with their implementation and performance under the CoolFlux BSP.

A simplified DAB transmission chain is processed as follows [6] [1]:

- Audio program signals are digitized and multiplexed together with ancillary data to produce an ‘un-coded’ bit-stream.
- The bit-stream is then encoded for forward error protection by adding redundant bits with appropriate, calculated values.

-
- During each consecutive 1 ms symbol, the ‘coded’ bits are divided into 1536 pairs, and each pair is differentially encoded with respect to its counterpart for the previous symbol.
 - The 1536 differentially encoded bit-pairs are presented to an inverse FFT where each is used to define the phase of a QPSK carrier; collectively, they specify the spectrum of a 1536-carrier signal.
 - The inverse FFT synthesizes a time-domain signal which has the specified spectrum, and this signal is converted to analogue form, frequency converted then transmitted. This is the OFDM generation process, and it is repeated symbol-by-symbol.
 - In the receiver, the incoming OFDM signal is frequency-converted to lower frequencies (appropriate to the hardware), digitized and applied to an FFT. Here the spectrum is analyzed symbol-by-symbol, and the phases of the 1536 carriers are determined. This corresponds to OFDM decomposition.
 - The high-resolution digital complex number which represents the phase of each carrier is divided by the value for the previous symbol in order to detect the differential QPSK.
 - The resulting 1536 differentially decoded numbers are passed to an error-correction decoder where the redundant data and the ‘soft-decision’ detail are used to reconstruct the ‘un-coded’ bit-stream, symbol-by-symbol, as accurately as possible.
 - The reconstructed bit-stream is de-multiplexed and the audio program data are converted back to analogue signals, which are reproduced by a loudspeaker.

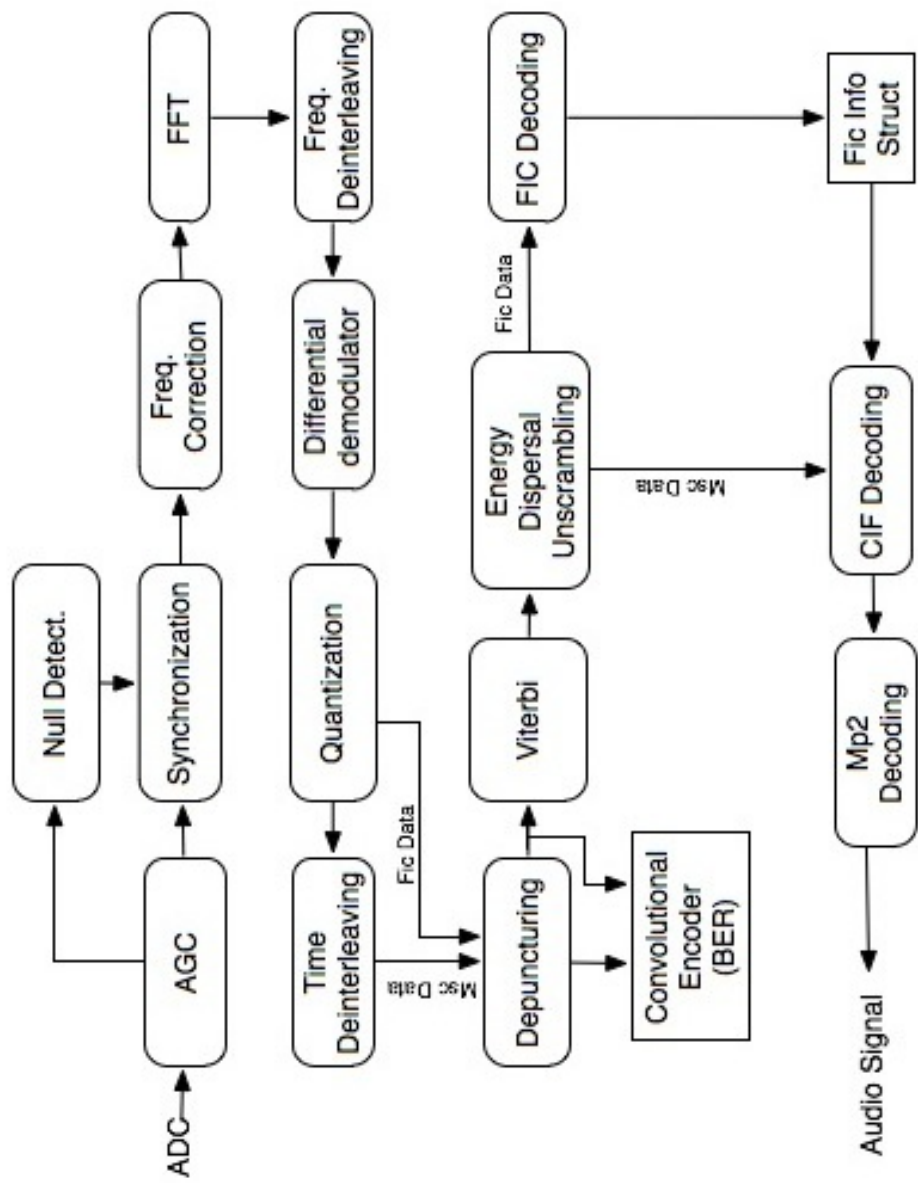


Figure 3.1: A simplified DAB transmission system

3.1 Automatic Gain Control

Automatic gain control (AGC) is an adaptive system found in many electronic devices. The average output signal level is fed back to adjust the gain to an appropriate level for a range of input signal levels. For example, without AGC the sound emitted from an AM receiver would vary to an extreme extent from a weak to a strong signal; the AGC effectively reduces the volume if the signal is strong and raises it when it is weaker^[36].

Because of mobile operation, the average signal amplitude constantly varies by about 20 dB. Hence, for COFDM receivers, careful AGC design is a vital feature. A special scheme called a null symbol, a break in the transmitted signal of 1 ms in DAB transmission mode I, for example, is used for synchronization^[37].

In the case of the DAB input signal, this must be scaled up or down to make use of the 24 bits of resolution available within the architecture. The power reference for the CoolFlux is around -12dB. Initially, the incoming signal is multiplied by a gain factor set to 1 (no amplification is performed). The average power is computed during a fixed window of IQ-samples. After that the gain is turned up or down depending on whether the average power of the window is greater or lower respectively than the power reference.

A low pass filter is required in order to avoid the average power to go up or down too fast due to spurious abrupt (i.e. high frequency) changes in the power of the incoming signal. As an example of a possible sharp change in the signal power is the reception of the null symbol. Without the low pass filter, the null symbol would be amplified up to -12dB, thus making its detection impossible.

A low pass filter can be implemented in software as follows:

$$AvgPwr = Tav * IQpwr + (1 - Tav) * AvgPwr$$

$IQpwr$ is the power of the current IQ-sample. $AvgPwr$ is the average power of all samples received so far within the current window. Tav is a parameter of the filter related to the frequency you want to filter. Notice that If you increase Tav , you force the power of the current symbol to contribute stronger to the average power.

Once the average power of a complete window has been calculated it is time to adjust the gain factor. If the average power is greater than the power reference, the gain factor

is decreased by a small amount. On the other hand, if it is lower then the gain factor is increased. Note the word slightly in the last sentence. This is because, in order to avoid the gain factor to be oscillating over and over again, we define a range of values for which no change of the gain factor is performed. Typically, this range is around

$$[0.9 * PowerReference, 1.1 * PowerReference]$$

With all this at hand, we can write the pseudo-code for the AGC:

```

while true do
    AvgPwr = 0;
    gain = 1;
    pwrRef = -12dB;
    tav = 1/213;
    for i = 0 to WindowSize do
        current IQ - Sample = current IQ - Sample * gain;
        AvgPwr = tav * IQpwr + (1 - tav) * AvgPwr;
        if (AvgPwr < 0.9 * PwrRef) then
            gain = 1.1 * gain;
        end if
        if (AvgPwr > 1.1 * PwrRef) then
            gain = 0.9 * gain;
        end if
    end for
end while
```

As an example of the workings of the last algorithm, in picture 3.2 we show an example of a real DAB signal received at NXP Offices in Leuven. It turned out that the power of the incoming signal was not very good to be subsequently processed. Nevertheless, as can be seen the AGC performs well its task and amplifies the signal to a amplitude such that it can be processed with all the available resolution in the CoolFlux architecture (24 bits).

For a better understanding of the AGC block we show in picture 3.3 the average signal power of the last signal (in blue) in superposition with the gain factor (in red). Presumably the power of the input signal is increased (maybe due to multipath propagation) at around point 12 in the x-axis. Consequently, the gain factor is immediately decreased to maintain the power of input signal at safe levels. As an observation, an excess in power does not

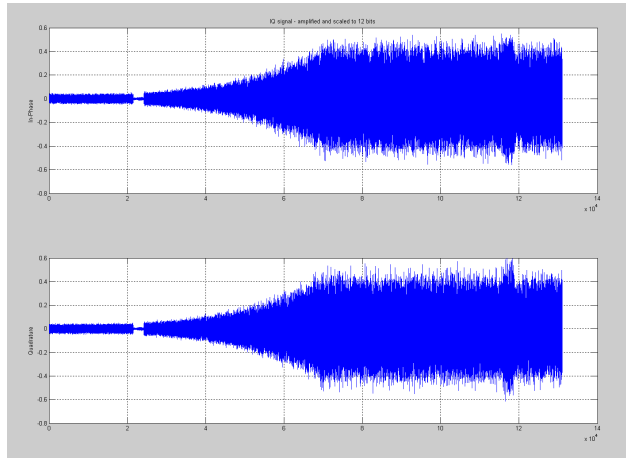


Figure 3.2: AGC amplifying a real DAB signal. NXP Offices (Leuven)

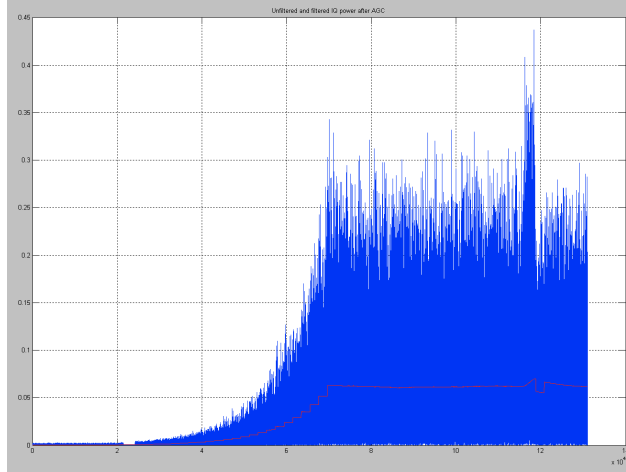


Figure 3.3: Average signal power in superposition with the gain factor.

make the DSP to blow up, but it might cause some operations in the demodulation chain to overflow, thus corrupting the information.

3.2 FFT

The FFT and its relation with DAB was explained in chapter 1. Recall that it is used to extract each of the 1536 subcarriers of the input signal.

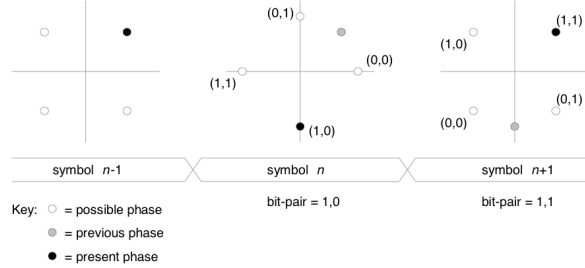
Two implementations of the FFT were tested, namely the radix 2, and radix 4. These FFTs were already implemented by the team of NXP, so we did not have to rewrite it. Our

work was to analyze both the number of MIPS consumed by each FFT and the error of the output vector. Each input sample to the FFT is a complex number with type `complex12`. Thus, both the real part and the imaginary part are represented with 12 bits. Note that we are in a fixed point architecture, so the precision of the FFT is more limited than say, a float point implementation. To allow a fast computation of the FT, the size of the input buffer must be a power of 2. In DAB mode I, there are 1536 subcarriers, so the number of points of the FFT is 2048. Note that $2048 - 1536 = 512$ output samples are not actually used.

3.3 Differential Demodulation

The DAB system uses a different method whereby the QPSK modulation on each carrier is applied differentially; that is, 2 data bits are signaled by the change of phase of a carrier at each symbol boundary, rather than the absolute phase. Detection can be achieved in the receiver by storing each output from the FFT for one symbol and comparing, in some way, the new value with the previous value. This avoids the need for an absolute phase reference, which can simplify the receiver implementation, and correct operation resumes quickly after a deep fade as soon as two consecutive symbols have been received successfully. The disadvantage is impaired performance in the presence of noise and interference (i.e. the previous received symbol could be in error). Up to 3 dB greater S/N is needed to match the performance of coherent detection in the absence of fading.

In the DAB system, the chosen method of modulation is ‘ $\pi/4$ offset D-QPSK’, where the offset is 45 degrees (i.e. $\pi/4$ in radians). The four modulation states are signaled by ± 45 degrees and ± 135 degrees changes of the carrier phase at the start of each new symbol, and this avoids 180 degrees phase changes. In practice, this requires only a little further manipulation of the complex numbers. In absolute terms, there are eight possible phase states, four of which are available in any one symbol, and the phase reference (from the previous symbol) rotates by multiples of 45 degrees from symbol to symbol. These features are illustrated in Fig. 3.4, where the phase of one carrier is shown during three consecutive symbols; the actual phases shown are examples of many possible combinations.


 Figure 3.4: $\pi/4$ offset QPSK

Recall that the input signal is DQPSK modulated. Therefore, the coded data is the difference of phases between the current OFDM symbol (1536 carriers) and the previous one, both of which are held in two buffers in XMEM. Let $z[i], z'[i]$ be the i-th sample in the input buffer and the previous buffer respectively. It can be shown that the phase of complex number r, where

$$r[i] = z[i]\overline{z'[i]}$$

is the difference of phases between $z[i]$ and $z'[i]$.

3.4 Frecuency de-interleaving

Apart from the Phase Reference symbol-block, 75 symbol-blocks of data, or 230400 bits make up each transmission frame. In principle, these can be formed into a serial bit-stream to be applied to the 1536 carriers by D-QPSK and OFDM during 75 consecutive symbols, preceded by the null and Phase Reference symbols. By dividing the bit-stream into 75 blocks of 3072 consecutive bits, and associating pairs of bits within a block, 1536 bit-pairs can be made available during each symbol to be mapped onto the carriers.

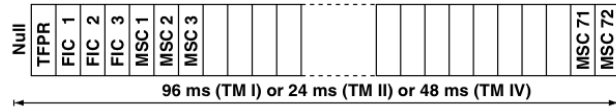


Figure 3.5: Transmission frame structure

If the mapping was a simple one-to-one relationship (e.g. the first two incoming bits

were associated as a bit-pair, and this always modulated the lowest-frequency carrier, etc.), static selective fading or relatively narrow-band interference could impair one or more of the sub-channels selectively; they could suffer most of the errors. Even in the case of mobile reception, long strings of bits would be subject to relatively correlated fading events and this could give rise to bursts of errors. As noted before, this is the least favorable condition for successful error correction by a Viterbi decoder.

Instead, the mapping is based on a static pseudo-random series, and when the bit-pairs are recovered in the receiver, fading and interference events which are correlated amongst groups of adjacent carriers are dispersed within the bit-stream (i.e. they are dispersed in time). Subsequent bit-pairs are then affected by events which are uncorrelated in the frequency domain, and the dispersal of clusters of bit-errors improves the performance of the Viterbi decoder. This process is known as frequency interleaving.

In practice, the bit-pairs are formed by partitioning the incoming bit-stream into blocks of 3072 consecutive bits and associating the 1st bit with the 1537th bit; the 2nd bit with the 1538th bit; and so on. This adds a further element of dispersal.

The data carried in the Phase Reference symbol are not subjected to frequency interleaving but are available as a further 1536 bit-pairs mapped to particular carriers.

Each of the 1536 bit-pairs to be transmitted is given an index, 0 to 1535, and each of the 1536 carriers is given an index, -768 to 768, omitting 0 which corresponds to the un-modulated centre carrier. The series then relates the bit-pair index to the carrier index, and is constructed as follows.

First, an intermediate series is constructed, starting with 0 as the value of the first term. The value of the next term is calculated by multiplying the value of the previous term by 13 and adding 511, with the proviso that if the result is greater than 2047 then 2048 is repeatedly subtracted from it until the result is less than 2048 but positive (i.e. the result is taken modulo 2048). This is repeated to yield 2048 different values; 0, 511, 1010, 1353, ..., 1221.

Then, from the intermediate series, only those values are selected which lie in the range 256 to 1792, omitting all others and 1024 (the centre carrier again). This yields 1536 different values, and 1024 is subtracted from each value giving -513, -14, 329, ..., 197. The

position of each value in this series gives the bit-pair index, 0, 1, 2, ..., 1535, and the value gives the carrier index, so the first bit-pair is directed to the carrier indexed -513, and so on.

Consecutive bit-pairs are separated by widely varying amounts, ranging from about 40 carriers (i.e. their information is transmitted using frequencies separated by at least 40 kHz), up to more than 1400 (i.e. 1.4 MHz separation).

By this process, the resulting dispersal-in-time of errors in the received, de-interleaved bit-stream is limited to within one symbol-block, but errors are further dispersed by the time interleaving which is applied ‘outside’ the frequency interleaving^[6].

3.5 Quantization

Once the differential demodulation has been carried on, we must convert the resulting complex numbers to actual bits. There exists two approaches to this problem, namely hard decision and soft decision.

3.5.1 Hard Decision

First we present the hard decision algorithm which might be simpler:

```
for i = 0 to 1535 do
    r = real(input[i]);
    i = imag(input[i]);
    if (r > 0) then
        output[i] = 1;
    else
        output[i] = -1;
    end if
    if (i > 0) then
        output[i + 1536] = 1;
    else
        output[i + 1536] = -1;
    end if
end for
```

Note that a bit in this case is not represented by ‘1’ and ‘0’ as the reader might have expected. Instead, the two values ‘1’ and ‘-1’ are used.

In picture 3.6 we show a noiseless constellation diagram resulting from the differential demodulator. This output is the input to the quantization module.

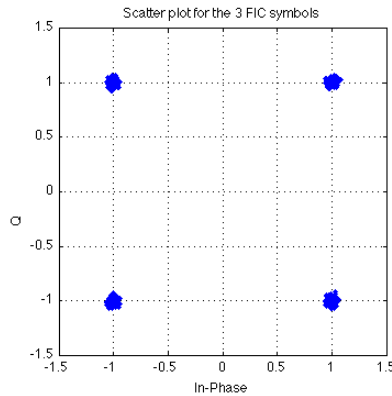


Figure 3.6: Constellation diagram without noise.

As a curiosity, the bits in the above constellation diagram (figure 3.6) belong to a real audio signal. The first quadrant corresponds to the bits (1,1), the second to (-1,1), the third to (-1,-1) and the fourth to (1,-1). This signal is absented from noise. This was only shown with academic purposes. In MATLAB we can add white Gaussian Noise to simulate a more realistic channel. See that the more noise we add, the more and more away are the points from each other on the constellation diagram.

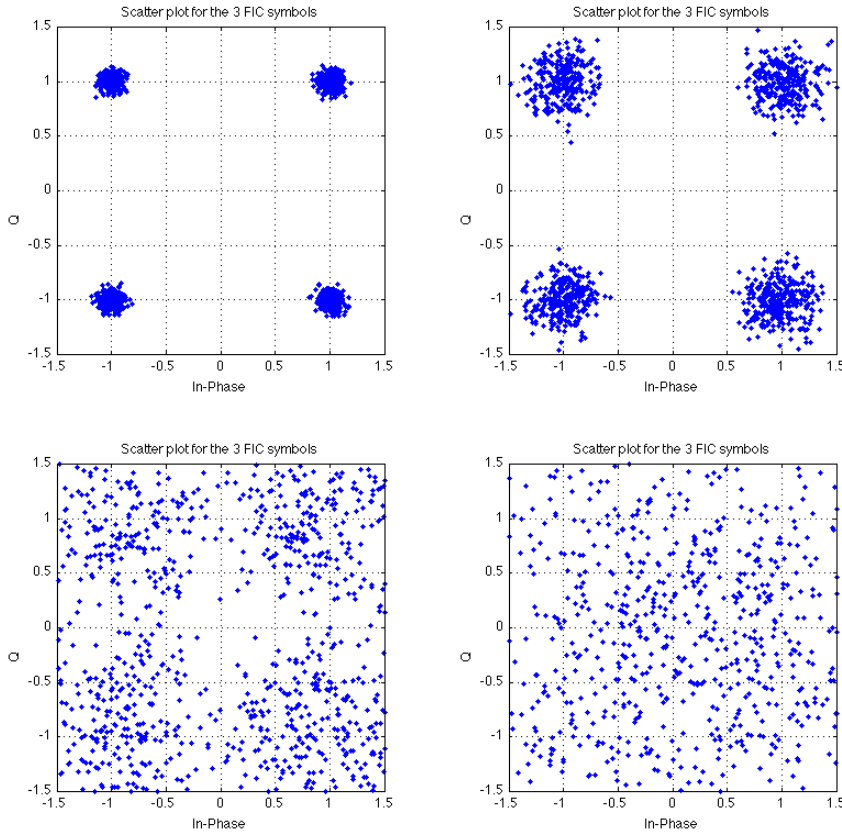


Figure 3.7: Constellation diagram adding noise.

We see that it is possible for a noisy signal that the values of some bits are flipped (those close to the quadrant boundaries), thus corrupting the information. We shall see that even in this case, we can recover the original signal with error correction codes.

3.5.2 Soft Decision

For a transmission channel which introduces only Gaussian noise (such as a satellite down-link), it is found that a 3-bit representation is optimum, giving 2 dB improvement over hard-decision. In this case, an infinite number of bits would only increase the improvement to about 2.25 dB. When the channel also introduces fading which cannot be removed by conventional AGC, there can be value in increasing the resolution to 4 bits .

A multi-bit representation of the demodulator output signal contains an indication of

the ‘confidence’ with which each bit was demodulated. For example with a three-bit word: given ‘000’, it can be inferred with great confidence that a ‘0’ was transmitted, but ‘010’ suggests that it was probably a ‘0’, etc. The two less-significant bits of each word can be considered as a weighting factor, and this can be applied in decisions made within the Viterbi decoder. A neutral value half-way between ‘000’ and ‘111’ would indicate no confidence at all, or zero weighting, so no decisions should be made on the basis of this word^[6].

3.6 Time De-Interleaving

We have already seen the functionality of the frequency interleaving. For more tolerance to burst noise, a time interleaving of output data is also performed in the transmitter. Instead of sending the bits in the order they are generated in the original data stream, we introduce some rule for delaying each bit to transmit. In this way we make that close bits in the original non time de-interleaved stream (that are likely related to each other) be more dispersed. If some noise affects the channel during a period of time whilst transmitting a frame, only a group of non-related bits will be actually corrupted. In addition, the Viterbi decoder, (see below) which was one of the best methods to recover errors in a bit stream at the time of the DAB specification was written, is able to repair only a corrupted bit stream lasting less than a critical duration. By delaying some bits at the transmitter and reordering them at the receiver we avoid the channel to damage segments of the stream data of longer length than the critical duration^[6].

The bits that compose a frame are each delayed by different amounts of subsequent frames. The same amount is always applied to bits that occupy the same position in different frames. Time interleaving shall be applied to the output of the convolutional encoder for all sub-channels of the Main Service Channel (MSC). It shall not be applied to the FIC because this must be processed faster than the MSC. The rule is the following:

Let’s form groups of 16 bits for the current frame, b_0, b_1, \dots, b_{15} . Let s be a string of bits and f be a function defined as

$$f(s) = \text{reverse}(s)$$

	out																		
q₀	b _{r-15,0}	b _{r-14,0}	b _{r-13,0}	b _{r-12,0}	b _{r-11,0}	b _{r-10,0}	b _{r-9,0}	b _{r-8,0}	b _{r-7,0}	b _{r-6,0}	b _{r-5,0}	b _{r-4,0}	b _{r-3,0}	b _{r-2,0}	b _{r-1,0}	b _{r,0}			
q₁	b _{r-7,1}	b _{r-6,1}	b _{r-5,1}	b _{r-4,1}	b _{r-3,1}	b _{r-2,1}	b _{r-1,1}	b _{r,1}											
q₂	b _{r-11,2}	b _{r-10,2}	b _{r-9,2}	b _{r-8,2}	b _{r-7,2}	b _{r-6,2}	b _{r-5,2}	b _{r-4,2}	b _{r-3,2}	b _{r-2,2}	b _{r-1,2}	b _{r,2}							
q₃	b _{r-3,3}	b _{r-2,3}	b _{r-1,3}	b _{r,3}															
q₄	b _{r-13,4}	b _{r-12,4}	b _{r-11,4}	b _{r-10,4}	b _{r-9,4}	b _{r-8,4}	b _{r-7,4}	b _{r-6,4}	b _{r-5,4}	b _{r-4,4}	b _{r-3,4}	b _{r-2,4}	b _{r-1,4}	b _{r,4}					
q₅	b _{r-5,5}	b _{r-4,5}	b _{r-3,5}	b _{r-2,5}	b _{r-1,5}	b _{r,5}													
q₆	b _{r-9,6}	b _{r-8,6}	b _{r-7,6}	b _{r-6,6}	b _{r-5,6}	b _{r-4,6}	b _{r-3,6}	b _{r-2,6}	b _{r-1,6}	b _{r,6}									
q₇	b _{r-1,7}	b _{r,7}																	
q₈	b _{r-14,8}	b _{r-13,8}	b _{r-12,8}	b _{r-11,8}	b _{r-10,8}	b _{r-9,8}	b _{r-8,8}	b _{r-7,8}	b _{r-6,8}	b _{r-5,8}	b _{r-4,8}	b _{r-3,8}	b _{r-2,8}	b _{r-1,8}	b _{r,8}				
q₉	b _{r-6,9}	b _{r-5,9}	b _{r-4,9}	b _{r-3,9}	b _{r-2,9}	b _{r-1,9}	b _{r,9}												
q₁₀	b _{r-10,10}	b _{r-9,10}	b _{r-8,10}	b _{r-7,10}	b _{r-6,10}	b _{r-5,10}	b _{r-4,10}	b _{r-3,10}	b _{r-2,10}	b _{r-1,10}	b _{r,10}								
q₁₁	b _{r-2,11}	b _{r-1,11}	b _{r,11}																
q₁₂	b _{r-12,12}	b _{r-11,12}	b _{r-10,12}	b _{r-9,12}	b _{r-8,12}	b _{r-7,12}	b _{r-6,12}	b _{r-5,12}	b _{r-4,12}	b _{r-3,12}	b _{r-2,12}	b _{r-1,12}	b _{r,12}						
q₁₃	b _{r-4,13}	b _{r-3,13}	b _{r-2,13}	b _{r-1,13}	b _{r,13}														
q₁₄	b _{r-8,14}	b _{r-7,14}	b _{r-6,14}	b _{r-5,14}	b _{r-4,14}	b _{r-3,14}	b _{r-2,14}	b _{r-1,14}	b _{r,14}										
q₁₅	b _{r,15}																		

Figure 3.8: Time De-Interleaving data structure

where $\text{reverse}(s)$ is the original string put in reverse order. So for example, $\text{reverse}(1010) = 0101$. The bit b_i are delayed by $\text{reverse}(i)$ frames. For example, in mode I, the frame duration is 96ms. Thus bit 0 will be transmitted without delay, bit no. 1 will be transmitted with a delay of 96 ms, bit no. 2 will be transmitted with a delay of $2*96$ ms, and so on, until bit no. 15 will be transmitted with a delay of $15*24$ ms. A buffer is required to store the bits that will be transmitted later. In fact, this is the most critical module in terms of memory requirements for the DAB. Note that when we start receiving bits, we must wait 16 frames (1536 ms) in order to fulfill the buffer.

The number of bits within a subchannel is a multiple of 16, so without loss of generality we will consider in a first sight a group of 16 bits. Let r be the current frame being processed. So $b_{r-t,i}$ is the i -th bit within the frame emitted t frames ago. To delay the bits correctly we implemented a data structure consisting of 1 array of 16 circular queues (FIFO), each one of a size equal to $\text{reverse}(i)$. Bits are inserted always at the end of the queue. Picture 3.8 shows this data structure and how bits are inserted.

Argument	Type	Description
P	See below	The pointer value to be update
offs	int	The increment (or decrement)
Start	See below	The start address of the array
Len	int	The length of the circular buffer

Figure 3.9: Structure of the circular buffer

The output is made out of all bits in order from the first position of each queue to the last one. So, according to the picture, the output would be:

$$(b_{r-15,0} b_{r-7,1} b_{r-11,2} b_{r-3,3} b_{r-13,4} b_{r-5,5} b_{r-9,6} b_{r-1,7} b_{r-14,8} b_{r-6,9}$$

$$b_{r-10,10} b_{r-2,11} b_{r-12,12} b_{r-4,13} b_{r-8,14} b_{r,15})$$

Note that the first bit is the first bit of the frame emitted 15 frames ago, the second bit is the second bit emitted 7 frames ago, and so on.

The CoolFlux BSP has special functions to support circular buffers. As explained in the CoolFlux BSP Assembly Programmers Manual^[7], the start address of such circular buffers must be aligned to a start address that is a multiple of a power of 2. The power of 2 must be equal to or higher than the length of the buffer. To efficiently support circular buffers, two special functions are available to update pointers:

```
TP* cyclic_add(TP*p, int offs, TP* start, int len);
TP* cyclic_add_enc(TP*p, int offs, TP* start, int len_or);
```

The *cyclic_add* function adds an offset offs to a pointer in a cyclic buffer. When the pointer reaches the end of the buffer, the pointer is automatically wrapped.

On the CoolFlux BSP, the start address is deduced by the hardware from the address of the pointer p, the size of the array, and the constraint of correct alignment.

An obvious way to extend the structure in figure 3.8 solution to any multiple of 16 bits would be to replicate the last structure n times, one below the other, giving a total of $16n$ queues. However, $16n$ pointer update operations would be required each time a frame is received, making it quite inefficient.

A more efficient way is to reserve memory for one queue of a given size consecutively

	1 st queue				2 nd queue				3 rd queue			
q₃	b _{r-3,3}	b _{r-2,3}	b _{r-1,3}	b _{r,3}	b _{r-7,3}	b _{r-6,3}	b _{r-5,3}	b _{r-4,3}	b _{r-11,3}	b _{r-10,3}	b _{r-9,3}	b _{r-8,3}

Figure 3.10: deinterleaver for any multiple of 16 bits

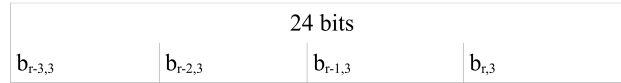


Figure 3.11: Data Type isimd6

after the other of the same size (so, in the same row in picture 3.8). Thus, only one pointer is needed to mark the first element of the first queue. The first elements of the rest of the queues can be deduced from the pointer to the first element of the first queue, since they are within a fixed offset from it. For example, suppose 48 bits are received in a interleaved fashion. Thus, the third row of the above table would be that on picture 3.10

Note that the first element of the second queue is the address of the first element of the first queue plus 4. With this scheme, only 16 pointer updates are needed for each frame.

Another final improvement consists on packing several bits in a single word of 24 bits. So far we used one word for each input bit, now we will pack 4 input bits into a single word, thus reducing the memory requirements by four. The BSP architecture does support the data type simd12, which makes possible to pack two integers into one word. However, it does not implement the type simd6, which would be required for this application. Nevertheless, we emulated this data type in software by making use of bit operations like masks, shifts, etc (Figure 3.11). The counterpart is that more cycles of overhead will be added to the running time. As ever, some compromise must be found between memory space and number of cycles (and of course energy consumption).

The input size depends on the subchannel configuration and so does the performance. During the demodulation of a DAB signal (mode II) with 50 frames and a subchannel size of 208 capacity units (CU) we obtained 2053293 cycles in total for the time de-interleaver. Since each frame in mode II takes 24ms, we can easily compute the number of MIPS

$$2053293 / 1M / 24mS / 50frames = 1.71MIPS$$

According to the DAB standard, the maximum size allowed for a subchannel is of 416 CU's for each frame, giving a bit rate of 384kbit/s. Since each CU contains 64 bits, the subchannel maximum size has a total of 26624 bits. Each basic structure as the one shown in the picture above is made up of $(1+2+\dots+16) = 136$ words, and since each word holds 4 bits, $16 \times 4 = 64$ bits can be de-interleaved with 136 words. Hence, the number of words needed to fully de-interleave a subchannel of maximum size is 56576 (55.25 KB).

3.7 Errors Detection and Correction

The convolutional coding used in the DAB system employs these principles but is considerably more complicated than the examples given so far. The constraint length is 7 so the encoder has 64 states. Fundamentally, it uses 4 generator polynomials and the generated bits are transmitted in a fixed sequence cycling through the 4 bits, so the encoder operates at rate 1/4. This can provide very powerful error correction, albeit with extreme consumption of the available bit-rate^[1].

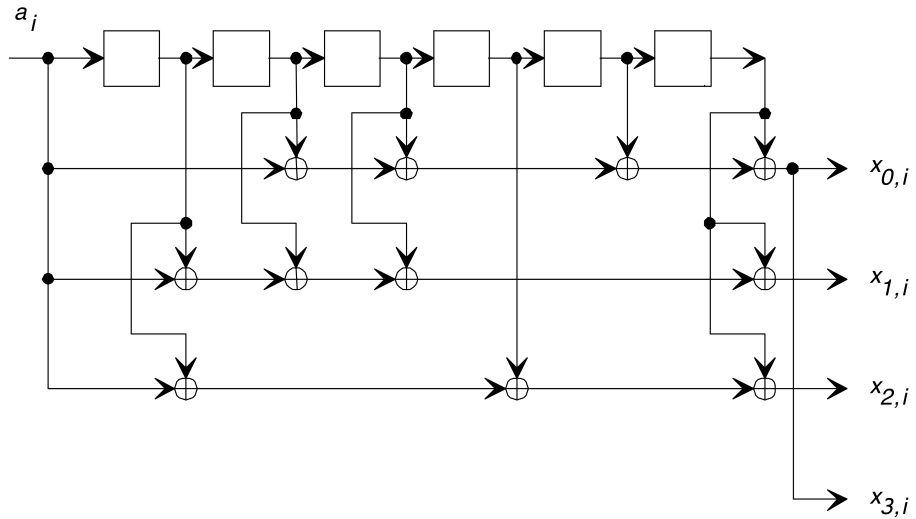


Figure 3.12: DAB convolutional encoder

$$x_{0,i} = a_i \oplus a_{i-2} \oplus a_{i-3} \oplus a_{i-5} \oplus a_{i-6}$$

$$x_{1,i} = a_i \oplus a_{i-1} \oplus a_{i-2} \oplus a_{i-3} \oplus a_{i-6}$$

$$x_{2,i} = a_i \oplus a_{i-1} \oplus a_{i-4} \oplus a_{i-6}$$

$$x_{3,i} = a_i \oplus a_{i-2} \oplus a_{i-3} \oplus a_{i-5} \oplus a_{i-6}$$

In the corresponding trellis, and therefore the Viterbi decoder, four paths emerge from each node. At the higher levels, there are 64 nodes in each level and four paths enter each node; one path amongst two must be chosen at each of these nodes. Each branch represents a sequence of four transmitted bits.

The coding gain of a convolutional code depends on the code rate, the constraint length and uniqueness properties endowed by the generator polynomials; their choice is not obvious, and may be the result of extensive computer searches (as may be the puncturing codes).

Assessment of the number of errors can be corrected is quite complicated because of the unbounded length of the code-word. Nevertheless, one useful parameter in the context of Viterbi decoding is the ‘free distance’. This is the minimum Hamming distance between any two code-words as the length, and the number of code-words considered, approaches infinity. On the basis that truncating the length of the Viterbi decoder (from infinity) to four or five times the constraint length incurs little penalty, the free distance is a first-order guide to the number of errors that can always be corrected in an input sequence the length of the decoder. The coding used in the DAB system is based on an un-punctured code for which the free distance is 10, so this indicates a capacity for always correcting up to 4 errors in the decoder trellis simultaneously.

The combination of a convolutional encoder and a Viterbi decoder works well in the presence of a continuous stream of randomly placed errors, which may be caused by noise or inter-symbol interference. For the non-coded case, the BER of the recovered bit-stream would increase, with reducing S/N of the input signal, as illustrated in Fig. 3.13^[6]

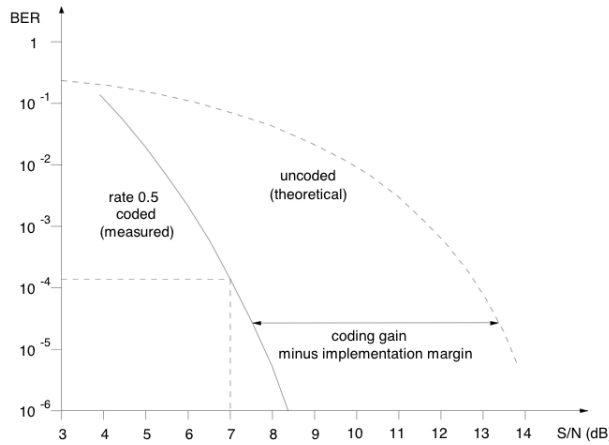


Figure 3.13: Relationship between BER and S/N ratio

3.8 Energy Dispersal Unscrambling

In order to ensure appropriate energy dispersal in the transmitted signal, the individual inputs of the energy dispersal scramblers shall be scrambled by a modulo-2 addition with a pseudo-random binary sequence (PRBS), prior to convolutional encoding.

The PRBS shall be defined as the output of the feedback shift register of figure 3.14. It shall use a polynomial of degree 9, defined by:

$$P(X) = X^9 + X^5 + 1$$

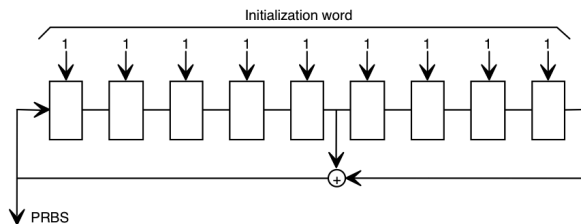


Figure 3.14: PRBS generation.

The initialization word shall be applied in such a way that the first bit of the PRBS is obtained when the outputs of all shift register stages are set to value “1”. The first 16 bits of the PRBS are given in table 3.15^[1].

bit index	0	1	2	3	4	5	6	7	8	9	10	11	12	13	14	15
bit value	0	0	0	0	0	1	1	1	1	0	1	1	1	1	1	0

Figure 3.15: PBRS indexing table.

3.9 Synchronization channel

Many of the processes in the DAB receiver require accurate synchronization with aspects of the frequency and timing of the incoming signal, and in mobile reception conditions, all of these aspects can be modified by the Doppler shift.

The following aspects of synchronization need to be considered:

- The rate at which FFT computations are carried out must be equal to the reciprocal of the total symbol duration of the incoming signal; to avoid inter-carrier crosstalk.
- The channel decoding and de-multiplexing process must be clocked at the same rate as data appear in the incoming signal; so the correct data are processed and selected.
- The frequencies of components of the baseband signal input to the FFT must be such that the carrier frequencies lie precisely on the correct ‘teeth’ of the comb with frequency separation equal to the reciprocal of the active symbol duration; to avoid corruption of the differential coding and to avoid inter-carrier crosstalk.
- The FFT processing window must be timed to start at the point in each total symbol which makes the greatest constructive use of receivable multipath signals.

Synchronization of a DAB receiver is performed in several steps:

- Coarse time or frame synchronization
- Coarse frequency synchronization on carrier accuracy
- Fine frequency synchronization on sub-carrier accuracy
- Fine time synchronization.

There is a special OFDM symbol called ‘Null-symbol’. The Null-symbol of the DAB transmission frame provides a simple and robust way for the coarse time synchronization,

which is also called frame synchronization. The underlying idea is to use a symbol with reduced signal level which can be detected by very simple means. In practice a short time power estimation is calculated which is then used as input to a matched filter. This filter is simply a rectangular window with a duration according to the Null-symbol length. Finally a threshold detector indicates the beginning of a DAB frame.

Coarse and fine frequency synchronization can be performed using the by means of an OFDM symbol called the “TFPR symbol (Time Frequency Phase Reference)” in the frequency domain. This step clearly requires a sufficiently exact coarse time synchronization. Frequency offsets are calculated using the various CAZAC (Constant Amplitude Zero Auto-Correlation) sequences inside the TFPR symbol (see below). These sequences provide a tracking frequency error range of about +32 carriers.

Fine time-synchronization is performed by calculating the channel impulse response based on the actually received TFPR symbol and the specified TFPR symbol stored in the receiver^[6].

3.9.1 Null Symbol Detection

All the carriers are attenuated by at least 20 dB for the 1.297 ms duration of the null symbol (in Mode 1). This discontinuity can be detected from the envelope of the incoming RF signal.

In order to detect the null symbol we must set up a window of size 512 words for which we calculate the average power of the incoming signal. The idea is that the average power must fall below a given threshold in order to infer the null symbol is coming in. When the average power falls below a given threshold, we can be certain the null symbol is coming in. Let $s = a + bi$ be some sample. The power of s is computed according to this formula:

$$P(s) = (a + bi)(a - bi) = a^2 + b^2$$

In picture 3.16 we show the average value of a real DAB signal (mode I). You might note the abrupt falls of the power during the detection of the null symbol. As expected, the null symbol is presented each 96 ms for a DAB signal in mode I.

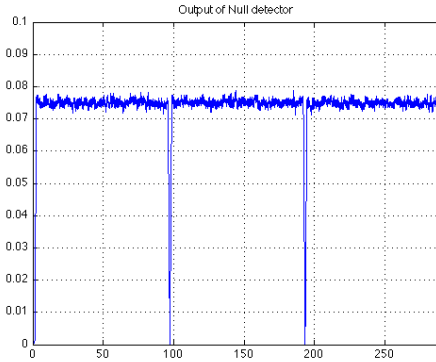


Figure 3.16: Null symbol detection

It might be the case that the average power falls incidentally below the threshold for a very short time due for instance to some obstacle in the path. This event might be misinterpreted as the presence of the null symbol. To avoid the possibility of such a false positive we force the average power to pass through a low pass filter. In this way, spurious changes in the signal power will be attenuated. An example of a real filtered signal is represented in picture 3.17 with pink color. The red line is an indicator that changes from 0.05 to 0 when the filtered average power of the signal falls below the decision threshold, or equivalently when the null symbol is detected. Note that the filtered signal is much softer than the unfiltered one.

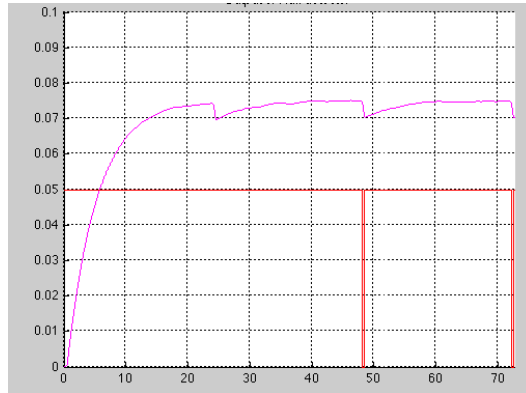


Figure 3.17: Low pass filtered signal.

So up until now we have performed the coarse time synchronization, and so we are ‘almost’ at the beginning of one frame. The TFPR symbol starts ‘approximately’ within a

fixed offset (measure in number of samples) from the point where the average filtered power falls below the aforementioned threshold. Such approximation is not permissible in order to start demodulating the actual audio signal. In fact, the TFPR serves as a symbol to do the fine time synchronization, the coarse and fine frequency synchronizations.

3.9.2 TFPR symbol

During the TFPR symbol, all carriers are transmitted at normal power with the normal symbol duration and guard interval; these are necessary requirements for its use as the phase reference for all carriers.

The carriers are modulated in a fixed pattern and this pattern is reproduced when the incoming signal is analyzed by the FFT in the receiver. However, the position of the pattern within the array of numbers output by the FFT depends on the frequencies of the received signal and the RF local-oscillator in the receiver. The objective is to locate the pattern precisely at a particular position so the data conveyed by the carriers during the following frame can be identified uniquely. The same pattern is stored in the receiver, so the frequency error can be determined by measuring the misalignment between the stored and received patterns.

The TFPR symbol also facilitates measurement of the impulse response of the transmission channel, and fine time synchronization can be achieved using this; this will be discussed later.

The TFPR symbol-block has the normal capacity of 1536 bit-pairs, in Mode 1, and the whole of this capacity is used for synchronization functions. The data are self-contained within the symbol-block and can be decoded without reference to an earlier symbol. The chosen fixed pattern has properties which assist its recognition in the presence of noise and interference; it is based on a CAZAC (Constant-Amplitude Zero-Autocorrelation) sequence.

A CAZAC sequence is a sequence of complex numbers, which may be called elements, which has the following characteristics:

- Each element has the same magnitude; for example, its value can be +1, +j, -1 or -j. This accounts for ‘Constant Amplitude’.

- If the sequence is multiplied, element by element, by its complex conjugate, the sum of the products is a large number; this would be true for many sequences. However, if the sequence is shifted by one element (i.e. the first number takes the place of the second one, etc., and the last number takes the place of the first one), and the shifted sequence is multiplied by the conjugate of the original sequence, the sum of the products is zero. Furthermore, the same zero result occurs for any amount of shift, less than the length of the sequence, in either direction. This means that the sequence has ‘Zero Autocorrelation’, and this property is relatively uncommon.

‘Correlation’ is the process of multiplying the element values and accumulating the result, and the ‘auto’ prefix indicates that the process is carried out on a sequence and the conjugate of the same sequence. An example of a 16 element CAZAC sequence, its conjugate and the autocorrelation with no shift are shown in Figure 3.18; note that the conjugate has the signs of the ‘j’s reversed.

CAZAC sequence	$\begin{array}{ c c c c c c c c c c c c c c c c c } \hline j & -1 & -j & 1 & -1 & 1 & -1 & 1 & -1 & -j & -1 & j & 1 & 1 & 1 & 1 & 1 \\ \hline \end{array}$
x	
conjugate sequence	$\begin{array}{ c c c c c c c c c c c c c c c c c } \hline -j & -1 & j & 1 & -1 & 1 & -1 & 1 & j & -1 & -j & 1 & 1 & 1 & 1 & 1 \\ \hline \end{array}$
=	
	$1+1+1+1+1+1+1+1+1+1+1+1+1+1+1+1 = 16$

Figure 3.18: a 16-element CAZAC sequence, its conjugate, and the autocorrelation with no shift.

Performing the autocorrelation with a shift of 1 element (or any other discrete amount up to 15 elements) gives the zero result, as shown in Fig. 3.19;. Note that the zero result arises because of cancellation, so it is essential that all elements of the sequence be represented in the autocorrelation calculation; if the sequence was truncated for some reason, the ‘ZAC’ property would be lost.

The result for any discrete amount of shift can be presented as a histogram, as shown in Fig. 3.20;. A shift of 16 elements, or any multiple, restores the original sequence so the autocorrelation peak is said to be ‘periodic’.

Some useful properties of a CAZAC sequence are as follows:

$$\begin{array}{c}
 \text{---} \\
 | \quad j \quad -1 \quad -j \quad 1 \quad -1 \quad 1 \quad -1 \quad 1 \quad -j \quad -1 \quad j \quad 1 \quad 1 \quad 1 \quad 1 \quad 1 \quad 1 \\
 | \quad j \quad -1 \quad j \quad 1 \quad -1 \quad 1 \quad -1 \quad 1 \quad j \quad -1 \quad -j \quad 1 \quad 1 \quad 1 \quad 1 \quad 1 \quad 1 \\
 \text{x} \\
 = \\
 -j \quad -j \quad -j \quad -j \quad -1 \quad -1 \quad -1 \quad -1 + j + j + j + j + 1 + 1 + 1 + 1 = 0
 \end{array}$$

Figure 3.19: The autocorrelation with shift of one.

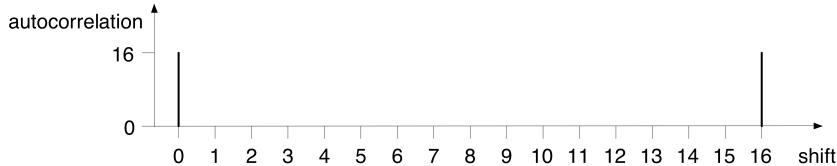


Figure 3.20: Autocorrelation VS Shift.

- If all elements of the original sequence are multiplied by some constant factor, which may be complex, the magnitude of the result becomes multiplied by the same factor and the zero autocorrelation property is preserved.
- If the original sequence is corrupted by the addition of one or more shifted versions of the same sequence, individual correlation peaks are found for each of the sequences at appropriate shifts. Last property applies, so if the different sequences are multiplied by constants, the complex values of correlation are multiplied in the same way.
- If the original sequence is corrupted by noise or interference, some or all elements will have modified values and, generally, the result will be a complex number. In that case, up to a certain degree of corruption, the correlation for zero shift will still have the greatest magnitude. The ruggedness of such a sequence can be demonstrated by adding a 16-element sequence of random numbers (from the set $+1, +j, -1, -j$), as shown in Fig. 3.21. This corresponds to 0 dB signal-to-noise ratio, but the correlation peak for zero shift can be clearly identified.

Essentially, the added sequence would need to mimic the original CAZAC sequence

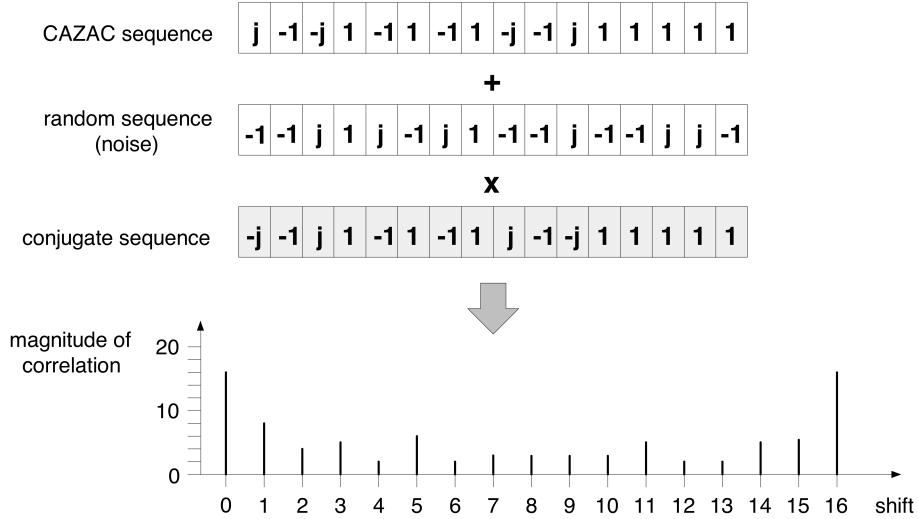


Figure 3.21: correlation with added noise.

(or some multiplied and/or shifted version) for a large false correlation peak to be generated, and the likelihood of this occurring is reduced by lengthening the sequence.

- If several of the original CAZAC sequences are concatenated end-to-end and the correlation is performed between any group of 16 consecutive elements and the 16-element conjugate sequence, the result will be periodic correlation peaks. If the amount of shift is limited to less than ± 16 elements, then a single central correlation peak can be produced, with reduced correlation either side. Fig. 3.22 shows the sequence extended by 8 elements at each end; in this case, the conjugate sequence can be shifted by up to 8 elements in either direction^[6].

3.9.3 Coarse Frequency Correction

These properties are used to provide AFC in the DAB receiver. A large number of such 32-element extended CAZAC sequences are transmitted simultaneously in the Phase Reference symbol-block. Each element value is conveyed by the phase modulation one carrier, and each sequence is contained in the modulation of 32 consecutive carriers (working from the low-frequency end of the ensemble, for example).

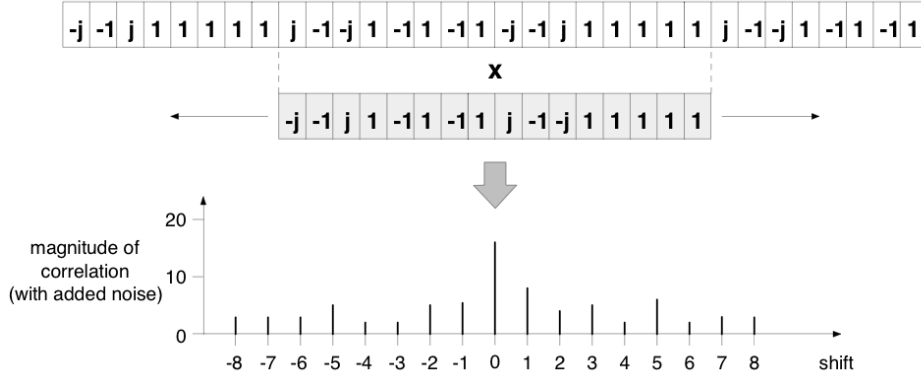


Figure 3.22: Correlation with an extended sequence

In the receiver, the sequences are reproduced in the array of complex numbers output by the FFT, and the conjugate sequence is held in ROM, so the correlation can be performed as previously described. If the time-domain signal input to the FFT has no frequency error, then the reproduced sequence will be aligned in some particular way with the FFT outputs, but if a large frequency error exists (i.e. one or more times the carrier frequency separation), the reproduced sequence will be shifted with respect to those outputs. This can be detected by shifting the stored conjugate sequence or changing the local-oscillator frequency, and searching for the correlation peak. Coarse AFC can be provided in this way, with a capture range of at least ± 8 carrier separations (i.e. ± 8 kHz in Mode 1).

The Phase Reference symbol-block is not subjected to frequency-interleaving because this would require additional processing in the receiver and it would confer no advantage in conditions of selective fading; a CAZAC sequence is equally sensitive to corruption of adjacent or non-adjacent elements. Also, time interleaving cannot be used because the AFC needs to be updated from transmission frame to frame in order to optimize the receiver performance in conditions of changing radio frequency (i.e. oscillator drift or changing Doppler shift), and the attendant time-delay could not be tolerated.

Consequently, the ruggedness of this system is dictated by the length of the CAZAC sequences alone. However, very long sequences (i.e. across many carriers) could be corrupted by variations in the phase/frequency response of the transmission channel. The use of a large number of shorter sequences is relatively beneficial because the complex results of individual

correlations can be added together as vectors, and the magnitude of the resultant used for AFC; this has the effect of averaging noise, interference and channel variations^[6].

3.9.4 Fine Frequency Correction

Having achieved coarse AFC, the residual frequency error will be less than the carrier frequency separation. One effect of a small frequency error is to cause crosstalk between the FFT outputs so the correlation peak will be dispersed to some degree; the magnitude of the correlation will rise and fall as the conjugate sequence is shifted, and the true peak will lie between two discrete amounts of shift.

Take, for example, four adjacent carriers (labelled D, E, F and G to facilitate this explanation) which carry part of one of the CAZAC sequences (elements labelled P, Q, R and S). The FFT in the receiver operates like a bank of band-pass filters followed by demodulators; each filter has a $\sin f/f$ frequency response, f being the relative frequency, which is broad but exhibits distinct nulls. With no frequency error, the nulls coincide with the frequencies of the adjacent carriers as illustrated in Fig. 3.23, so there is no crosstalk. Only one of the frequency responses is shown fully in order to preserve clarity.

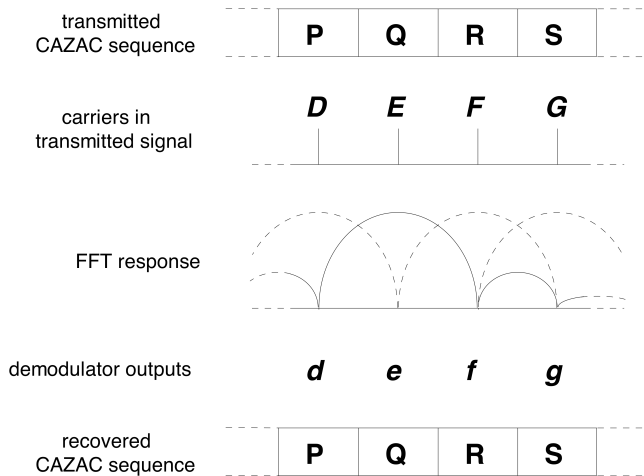


Figure 3.23: transmission and reception of four carriers with no frequency error

Each filter/demodulator outputs a complex number (labelled d, e, f and g) which carries

information about the phase of one carrier, and the received CAZAC sequence can be recovered from these.

In the presence of a frequency error, the number output by each filter contains contributions from all of the carriers; that is, crosstalk. The strongest component represents the closest carrier, and the relative amplitudes of the other components depend on the relative frequencies of the carriers they represent (with a $\sin f/f$ variation).

Considering the filter/demodulator which outputs the number e in the absence of an error; in the presence of an error, its output number will contain a component e' (the prime ' indicates some difference from e ; principally a smaller amplitude), f'' (with an amplitude even smaller than f), d''' , and many other components with much smaller amplitudes. The next higher-frequency filter/demodulator will output a number containing f', g'', e'' , etc., and so on for all filter/demodulators. This is illustrated in Fig. 3.24.

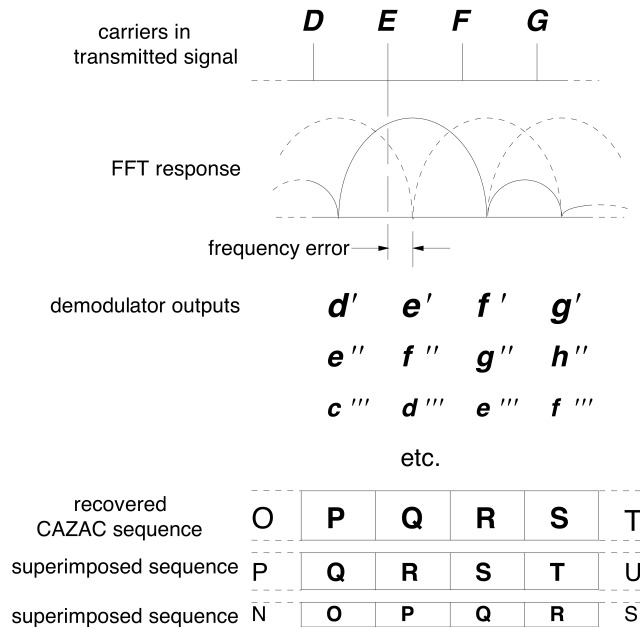


Figure 3.24: transmission and reception of four carriers with frequency error

The numbers output by the FFT represent the phasor sums of these components, so the array of numbers contains many shifted versions of the CAZAC sequence superimposed with different amplitudes. This is indicated in Fig. 3.24 by the use of smaller typefaces.

When the correlation is performed, these different amplitudes are preserved in the numerous values of correlation which are found at different discrete shifts, as illustrated in Fig. 3.25.

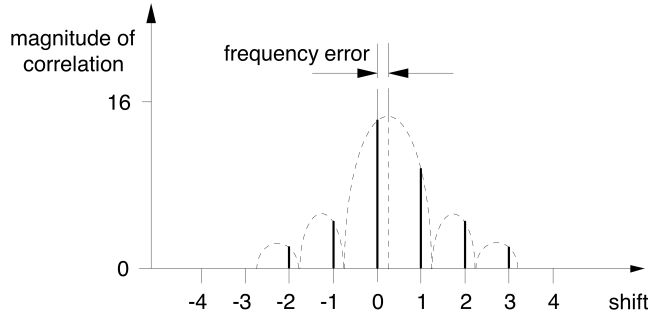


Figure 3.25: magnitude of correlation vs. shift with a small frequency error

The variation of the magnitude of the correlation, at each discrete shift, with increasing frequency error, follows a $(\sin x/x)^2$ law as illustrated by the dashed line in Fig. 3.25; the square is introduced by taking the magnitude. In this case, the variable x is the sum of the magnitude of the error and the amount of shift, multiplied by π .

The amount of shift is an integer, so for a given error, $\sin x$ has the same value for all shifts. Therefore, the magnitude at each shift is proportional to $(1/x)^2$ and individual values are related to one another by a quadratic equation (i.e. of the form $a + bx + cx^2 = 0$). The magnitude of the error can then be calculated from the magnitude of the correlation at different shifts, and the sign of the error can be established with an additional measurement. The middle three values offer the greatest signal-to-noise ratio and, therefore, the greatest accuracy. Some straightforward arithmetic involving these three values provides a number representing the magnitude and sign of the frequency error^[6].

3.9.5 Fine time synchronization

Having achieved fine frequency control, the Phase Reference symbol-block can then be used to achieve fine time synchronization of the FFT processing window in the receiver. In order to make the greatest constructive use of multipath signals it is necessary to measure the impulse response of the transmission channel and to time the beginning of the processing

window on the basis of a calculation which weights the relative importance of different multipath signals. The impulse response can be measured as follows.

The array of complex numbers output by the FFT (partly illustrated in Fig. 3.23) represents the amplitudes and phases of the carriers transmitted in the Phase Reference symbol-block multiplied by the complex (amplitude and phase) frequency response of the channel, albeit sampled at the carrier frequencies. The (time) impulse response is related to the channel frequency response by the inverse Fourier transform, so a sampled version of the impulse response is related to this sampled frequency response by the inverse DFT, and this can be performed using an inverse FFT; quite separate from the ‘main’ FFT used for OFDM decomposition.

The channel frequency response is revealed by holding the definition of the Phase Reference symbol-block in the receiver as an array of complex numbers in ROM, and by dividing the main FFT outputs by their counterparts in this stored array. The resulting array is then applied to an inverse FFT which outputs a further array representing the impulse response. The magnitudes of elements in this array are then calculated and can be used to derive the timing reference for the following transmission frame. This involves searching for the peaks and applying an algorithm for the chosen timing strategy in order to derive a number representing the amount by which the timing of the main FFT processing window should be advanced or retarded.

For accuracy in this method, the transmitted signal must have a constant Power Spectral Density (PSD) at different frequencies within the bandwidth of the DAB ensemble (i.e. its spectrum must be ‘white’) for the duration of the Phase Reference symbol. With this provision, the same ‘gain’ can be applied at all frequencies to avoid distorting the influence of channel noise. To a first order, and certainly over the period of only one symbol, the PSD is effectively constant because the carriers are all transmitted with the same amplitudes. This might not be the case if the spectrum of the DAB signal were considered over a period of many symbols because it would also depend on the carrier phases.

The Phase Reference symbol-block has been described here as it is defined in the frequency domain, that is, at the input to the inverse FFT in the transmitter or the output of the main FFT in the receiver, and not in terms of the time-domain signal that is transmit-

ted. The time-domain signal is related to this by the Fourier transform. Now, the PSD of a signal in one domain is related by the Fourier transform to the autocorrelation function of the transformed signal in the other domain. In this case, the autocorrelation function of the DAB signal described in the frequency domain is that of the CAZAC sequences, which could be described as an ‘impulse’. The Fourier transform of an impulse is a constant value (viz. for a true impulse in the time domain, the frequency spectrum is ‘white’), so it follows that the PSD of the transmitted DAB signal, described in the time domain, is constant. If the Phase Reference symbol was repeated, the PSD would be constant over the duration of any number of repeated symbols.

Another benefit of the constant amplitude nature of the Phase Reference symbol-block is that the process of division by the stored array in the receiver only has the effect of subtracting phases. The same effect can be achieved by multiplying the array output by the main FFT by a stored array representing the conjugate of the PhaseReference symbol-block, and multiplication is an easier process to carry out digitally. Generally, this would introduce a scaling factor, equal for all elements of the array, but in this case the stored values all have unit amplitude so there is no scaling factor.

Described as an array, the Phase Reference symbol-block has 1536 elements in Mode 1, so a 2048-sample inverse FFT must be used. The samples output by the inverse FFT represent the duration of the active symbol, so the resolution of the impulse response is then about $0.5 \mu\text{s}$. It is worth noting that absolute magnitudes are not important in this case; indeed they depend on the action of AGC which is entirely separate from the processing of the Phase Reference symbol. An example of an impulse response is illustrated in Fig. 3.26^[6].

3.10 Transport mechanisms

The DAB system is designed to carry several digital audio signals together with data signals. Audio and data signals are considered to be service components which can be grouped together to form services.

The DAB system transmission frame consists of three different channels:

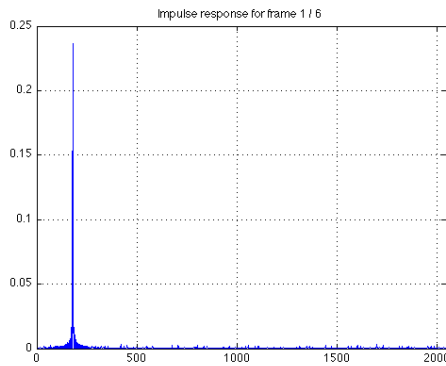


Figure 3.26: example of an impulse response for a multipath channel

1. Main Service Channel(MSC):

Used for carrying audio and data service components. The MSC is a time-interleaved data channel divided into a number of sub-channels which are individually convolutionally coded, with equal or unequal error protection. Each sub-channel may carry one or more service components. The organization of the sub-channels and service components is called the multiplex configuration;

2. Fast Information Channel(FIC):

The FIC is a non time-interleaved data channel with fixed equal error correction. FIC carries information about the organization of the MSC subchannels, such as information on the multiplex structure and, when necessary, its reconfiguration. Optionally FIC may include service information, conditional access management information and data service;

3. Synchronization channel:

The Synchronization Channel provides a phase reference and is used internally for demodulator functions such as transmission frame synchronization, automatic frequency control, transmitter identification, and channel state estimation. Each channel supplies data from different sources and these data are provided to form a transmission frame.

The Synchronization channel, the Fast Information Channel and the Main Service Chan-

nel form a transmission frame (see figure below 3.27). The MSC occupies the major part of the transmission frame.

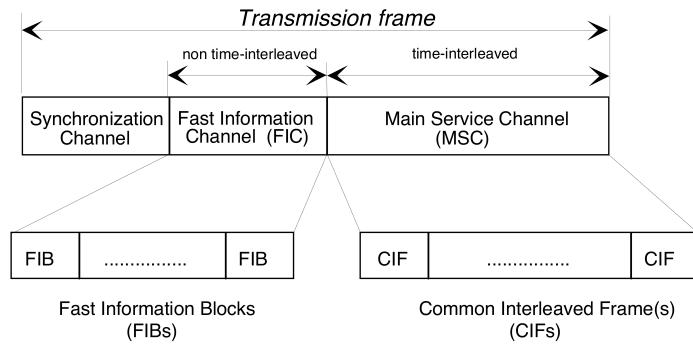


Figure 3.27: DAB Transmission mode independent description.

Each transmission frame is divided into a sequence of OFDM symbols, each symbol consisting of a number of carriers.

The Fast Information Block (FIB) and the Common Interleaved Frame (CIF) are introduced in order to provide transmission mode independent data transport packages associated with the FIC and MSC respectively.

The data, carried in the MSC, is divided at source into regular 24 ms bursts corresponding to the subchannel data capacity of each CIF. The CIF contains 55 296 bits, divided at 864 capacity units, 64 bits each.

Fast Information Block (FIB) is a data burst of 256 bits. The sequence of FIBs is carried by the Fast Information Channel FIC. The structure of the FIB is common to all transmission modes.

The synchronization channel symbols comprise the null symbol and the phase reference symbol. The null symbols are also used to allow a limited number of OFDM carriers to convey the Transmitter Identification Information (TII).

Both the organization and length of a transmission frame depend on the transmission mode. The Fast Information Block (FIB) and the Common Interleaved Frame (CIF) are introduced in order to provide transmission mode independent data transport packages associated with the FIC and MSC respectively.

Table(3.28) gives the transmission frame duration and the number of FIBs and CIFs which are associated with each transmission frame for the four transmission modes.

Transmission mode	Duration of transmission frame	Number of FIBs per transmission frame	Number of CIFs per transmission frame
I	96 ms	12	4
II	24 ms	3	1
III	24 ms	4	1
IV	48 ms	6	2

Figure 3.28: General transport characteristics of the transmission frame.

In transmission mode I, the 12 FIBs contributing to one transmission frame shall be divided into four groups which are each assigned to one of the CIFs contributing to the same transmission frame.

The information contained in the first three FIBs shall refer to the first CIF, the information contained in the fourth, fifth and sixth FIB to the second CIF, and so on. All FIBs contributing to a transmission frame, in transmission modes II and III, shall be assigned to the one CIF associated with that transmission frame. In transmission mode IV, the six FIBs contributing to one transmission frame shall be divided into two groups which are each assigned to one of the CIFs contributing to the same transmission frame. The information contained in the first three FIBs shall refer to the first CIF, and the information contained in the fourth, fifth and sixth FIB to the second CIF.

The general structure of the FIB is shown later, for a case when the useful data does not occupy the whole of a FIB data field. The FIB contains 256 bits and comprises an FIB data field and a CRC.

The following subclauses describe the formation of the FIC and MSC^[1].

3.10.1 Fast Information Channel (FIC)

The FIC is made up of FIBs.

3.10.1.1 Fast Information Block (FIB)

The general structure of the FIB is shown figure 3.29, for a case when the useful data does not occupy the whole of a FIB data field. The FIB contains 256 bits and comprises an FIB data field and a CRC.

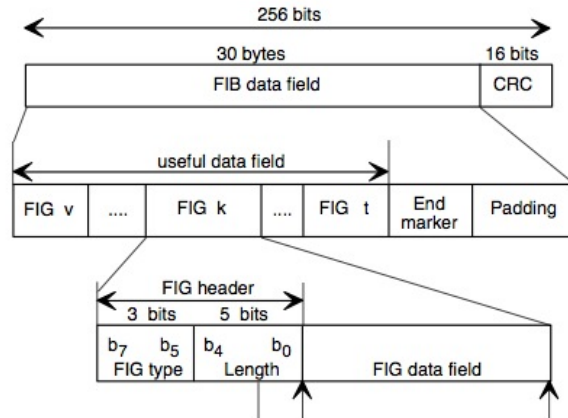


Figure 3.29: Structure of the FIB

3.10.1.2 Fast Information Group (FIG)

The FIG shall comprise the FIG header and the FIG data field. The following definitions apply:

- FIG header: shall contain the FIG type and the length:
 - FIG type: this 3-bit field shall indicate the type of data contained in the FIG data field. The assignment of FIG types is given in the following table:

FIG type number	FIG type	FIG application
0	000	MCI and part of the SI
1	001	Labels, etc. (part of the SI)
2	010	Reserved
3	011	Reserved
4	100	Reserved
5	101	FIC Data Channel (FIDC)
6	110	Conditional Access (CA)
7	111	In house (except for Length 31)

Figure 3.30: List of FIGs

- Length: this 5-bit field shall represent the length in bytes of the FIG data field and is expressed as an unsigned binary number (MSb first) in the range 1 - 29.

Values 0, 30 and 31 shall be reserved for future use of the FIG data field except for 31 ("11111") when used with FIG type 7 ("111") which is used for the end marker.

- FIG data field

Generally, FIGs may be arranged in any order except where special operational requirements dictate otherwise. FIGs shall not be split between FIBs. An example of FIG type is shown below(fig 3.31).

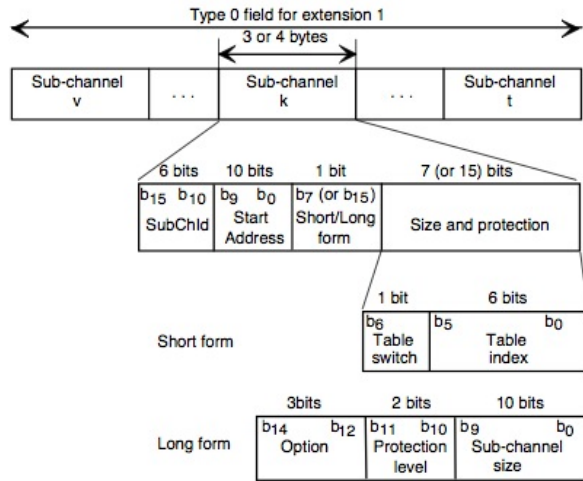


Figure 3.31: Structure of the subchannel organization field.

This image shows the structure of a FIB type 0 and FIG type 1 field, it is used for the subchannel organization. Each subchannel is defined by its own ID. As an example of the fields contained into a FIG data field we describe:

- SubChId(Sub-channel Identifier), this 6-bit field, coded as an unsigned binary number, shall identify a sub-channel.
- Start Address: this 10-bit field, coded as an unsigned binary number (in the range 0 to 863), shall address the first Capacity Unit (CU) of the sub-channel.
- Short/Long form: this 1-bit flag shall indicate whether the short or the long form of the size and protection field is used, (0:short form, 1:long form).

- Sub-channel size: this 10-bit field, coded as an unsigned binary number (in the range 1 to 864), shall define the number of Capacity Units occupied by the sub-channel.

The remaining fields are out of the aim of this documentation.

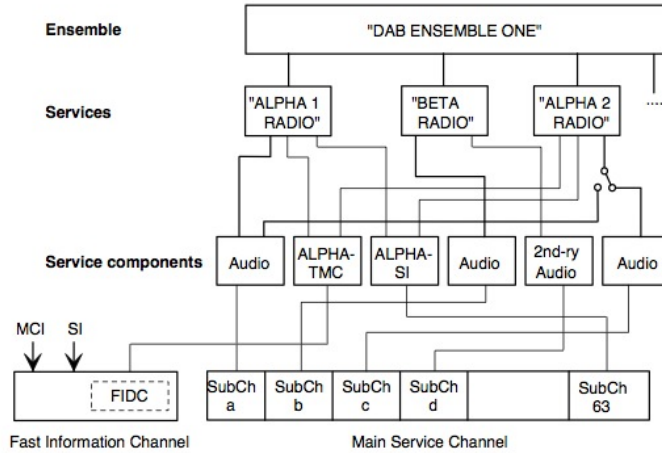


Figure 3.32: An example of the DAB service structure

The organization of the sub-channels, services and service components in an ensemble is managed by the MCI. The MCI serves five principal functions:

- To define the organization of the subchannels in terms of their position and size in the CIF and their error protection;
- To list the services available in the ensemble;
- To establish the links between service and service components;
- To establish the links between service components and subchannels;
- To signal a multiplex re-configuration.

As FIC symbols come in, they are processed. In each FIC data different FIG types are contained, usually these types are 0, 1 and 7. Once all the symbols into a frame has been processed, one structure for recovering the information is created. All services are stored which their respective service component. For each service component just one subchannel belongs, identified by its subchannel ID^[1]

3.10.1.3 Calculation of the CRC word

A 16-bit Cyclic Redundancy Check word is calculated on the FIB data field. The implementation of CRC-codes for data and audio transmission allows the detection of transmission errors at the receiver side. For this purpose CRC words shall be included in the transmitted data. These CRC words shall be defined by the result of the procedure described here. A CRC code is defined by a polynomial of degree n:

$$G(x) = x^n + g_{n-1}x^{n-1} + \dots + g_2x^2 + g_1x + 1, n \geq 1,$$

$$g_i \in \{0, 1\}, i = 1 \dots n - 1.$$

The CRC calculation may be performed by means of a shift register containing n register stages, equivalent to the degree of the polynomial. The stages are denoted by $b_0 \dots b_{n-1}$, where b_0 corresponds to 1, b_1 to x_1 , b_2 to x_2 , ..., b_{n-1} to x_{n-1} . The shift register is tapped by inserting XORs at the input of those stages, where the corresponding coefficients g_i of the polynomial are “1”.

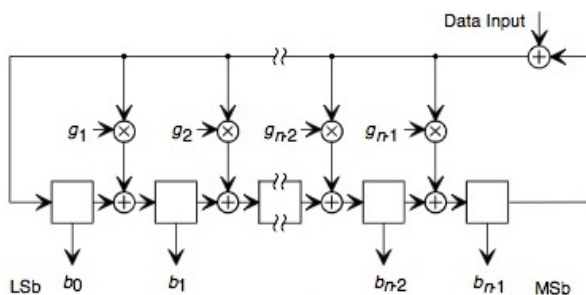


Figure 3.33: General CRC block diagram

At the beginning of each CRC word calculation, all shift register stage contents shall be initialized to "1". The CRC word shall be complemented (1's complement) prior to transmission. If the final output of the shift register and the CRC-check word in the DAB audio frame are not identical, a transmission error has occurred in the protected field of the audio bit stream.

After applying the first bit of the data block (MSb first) to the input, the shift clock causes the register to shift its content by one stage towards the MSb stage (b_{n-1}), while

loading the tapped stages with the result of the appropriate XOR operations. The procedure is then repeated for each data bit. Following the shift after applying the last bit (LSb) of the data block to the input, the shift register contains the CRC word which is then read out. Data and CRC word are transmitted with MSb first. The CRC codes used in the DAB system shall be based on the following polynomials:

$$G(x) = x^{16} + x^{12} + x^5 + 1$$

$$G(x) = x^{16} + x^{15} + x^2 + 1$$

$$G(x) = x^8 + x^4 + x^3 + x^2 + 1$$

Note that all CRCs has to be passed correctly to ensure a good reception of the data. For mode I, 3 CRCs for each FIB block have to be checked so in total 12 CRC are tested^[1].

3.10.2 Main Service Channel (MSC)

The MSC is a time-interleaved data channel used to carry the audio and data service components, together with possible supporting and additional data service components. The MSC is divided into a number of subchannels. Each of the subchannels is individually convolutionally coded with equal or unequal error protection. Each subchannel may carry one or more service components.

The MSC is made up of Common Interleaved Frames (CIFs). The CIF contains 55 296 bits. The smallest addressable unit of the CIF is the Capacity Unit (CU), comprising 64 bits. Therefore, the CIF contains 864 CUs, which shall be identified by the CU addresses 0 to 863. The MSC is divided into sub-channels. Each sub-channel shall occupy an integral number of consecutive CUs (and is individually convolutionally encoded). Each CU may only be used for one sub-channel. A service component is a part of a service which carries either audio or general data.

The data, carried in the MSC, shall be divided at source into regular 24 ms bursts corresponding to the sub-channel data capacity of each CIF. Each burst of data constitutes a logical frame. Each logical frame is associated with a corresponding CIF. Succeeding CIFs

are identified by the value of the CIF counter, which is signaled in the MCI . The logical frame count is a notional count which shall be defined as the value of the CIF counter corresponding to the first CIF which carries data from the logical frame^[1].

3.11 Audio Coding

MPEG-1 Audio Layer II (**MP2**) is the audio compressing format defined for DAB. It uses a lossy compression algorithm that was designed to greatly reduce the amount of data required to represent an audio recording and sound like a decent reproduction of the original uncompressed audio for most listeners. For transmission mode I the sampling rate is set at 48 kHz. The format is based on successive digital frames of 1152 sampling intervals with four possible formats:

- Mono format
- Stereo format
- Intensity encoded joint stereo format (stereo irrelevance)
- Dual channel (uncorrelated) format.

MP2 splits the input audio signal into 32 sub-bands, and if the audio in a sub-band is deemed to be imperceptible for the human auditory system then that sub-band is not transmitted.

Conversely MP2 shows a better behavior than MP3, in the time domain, due to its lower frequency resolution which implies less codec time delay (simpler editing) and native ruggedness to the digital recording and digital transmission errors.

Moreover, the MP2 sub-band filter bank provides an inherent transient concealment feature due to the specific temporal masking effect of its mother filter. This unique characteristic of the MPEG-1 Audio family codecs implies a very good sound quality on audio signals with rapid energy changes such as percussive sounds both on the MP2 and the MP3 codecs which use the same basic sub-band filter bank.

The simplified block diagram of the audio decoder in the receiver, shown in the following figure(3.34), accepts the DAB audio frame in the syntax defined later which is a conformant subset of the MPEG Audio Layer II.

This allows the use of an MPEG Audio Layer II decoder. The DAB audio frame shall be fed into the audio decoder, which unpacks the data of the frame to recover the various elements of information. The reconstruction block shall reconstruct the quantized sub-band samples. An inverse filter bank shall transform the sub-band samples back to produce digital PCM audio signals at 48 kHz sampling frequency^[1].

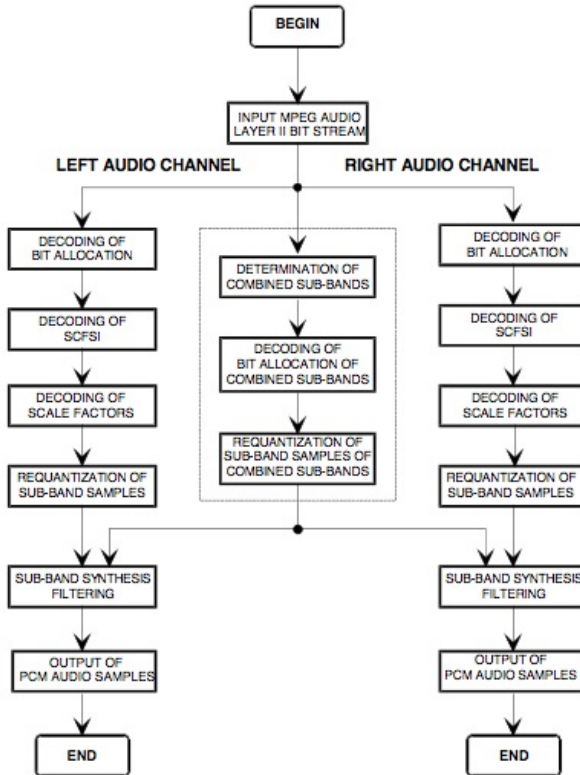


Figure 3.34: General MPEG Audio Layer II stereo encoder flow chart.

3.11.1 Formatting of the audio bit stream

The frame format of the audio encoder shall take the bit allocation, ScFSI(Scale Factor selection information), ScF and the quantized sub-band samples together with header information and a few code words used for error detection to format the MPEG Audio Layer II bit stream. It shall further divide this bit stream into audio frames, each corresponding to 1152 PCM audio samples, which is equivalent to a duration of 24 ms in the case of 48 kHz sampling frequency and 48 ms in the case of 24 kHz sampling frequency. The principal

structure of such an MPEG Audio Layer II frame with its correspondence to the DAB audio frame can be seen in figure 3.35.

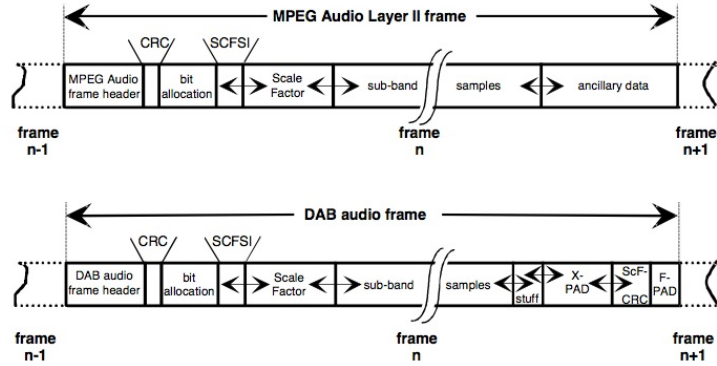


Figure 3.35: Frame structure of MPEG Audio Layer II and corresponding DAB audio frame.

Each audio frame starts with a header, consisting of a syncword and audio system related information.

A Cyclic Redundancy Check (CRC), following the header protects a part of the header information, the bit allocation, and the ScFSI fields. After the CRC follows bit allocation, ScFSI and Scale Factors. The sub-band samples, which will be used by the decoder to reconstruct the PCM audio signal, are the last audio data part in the MPEG Audio Layer II frame before the ancillary data field. This ancillary data field, which is of variable length, is located at the end of the MPEG Audio Layer II frame.

An adaptation of the MPEG Audio Layer II frame to the DAB audio frame is performed in order to introduce:

- specific DAB Scale Factor Error Check (ScF-CRC);
- a fixed and a variable field of Programme Associated Data (F-PAD and X-PAD).

The first four bytes of the DAB audio frame contain the MPEG Audio header. This header carries information for the audio decoder. In the DAB system, some of this information is currently defined as static information. This is:

- Syncword(set to external synchronization of the audio decoder).
- Layer: set to Layer II (layer = Layer II).

- protection_bit: set to CRC protection on.

3.11.2 CRC check for audio side information

A CRC-check word for detecting errors within the significant side information of a DAB audio frame has been inserted in the bit stream just after the DAB audio frame header.

The error detection method used is "CRC-16" whose generator polynomial is:

$$G_1(x) = x^{16} + x^{15} + x^2 + 1$$

The bits included into the CRC-check are:

- 16 bits of DAB_audio_frame_header(), starting with bit_rate_index and ending with emphasis;
- a number of bits of audio_data(), starting with the first bit. These bits include bit allocation information and ScFSI.

The initial state of the shift register for the calculation of the CRC is "1111 1111 1111 1111". If the final output of the shift register and the CRC-check word in the DAB audio frame are not identical, a transmission error has occurred in the protected field of the audio bit stream^[1].

Frame structure of coded bit stream: valid for 1152 PCM audio input samples (stereo mode)

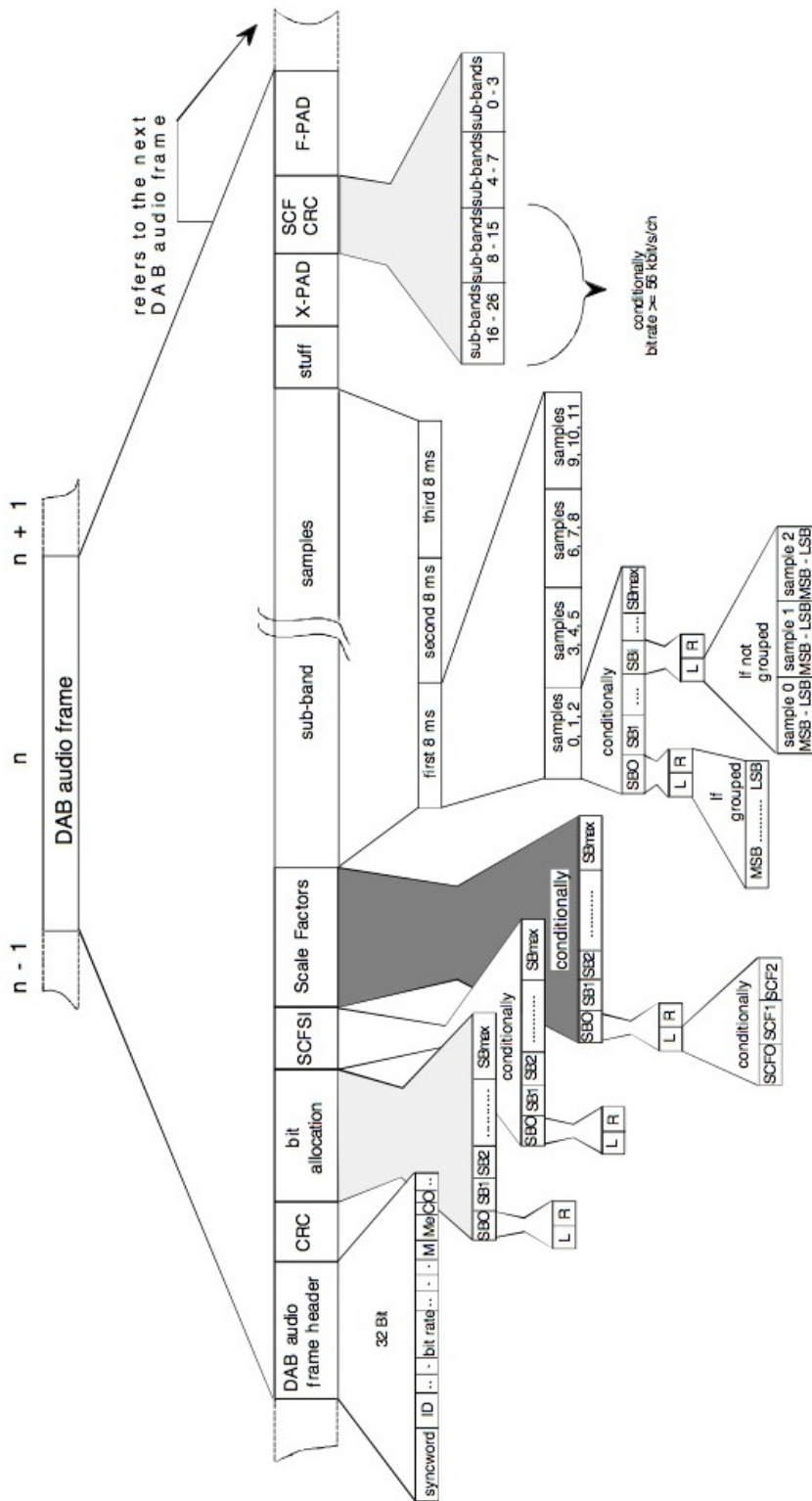


Figure 3.36: Frame structure of MPEG Audio Layer II

Chapter 4

Hardware implementation of the DAB demodulator

4.1 An overview to CoolFlux BSP

The implementation of our application was done on the CoolFlux BSP(Baseband Signal Processor) version 1.1.0, an embedded ultra low power C-programmable Baseband Signal Processor core which targets low-power communications baseband processing. The core is based on the similarly named CoolFlux DSP, which was designed for use in low-power audio applications and was introduced in 2004. This core, relative to the older one version, has been enhanced to increase its performance in baseband processing while retaining a small footprint and low power.

The CoolFlux BSP core will run at 290 MHz; power consumption (for the core only) is about 20 mW at 1.2 volts and 290 MHz in a 65 nm process. The core is designed to be used as a co-processor or in standalone mode, and can also be used as part of a multi-core system.

The CoolFlux BSP's 24-bit width is a holdover from the CoolFlux DSP: audio-oriented processors often use 24-bit data paths as a compromise as 24-bit data eases implementation of high-fidelity audio algorithms relative to a 16-bit machine, and reduces area and power

relative to a 32-bit design. As described below, the CoolFlux BSP can split its 24-bit data path into two 12-bit paths to increase computational throughput.

The CoolFlux BSP issues a single 32-bit instruction word per cycle, and enables an orthogonal instruction set and efficient C compiler. Unlike many DSPs, CoolFlux BSP does not offer a separate compressed, 16-bit instruction set. Wide instruction words often lead to high program memory use, which in turn can increase chip size and power consumption. The BSP has several features to keep code size low: multiple operations can be encoded in a single instruction to reduce code size on tasks that are parallelizable, and for sequential code, the core supports an instruction mode that essentially allows two 16-bit instructions to be packed into a 32-bit instruction.

As shown in figure 4.1, the CoolFlux BSP, includes two 24x24-bit multiply-accumulate (MAC) units; two 24/56-bit ALUs and one 24-bit ALU; two 24-bit data memories and a 32-bit program memory; and two address generation units. The key difference is that the new core supports three modes of operation rather than just one: scalar (used in the CoolFlux DSP core), SIMD, and complex. The mode is determined based on the class of instruction used and a status bit.

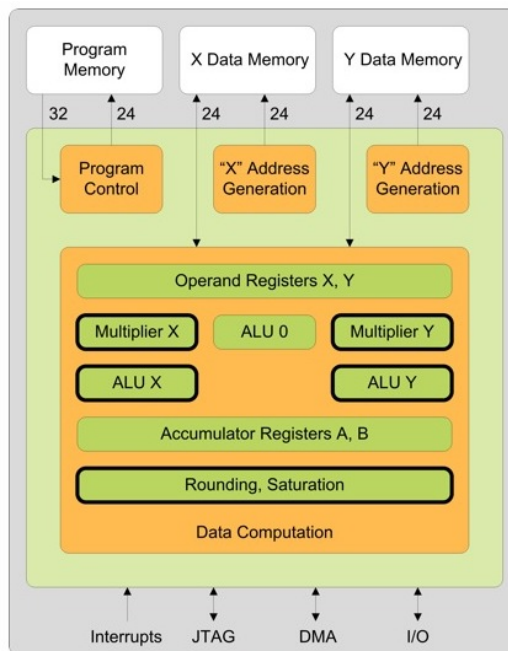


Figure 4.1: CoolFlux BSP architecture

In SIMD mode, each MAC unit (or ALU) is split such that it executes two 12-bit operations (the 56-bit ALUs can also perform dual 28-bit operations). In complex mode, the processor treats input data as a complex number with real and imaginary components, which can be 12 or 24 bits wide. The core can perform, for example, 12-bit complex multiplication (i.e., four real multiplications and two additions, as shown below) in two cycles, with single-cycle throughput:

$$(A_r \cdot B_i) + (A_i \cdot B_r), (A_r \cdot B_r) - (A_i \cdot B_i)$$

The core also explicitly supports complex addition and subtraction

$$(A_i + / - B_i, A_r + / - B_r)$$

and can execute 24-bit complex calculations (with lower throughput). The BSP supports a range of specialized instructions for SIMD arithmetic, complex arithmetic, FFTs, Viterbi processing, and the CORDIC algorithm.

The new SIMD and complex math capabilities enable the core to calculate two taps per cycle for a 12-bit complex FIR filter, for example, or execute a 12-bit (with 28-bit intermediate results) radix-4 256-point complex FFT in 2480 cycles. (By way of comparison, the CoolFlux DSP core requires 8930 cycles for a 24-bit (with 56-bit intermediate results), radix-2 FFT.) Overall, the SIMD and complex modes provide a significant speedup across a range of algorithms, but because they are 12-bit operations, the speedup comes at the cost of precision and dynamic range.

Like with the CoolFlux DSP, CoolFlux BSP has to be programmed in C. It has added C language extensions to support complex data types and SIMD data types, along with intrinsics for complex and SIMD functions.

The BSP has some unusual features, particularly its complex, 12-bit computational capabilities. Perhaps a key question is whether 12 bits is enough for many baseband operations. Based on several own analysis, their developers believe that it is particularly because the core can use larger intermediate results to maintain precision. And when it is not, users can switch to the (slower) 24-bit mode. How well customers are able to make use of the

cores' maximum throughput (using 12-bit data) will have a big effect on the performance they are able to squeeze out of the core^[16].

Power Consumption:

$31 \mu \text{ W/MHz} @ 0.8 \text{ V}$ (65 nm CMOS)

$70 \mu \text{ W/MHz} @ 1.2 \text{ V}$ (65 nm CMOS)

$40 \mu \text{ W/MHz} @ 0.8 \text{ V}$ (90 nm CMOS)

$90 \mu \text{ W/MHz} @ 1.2 \text{ V}$ (90 nm CMOS)

$53 \mu \text{ W/MHz} @ 0.8 \text{ V}$ (130 nm CMOS)

$120 \mu \text{ W/MHz} @ 1.2 \text{ V}$ (130 nm CMOS)

$390 \mu \text{ W/MHz} @ 1.8 \text{ V}$ in (180 nm CMOS)

Performance (Worst Case Commercial Conditions, standard VT):

$150 \text{ MHz} @ 1.8 \text{ V}$ 180 nm CMOS

$190 \text{ MHz} @ 1.2 \text{ V}$ 130 nm CMOS

$245 \text{ MHz} @ 1.2 \text{ V}$ 90 nm CMOS

$300 \text{ MHz} @ 1.2 \text{ V}$ 65 nm CMOS ($>5000 \text{ MOPS peak}$)

4.1.1 Baseband Signal Processor(BSP)

In telecommunications and signal processing, baseband is an adjective that describes signals and systems whose range of frequencies is measured from zero to a maximum bandwidth or highest signal frequency; it is sometimes used as a noun for a band of frequencies starting at zero.

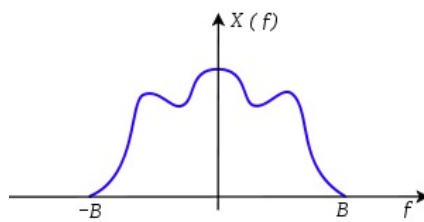


Figure 4.2: Spectrum of a baseband signal, amplitude as a function of frequency.

A signal at baseband is often used to modulate a higher frequency carrier wave in

order that it may be transmitted via radio. Modulation results in shifting the signal up to much higher frequencies (radio frequencies, or RF) than it originally spanned. A key consequence of the usual double-sideband amplitude modulation (AM) is that, usually, the range of frequencies the signal spans (its spectral bandwidth) is doubled. Thus, the RF bandwidth of a signal (measured from the lowest frequency as opposed to 0 Hz) is usually twice its baseband bandwidth. Steps may be taken to reduce this effect, such as single-sideband modulation; the highest frequency of such signals greatly exceeds the baseband bandwidth^[24].

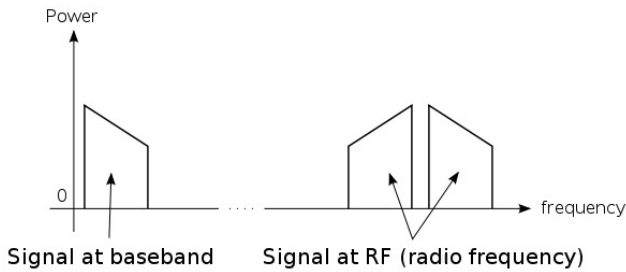


Figure 4.3: Comparison of the equivalent version of a signal and its AM-modulated RF version, showing the typical doubling of the occupied bandwidth.

4.1.2 DAB as a Real Time Application

A system is said to be real-time if the total correctness of an operation depends not only upon its logical correctness, but also upon the time in which it is performed. This was one of the main problems of the DAB implementation on the FPGA.

If the demodulator were not fast enough for processing all the OFDM symbols within the duration of one frame some data might be lost. Recall that the duration of one frame for DAB mode I is 96 ms. Due to this time constraint, some problems arose once we tested the code on the FPGA.

4.1.3 DAB hardware definition

Once all the software development process has concluded it is time to dump the code into the actual hardware to test it in real time. Up until now, the correctness of the code has been proved by means of the Target Simulator^[20]. First of all, the processor data path

must synthesized on the FPGA. The hardware description language chosen for this task has been VHDL. Special care was taken in considering the memory requirements. The quantity of memory of an embedded system is a critical aspect that must be taken in mind. Before mapping the actual memory into the FPGA we worked out the memory requirements for the design, taking into account the total memory of the FPGA and the worst case of the demodulation process (which corresponds to that of the maximum subchannel size at the maximum bit rate).

Once the FPGA was correctly configured and the software loaded on, the next step was to connect the FPGA with the external world and the debugger. A detailed description can be found below.

MATLAB Simulink proved to be an essential tool for easily interconnecting the FPGA with the rest of the hardware (oscilloscope, tunner, debugger, etc). In picture 4.4 we can see the global structure of the architecture during the first iteration of development process.

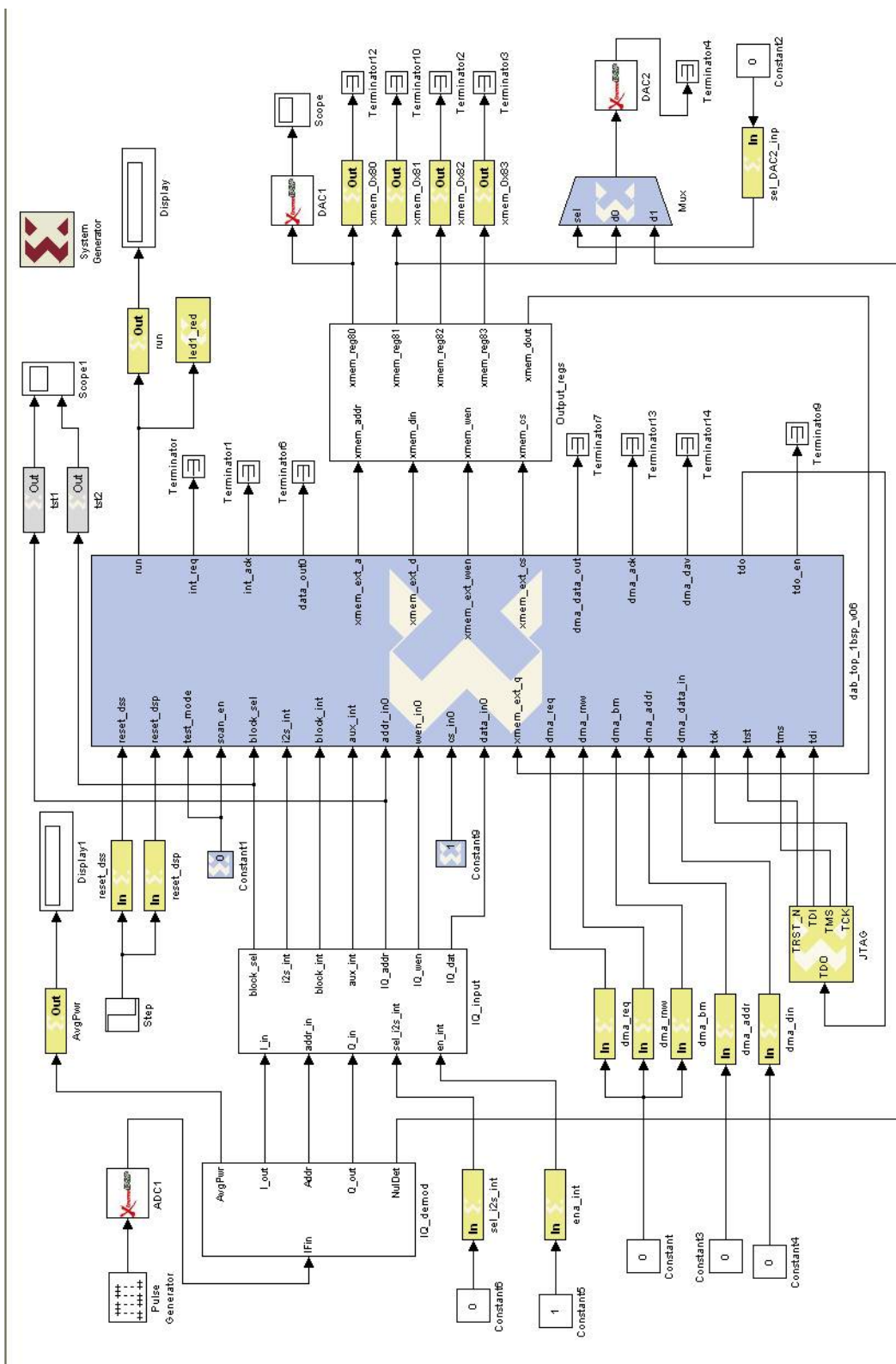


Figure 4.4: Simulink structure for DAB

In the picture, the main module -in blue- is the macro definition generated from the VHDL code for 1 BSP which, once the code has been synthesized is considered a black box system and cannot be modified within Matlab alone. The first very modest goal was to synchronize our demodulator with the broadcaster (not to listen at the actual sound), and so one BSP was enough for this task. Below we will present the complete datapath with the three BSPs.

It is not in the scope of this project the design of the hardware outside the FPGA so we shall limit ourselves to comment out these components from a bird sight. The oscilloscope is an essential device in order to debug the system in real time. On the oscilloscope we can study the shape of the desired signal in the time domain. The oscilloscope used for this project has two channels. What we want to show at the output channels in the oscilloscope must be previously selected through the sources ‘constant5’ and ‘constant6’ shown on the last scheme. A pulse generator is necessary as an input for the Analog Digital Converter as we can see at the top left of the image. This pulse generator marks the sampling rate of the input signal. There is also a JTAG module for testing purposes (later on we shall explain how it works).

IQ_demod schema corresponds with the AGC algorithm and Null Detection. The following module IQ_input takes the IQ signal coming from the AGC and writes the corresponding samples into the specified address(addr_in). These samples will be the input to the BSP.

Output_regs contains a set of registers where the values at the output of the BSP are allocated. They are connected to the scopes or else as an input to the BSP, returning the address of the next available word.

As can be seen in the picture, some scopes were added within the data path in order to facilitate the debugging process. These scopes can generate a graph with the required signals. Although they turned out to be quite helpful, these are not enough for completely debugging the program. The debugger provided by Target^[20] is essential in order to see the state of the DSPs -essentially registers and memories-. The debugger itself allows us to pause the execution at any time and check what is inside of each word of memory in such moment, or even dumping the content of the memories to a graph. Of course, whenever you

pause the real time execution, you might lose the synchronization with the transmitter. In this case, after watching at the desired state elements, the program might be reset, which means that the data structures of the demodulator must be properly initialized and another coarse synchronization must be performed.

4.1.4 Components Description

What follows is a technical description of the hardware components required to demodulate the radio signal.

4.1.4.1 Maxim 2172 v1.0.25

The MAX2172 direct-conversion to low-IF tuner for Digital Audio Broadcast is designed for digital audio broadcast and terrestrial digital multimedia broadcast (T-DMB) applications, covering an input frequency range of 168MHz to 240MHz (VHF-III), 1452MHz to 1492MHz (L-band), and also 87MHz to 108MHz (FM). The MAX2172 achieves a high level of component integration, allowing low power, and tuner-on-board designs. The direct-conversion to low-IF architecture eliminates the need for an IF-SAW filter while providing a balanced 2.048MHz center frequency baseband output to the demodulator.



Figure 4.5: MAX2172 Tuner

A sigma-delta fractional-N synthesizer is incorporated to optimize both close-in and wideband phase noise performances for OFDM applications where sensitivity to both 1kHz phase noise and wideband phase noise related to strong adjacent can be a problem [21].

This component allowed us to select the different channels of the digital radio broadcasters. In the area of Leuven, where this project was developed, two radio channels could

be selected which corresponded with both the flemish and the french emission. It turned out that both signals had more or less the same quality.

4.1.4.2 Tektronix TDS210

Tektronix TDS210 is a two channel digital real time oscilloscope used for testing. Offering an unbeatable combination of performance, reliability and versatility, the TDS200 Series offers breakthrough digital and real-time advantages.

By sampling at 10 and 16 times their bandwidths on all channels, the TDS200 Series oscilloscopes provide accurate real-time acquisition up to their full bandwidth.

Digital storage technology supports features including automatic measurements, peak detect, storage of two reference waveforms and five instrument setups and autoset. Peak detect and high sample rates minimize aliasing while capturing waveform details useful for the user.

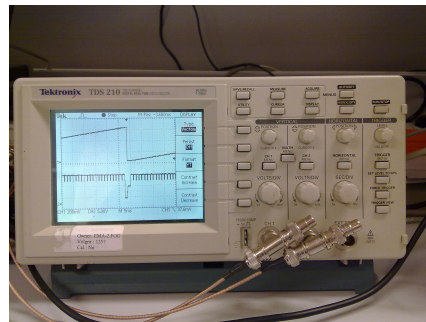


Figure 4.6: Tektronix TDS210 two channel digital real time oscilloscope

The user interface is similar to that of an analog oscilloscope, but with improvements that reduce learning time and increase efficiency. Knobs and buttons are grouped by function and provide direct access to controls, and each vertical channel has its own dedicated scale and position knobs. Readouts or menus are displayed on-screen at all times, allowing users to more quickly and accurately determine instrument settings. The display responds quickly to control adjustments and has a fast update rate^[25].

With this instrument we could carry out the testing, checking in real time the values from the input signal, registers and variables.

4.1.4.3 FPGA Board Virtex XC4VLX100

Simulation on real time of the DAB demodulator was done in an FPGA Board Nallatech by loading the data through the CoolFlux Debugger version 1.1.0.

Nallatech has its own API, FUSE, to manage the configuration, control, and communication with the rest of the system. With it comes Dimetalk that for some functions transform restricted type of C code, DIME-C, into VHDL and can generate the communication network between the various algorithm blocks, memory blocks I/O interfaces^[22].



Figure 4.7: FPGA Board Virtex XC4VLX100

4.1.4.4 PE 1542 DC Power Supply Philips

The PE 1542 is a stabilized D.C. power supply designed for supplying and testing electrical and electronic circuits. It produces three precise output voltages, which are galvanically separated. All outputs are protected against short circuit. Regulation of each output is achieved by transistor series-regulator stages. The transistor series-regulator gives continuously variable adjustments of the output voltages and currents with good accuracy and stability with minimum ripple. By means of control, each output voltage can be continuously varied from 0V to 20V or 7V, depending upon the channel^[23].

In our case a power of 3V was used.

4.1.4.5 Hewlett Packard 8596E Oscilloscope

The HP Agilent 8596E is an easy-to-use microwave Spectrum Analyzers with 9 kHz to 12.8 GHz range, that offers a wide range of performance, features, and optional capability to meet the measurement needs^[31].

This instrument allows us to visualize the radio signal broadcasting for the area of Belgium.

4.1.4.6 CoolFlux simulator, CoolFlux debugger, Chess compiler

Development toolkit designed and provided by NXP Semiconductors, with the architecture explained in the chapters above.

4.1.4.7 Reception Antenna

We employed a simple omnidirectional antenna. An electromagnetic field from any direction induces an alternating current at the antenna's terminals.

During the simulations of the DAB we could appreciate the phenomenon of multipath propagation (described earlier). Even somebody moving around the antenna could cause the signal to be attenuated. It could happen that due to hard signal distortions, the receptor might get desynchronized with the emitter. In this case, a resynchronization might be required.

4.1.4.8 JTAG(Joint Test Action Group)

Although it was originally designed for testing printed circuit board assemblies, today JTAG is also used for accessing sub-blocks of integrated circuits, making it an essential mechanism for debugging embedded systems which may not support any other debug-capable communications channel. Embedded systems development relies on debuggers talking to chips with JTAG to perform operations like single stepping and breakpointing^[35].

A JTAG interface is a special four/five-pin interface added to a chip, designed so that multiple chips on a board can have their JTAG lines daisy-chained together if specific conditions are met, and a test probe need only connect to a single "JTAG port" to have access to all chips on a circuit board. The connector pins are:

- TDI (Test Data In)
- TDO (Test Data Out)
- TCK (Test Clock)

- TMS (Test Mode Select)
- TRST (Test Reset) optional

Test reset signal is not shown in picture 4.8.

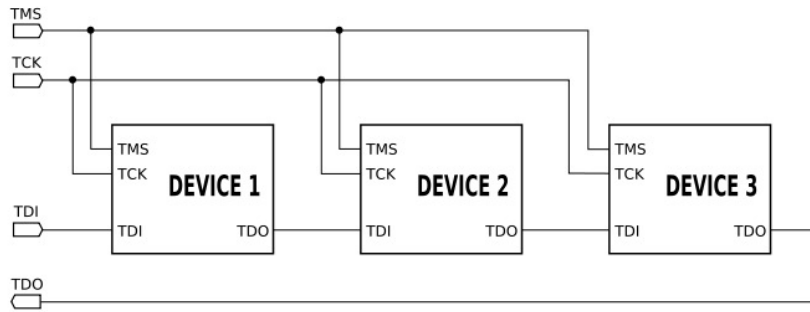


Figure 4.8: JTAG interface.

Since only one data line is available, the protocol is necessarily serial. The clock input is at the TCK pin. Configuration is performed by manipulating a state machine one bit at a time through a TMS pin. One bit of data is transferred in and out per TCK clock pulse at the TDI and TDO pins, respectively^[35].

The connection between different hardware components is shown in the schema 4.9:

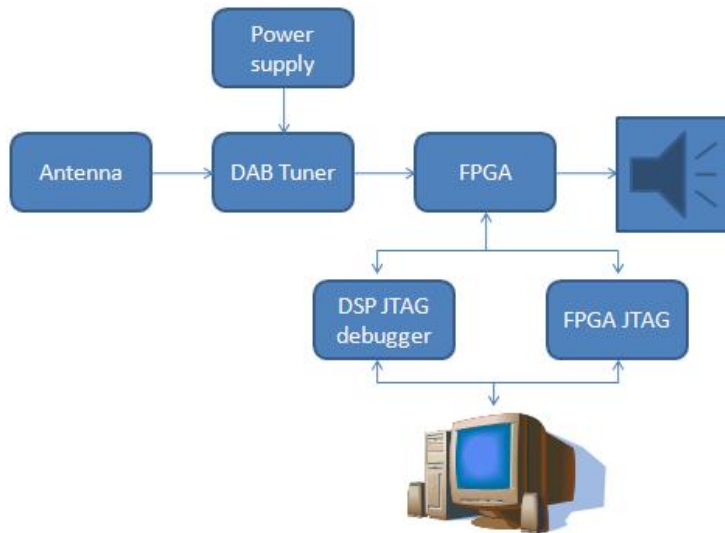


Figure 4.9: Components connection.

4.1.5 DAB demodulator datapath

The implementation of the DAB was done with several CoolFlux BSP cores due to the frequency constraints imposed by the FPGA Board. Whereas one CoolFlux BSP is able to run at 290 MHz in a real implementation, our FPGA runs at a maximum speed of about 50 MHz. The CoolFlux BSP has a CPI (Cycles per Instruction) of 1. Therefore, each BSP mapped on the FPGA might not process more than 50 MIPS.

The total amount of MIPS required for demodulating a DAB signal after several optimizations turned out to be around 80 (future improvements are expected to reduce this number). It might be expected that with two cores it would be possible to demodulate the signal in real time. However, the fact of having more than one core increases the number of MIPS due to the overhead of transferring the data amongst each other. Thus, the decision was to split up the demodulation chain into three DSPs. From now on, we shall refer them as BSP_0 , BSP_1 , BSP_2 .

It might not seem obvious that the separation of the functionality into 3 BSPs was not just a matter of dividing the code into serial-connected modules which pass the data from one to another. Memory requirements is another important issue to take care of. In a system on chip (SoC), the memory occupies essentially all the area of the chip, in comparison with the processing elements. Thus, the division was also made attending to the memory size available for set of processing modules^[17] .

The final division of the processing modules is shown in the next picture:

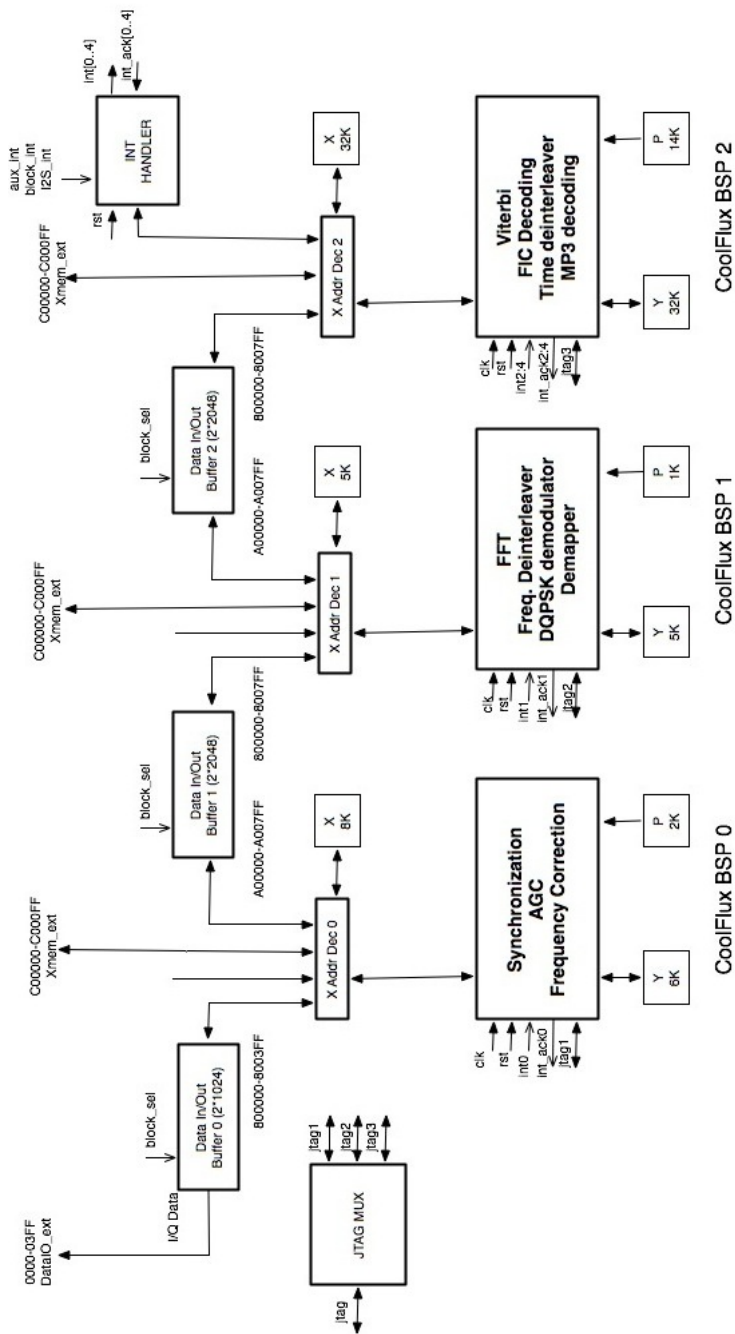


Figure 4.10: DAB Architecture.

Around the three BSP instances, several modules ensure the data flow between the different BSP's and from input to output. The I/Q data provided by the zero IF DAB front-end has to be stored into buffer 0. A couple of alternating buffers are present between each pair of cores.

There is a common JTAG module to access the three CoolFlux BSP instances.

Each BSP has its own local memory and an address decoder for X memory (see image 4.11). Each BSP has also an interrupt controller. When all data has been processed, the last core writes the output data (often audio) to customer-specific circuitry by using the external memory X as the output interface. Complex data-flow done in hardware is bi-directional. The next sections further detail the interconnection of the modules.

4.1.6 Local memories

Each CoolFlux BSP instance has three local memories(P, X and Y) . The memory sizes used in the design are described in the next table:

Instance	Memory	Size
CoolFlux BSP instance 0	P Memory	2 Kwords (0x000000-0x0007FF)
	X Memory	8 Kwords (0x000000-0x001FFF)
	Y Memory	6 Kwords (0x000000-0x0017FF)
CoolFlux BSP instance 1	P Memory	1 Kwords (0x000000-0x0003FF)
	X Memory	5 Kwords (0x000000-0x0013FF)
	Y Memory	5 Kwords (0x000000-0x00013FF)
CoolFlux BSP instance 2	P Memory	14 Kwords (0x000000-0x0037FF)
	X Memory	32 Kwords (0x000000-0x007FFF)
	Y Memory	32 Kwords (0x000000-0x007FFF)

Figure 4.11: CoolFlux DAB Local memories

4.1.7 Debug interface

Each instance of the CoolFlux BSP has a debugging unit. There is however only one JTAG interface that can communicate with any of these three instances. To do the multi-core debugging, a multi-core debugger was necessary, which was provided by NXP Semiconductors.

Each CoolFlux BSP instance has four hardware breakpoints. It is possible to stop all cores when any of the instances has hit a hardware breakpoint. In the multi-core debugger, it is possible to export a breakpoint from one core to another, which allows us to debug the BSP cores together in a relatively simple way.

When selecting Breakpoint for the BreakOut signals and BIO for the BreakIn signals, all instances of the CoolFlux BSP are interconnected and they all stop when one of the instances has hit a hardware breakpoint.

4.1.8 Interrupt interface

Each CoolFlux BSP instance has an interrupt controller. All interrupts go directly to the interrupt controller and it ensures that all interrupts are handled correctly and follow the priority scheme. The priority is taken when more than one interrupt is waiting to be handled. Once an interrupt is ongoing, it will not be interrupted by a higher priority interrupt, unless explicitly written in the software.

The interrupt controller detects a rising edge on the interrupt lines and the duration of the interrupt can be as small as one clock cycle.

Each BSP can generate an interrupt in its neighboring BSPs by writing to a certain I/O location. The interrupt is generated independently of what value was written. The table 4.12 indicates the mapping:

Interrupt Line	From BSP0	From BSP1	From BSP2
To BSP0	NA	0x20	NA
To BSP1	0x21	NA	0x20
To BSP2	NA	0x21	NA

Figure 4.12: CoolFlux DAB Interrupt generation IO addresses

4.1.9 Shared Buffers

We need some mechanism for communicating the input customer-specific circuitry with the first BSP and the BSPs between each other. To deal with this problem we were provided with a VHDL instance consisting of a couple of alternating shared buffers as shown in picture 4.13.

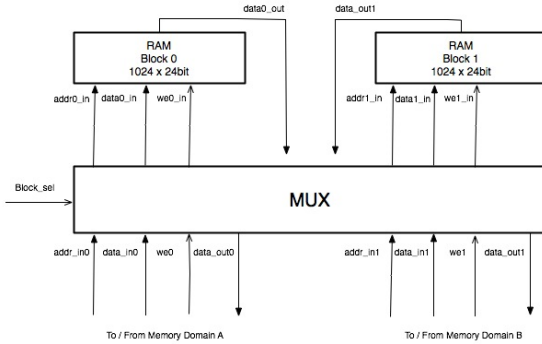


Figure 4.13: Shared buffer architecture

Each shared buffer connects two hardware modules in the design. The first shared buffer is between customer-specific hardware and CoolFlux BSP instance 0. The second shared buffer is between the CoolFlux BSP instance 0 and CoolFlux BSP instance 1. The third shared buffer is between the BSP_1 and BSP_2 . Each shared buffer contains 2 synchronous, physically independent, memories. The memories of shared buffer 0 are of 1024 word of 24 bits. The memories of shared buffer 1 and 2 are of 2048 words of 24bits.

While one memory is being accessed by one hardware module in block 0 memory domain, the second memory can be accessed by the second hardware module in block 1 memory domain.

At some point in time, this order can be changed. At that moment the second memory is accessed by the first hardware module, while the first memory can be accessed by the second hardware module.

This change is controlled by the signal `block_sel`. When this signal changes its value, the connections between two memories and the two interfaces of the shared buffer are swapped, so that there will never be a clash between the memories and the hardware modules. Note that for the running program, the addressing space always remains the same, independently of the actual physical memory that is being read. The memory block switching is hidden for the software.

This peripheral toggles the data buffers when the corresponding IO register is written. The buffers are toggled independently of what value was written. Each BSP can toggle any of its shared buffers by writing to a certain IO location.

The first BSP starts receiving the IQ data signal from the input buffer. The even and odd words of the input buffer keep the in-phase and quadrature components of the signal, respectively. The input buffer has space for a total of 512 IQ samples. When the input buffer is full, an interruption is triggered to swap the two input buffers. When the first BSP has finished to perform its tasks, it triggers a signal to activate the next BSP within the chain.

In sum, each BSP starts working as soon as it receives a signal from the previous BSP or a hardware interruption (only applicable for BSP_1).

Note that the total memory of the Board was just around 45KB, so all this space had to be divided and shared between the modules.

4.2 Description of the BSP instances

The aim of this section is to explain in more detail the BSP cores.

4.2.1 BSP_0 : Synchronization, Time correction, Save OFDM symbols

This BSP is responsible for the most arduous task in terms of signal processing, the synchronization of the input signal. The input to this BSP comes from the sampled radio signal, and once is processes by the synchronization algorithms, it is sent to the next BSP.

The first task of this BSP is to initialize all the data structures of the demodulator and in turn enable the interruptions. If the interruptions were set up before initializing the aforementioned data structures, an interruption could occur (thus starting the demodulation process) before all the parameters of the demodulator have the right values. In short, interruptions start disabled and are enabled after the initialization of the DAB data structures.

During the very first tests of the system in real time we had to face up a problem: the rate at which the demodulator processed the samples in the input buffer was slower than the sampling rate of the incoming signal, therefore the stored symbols in the input buffer were overwritten by the new samples before being processed. For avoiding this problem,

the first and obvious idea was merely to increase the memory, but the size necessary to buffer every OFDM symbol without losing data was 16K words, and this was inconceivable for the project.

A synchronous state machine was created with the aim of saving memory in the first BSP. In this way, instead of working with an ancillary buffer, the input buffer served both as input/output to/from the AGC and in turn as input to the Null Symbol Detection algorithm.

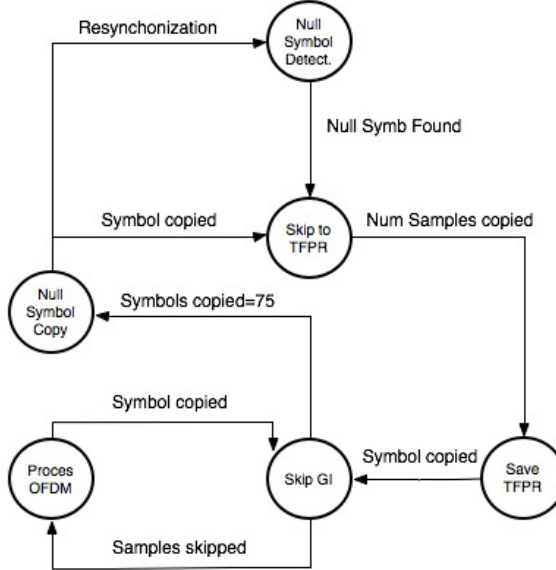
The synchronization processor mainly consists of two loops. The first is run when an interruption is received and computes the Automatic Gain Control with the help of the aforementioned state machine (both of which amplify the signal and store back the data into the input shared buffer). The other one is placed into the main call of the processor and applies the frequency and phase corrections.

When the BSP_0 has nothing to do, it is put into sleep mode (called by the function *sleep()* in the main loop). When the TFFR symbol has been copied to BSP_1 , BSP_0 starts with the calculation of the phase and frequency error and performs the corresponding correction.

Once the input buffer is full with IQ samples, a gain factor is applied to the input complex data, as we explained before. Normally, the gain factor is within the range $\{-2, 2\}$.

Each word of the input buffer stores either the in-phase or quadrature components of the signal successively. Thus, for each interruption a total of 512 samples are processed. Therefore, 512 is the maximum number of samples each state has to deal with. For this reason, if it were necessary to process a complete OFDM symbol (for example 2656 samples in the case of the null symbol), several loops in the same state had to be performed (in the case of the null symbol $2656/512 = 5.18$, so 6 loops must be executed).

In the next picture (4.14) we can see how the SM works:

Figure 4.14: State machine for BSP_0

- **NULL_DETECTION:**

This is the initial state, where the coarse time synchronization takes place (or a resynchronization if some problem occurs). As explained above, this state detects a drop in the signal for recognizing the null symbol. Since the input signal needs some time to be established (the gain must be adjusted to deal with the average power of the incoming signal), it is preferable to wait some frames before starting with the detection. Thus, our decision was to discard the first four null symbols.

Each time we are in this state, the minimum size between the maximum number of samples (512) and the remaining samples (if it were the case) are analyzed, as explained before.

The following pseudo-code illustrates this idea:

```
if state=NULL_DETECTION then
    usedSamples = min(remainingSamples, SamplesToSkip);
    remainingSamples -= usedSamples;
    SamplesToSkip -= usedSamples;
    buffer_pointer += usedSamples;
    if SamplesToSkip = 0 then
        Vars_state_Y = SamplesToRead;
        dab_nextState = state_Y;
    end if
end if
```

When the null symbol is found, the state machine jumps to the following state and the set of samples remaining from the end of the Null Symbol to the beginning of the TFPR Symbol (which is called WinOffsetNullSymbol) are discarded.

When a resynchronization is needed, every parameters in the DAB global register are reinitialized, and the processor starts executing in this state.

- **NUL_COPY:**

After recognizing the beginning of the signal, all BSPs are going to start working, but no one has information about the progress of the previous one, so we should implement some kind of control signal for verifying that everything is going correctly.

In this case, BSP_1 should know whether we are synchronized with BSP_0 or not. The way of doing that is by copying a special known symbol into the shared memory before writing the TFPR symbol, indicating the beginning of a frame. Immediately after that, an interruption is sent to BSP_1 , which indicates it to start processing.

In the future, the verification information might be managed also by interruptions.

- **SKIP_TO_TFPR:**

Once we have sent the signal to the following BSP, we continue by skipping the samples between the Null Symbol and the TFPR Symbol.

This is the time for applying the frequency correction of the frequency error calculated in the previous loop. In turn, the synchronization calculations performed during the current frame will be applied in the next one. This frequency correction is the same for every symbol in the ensemble.

- **SAVE_TFPR_FRQ_COR:**

With the new value of the frequency correction, a phase correction is applied to the TFPR Symbol. This symbol is also copied to the shared memory as will be done with the rest of the symbols.

The TFPR symbol is written twice in different buffers. One will be passed to the next core (BSP_1) and will be used as the previous symbol for the differential decoder (see last chapter). The other one is necessary because of its role as a synchronization symbol, and is used in the main loop. It is not possible to reuse this space of memory, because they have different life cycles, and when the TFPR symbol is used by BSP_1 , BSP_0 has already overwritten it.

Note that since the length of a symbol is bigger than 512 samples, this state is for sure executed more than once.

- **SKIP_GI:**

This is the state responsible of skipping the Guard Interval samples. For these samples, a different algorithm of Frequency correction is applied which is called Fast Frequency Correction and differs from the ordinary frequency correction algorithm in that it just adjusts the phase without using the Sine and Cosine Table. This algorithms allowed us to reduce the memory requirements and the processing time.

- **PROCESS_OFDM:**

Symbols are copied into the shared buffer, and then a signal is sent to BSP_1 . The frequency correction is also applied here.

In this BSP every subchannel is saved, as at this time we still do not know which ones are going to be used when the user selects a subchannel.

4.2.2 BSP_1 : FFT, Deinterleaving, Demapping

Once the signal is synchronized, the second BSP just have to start demodulating it when required, that is when a certain value is received as entry, in our case 0000FFFF FFFF0000. This entry is the one written in NULL_COPY state.

Since this value can never exist in digital signal, the recognition of this pattern will indicate the beginning of the new frame and can not be mistaken for a radio signal. This BSP is a module consisting of a chain of algorithms as explained in the figure 4.15:

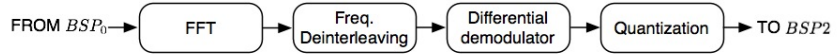


Figure 4.15: BSP_1 modules

The FFT requires all the input data ready by the time it starts running, so the 2048 words have to be written in the input buffer before the activating interruption is received. Note that the FFT is computed for the TFPR symbol again.

The last BSP needs to get all the ensemble but the Reference Symbol. To make sure the others are sent in the appropriate order, it is necessary to write into the shared buffer between the second and the third BSP which symbol has been processed.

After performing the quantization of the input stream, we obtain 1536 words out of 2048, so we can use the remaining space as extra space for any other task (recall that in a SoC, any available block of memory is quite welcome, even at the cost of complicating the code). In our case we just rewrite the number of the symbol in the 1536th position into the buffer. Following the same methodology an interruption is signaled to BSP_2 to make it start running once this BSP is done.

Throughout the implementation of this module, we had to face up some problematic issues concerning the processing time. Gradually, we added to the chain the modules illustrated in figure ?? taking into account the number of million of instructions per second (MIPS) each one contributed to the total time available for this core. Thanks to the compiler, we could further optimize the FFT and the quantization algorithm. In this way, we could fit the FFT, the frequency deinterleaver, the differential demodulator and the quanti-

zation to this BSP, thus liberating the last BSP (which was already quite overloaded) from performing even more computations.

4.2.3 *BSP₂: FIC and MSC Decoding. Audio decoding*

This is the last core of the three, and so at the end it must output the raw audio for being reproduced by customer-specific circuitry.

This first thing this processor does is to buffer all the OFDM symbols that conform the FIC. When the whole FIC data has been buffered, it is subjected to further processing (in turn the de-puncturing, viterbi and unscrambling modules). Once the FIC has been demodulated we extract the actual information from it. This information is stored in memory in a structure referred to as *FicInfo*. Recall from last chapter that the FIC gives us information about the subchannel configuration and services. This information includes the subchannel sizes, start and end addresses and so on. Hereinafter, the user might select one subchannel and the demodulation of the MSC begins. We only perform the demodulation of the OFDM symbols that form the subchannel, ignoring the rest of symbols. In other words, the symbols before and after the selected subchannel are skipped.

The demodulation of the MSC is slightly different from that of the FIC since now we must carry out a time deinterleaving of the bits. As pointed out in the last chapter, this module is critical in terms of memory. Once the bits are time reordered, we perform the depuncturing, viterbi and energy dispersal as we did with the FIC. Finally, the output of the energy dispersal serves as input to the MP2 decoder, which in turn produces the raw audio stream.

Chapter 5

Conclusions

The market of radio receptors has been up until now dominated either by static devices of considerable dimensions or as embedded devices in vehicles. Mobile receptors might be the most complex in terms of design due to the limitations both in size and power consumption. The lack of low cost mobile demodulators was one of the biggest motivations for scheduling this project in the company.

Advances in the field of electronics, concretely in integrated circuits, has had a huge impact in the industry of communications. The development and improvement of techniques of Very Large Scale Integration (VLSI) has stimulated the development of more powerful, smaller, faster and cheaper computers for specific applications. This technology has made it possible to implement highly sophisticated digital systems capable of performing digital signal processing that previously were done by analogical and more expensive means.

The high pressure from the consumers of more and more multimedia applications in their mobile devices has given rise to a growing interest for embedded specialized architectures of low power consumption. This means that achieving the maximum efficiency with the lowest power consumption, and of course at the lowest cost, has become one of the biggest challenges of the companies in the sector of DSP.

5.0.4 Start point

For the development of this project it has been essential a big effort from the members of the team, in order to understand the concepts that it englobes. Previously to the development of this project, it was necessary a deep study of both digital signal processing (not covered in the studies in Computer Engineering) and its applications to DAB and the CoolFlux BSP architecture. Nevertheless, thanks to the help of experts in the field we have been able to achieve the initial expectations.

In the following sections we explore the results obtained during the implementation and we conclude with the motives for which we think all the goals of the project have been accomplished.

5.0.5 Proposed and accomplished goals

The main objective of this project was to design a complete digital radio demodulator (following the standard of the european project DAB) for the architecture CoolFlux BSP (property of NXP Semiconductors) and perhaps, if there was time, simulating it on a FPGA. For such ambitious task it was required a highly optimized code in terms of memory consumption and execution cycles. The last two aspects play an important role in the actual power consumption.

Our initial goal was not only achieved, but we were able to simulate the demodulator on a FPGA and reproduce audio in real time from a real flemish broadcaster signal.

5.0.6 Future aspects

Thanks to the advantages that CoolFlux BSP together with its compiler offer us, in principle it could be possible to reduce even more the memory requirements and power consumption.

Once the software is tested enough and further optimized, the next step would be to implement a dedicated chip for the commercialization. At the present, there are several companies interested in this product for its installation in portable devices such as MP3 players, telephones and so on.

5.0.7 Difficulties found within the development phase

One of the main burdens has been that of developing a system that had to be able to process within very strict time constraints. In fact, this part took us around the fifty percent of our working time. Whereas one CoolFlux BSP is able to run at 290 MHz in a real implementation, our FPGA runs at a maximum speed of about 50 MHz. Therefore, the implementation of the DAB was done with several CoolFlux BSP cores due to the frequency constraints imposed by the FPGA Board.

Another important aspect to highlight is the necessity to reproduce a clean signal, free of errors. The algorithms written for this task, such as the Viterbi convolutional decoder, synchronization correction and CRC codes were another big difficulty.

For the sake of energy efficiency, the processor does not include a floating point unit. As programmers, we were not used to write algorithms in fixed point representation. Fixed point programming is much harder than the float point counterpart, since now the programmer is responsible of manually scaling the intermediate variables in order to not saturate the ongoing signal.

In addition, it is important to mention that we were provided with generic algorithms already implemented by the company such as the the MP2 decoder. For sure, this was an advantage in order to achieve our goals faster. However, the main difficulty in this case was to work around with code that was not written by us.

Appendices

Appendix A

The Fourier Transform

A.1 Motivation

In the field of functional analysis in mathematics, it has been fundamental to approximate a complex function by means of simpler or more convenient ones. In this way, properties of the former become easier to analyze by studying the properties of the latter functions. This is even more important in Physics and Engineering, where the ideal of Platonism held by the most pure mathematicians is replaced by applicability. Maybe, the first example we learn in our lives about reduction of an arbitrary complex function to a simpler one is that discovered by Taylor in which a function is approximated around a point by a polynomial with all the accuracy we want.

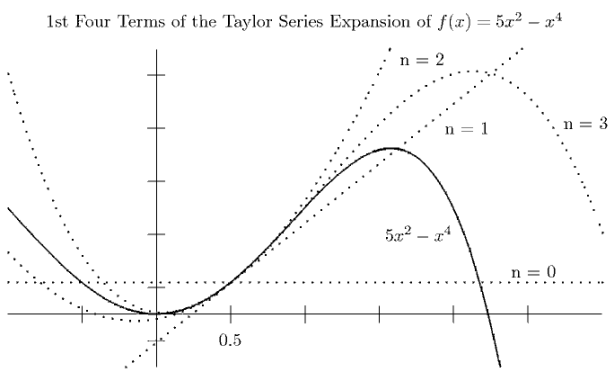


Figure A.1: A 4-degree polynomial approximated around point 0.5 by lower degree ones

But, what does this have to do with the first paragraph? Why did I mention the principle of the whole as a sum of the parts? Well, as we shall see, a function can be thought of as composed of atomic subsignals (which are simply sines and cosines) each one with a different frequency and with a different amplitude, just as matter is composed of atoms. This is known as Fourier Analysis. I do not intend to present the mathematical formality behind Fourier Analysis, rather I will try to introduce it in physical terms, with applications to Physics and Engineering. We shall think of a function as a physical signal varying in time. The classic notation of $f(x)$ is substituted by $f(t)$ and so on. Rather than emphasizing time as the independent variable, Fourier Analysis will allow us to think of a signal as a magnitude (think of it as information) varying in “frequency” (the so called frequency domain). This may sound quite bizarre right now, but my intention is to change this idea in the chapters that follow. A natural question is why we do ever want to deal with a signal in the frequency domain. Let’s say that signals might interact with other systems in the Universe in one way or another depending upon the frequencies (i.e subsignals) contained within the signal. The way a signal interacts with any other system is known as the frequency response of the system. For example, the sound emitted by two different instruments can be distinguished in part because they have different frequencies, and as a consequence of that, both signals interact differently with your ear and brain. If we are to code a sound in a computer, we will obtain a lot of advantage by filtering those frequencies in the record that the brain cannot perceive, presumably reducing the size of the file. After all, why do we want to store information that cannot be perceived?

Take the following step function, defined as:

$$f(x) = \begin{cases} 1 & \text{si } x < \pi \\ -1 & \text{si } x \geq \pi \end{cases}$$

It might not seem clear that it is composed of sinusoids, but hold on. Let’s plot the sine function $f(t) = \sin(t)$. Note that the frequency f is $\frac{1}{2}\pi$ Hz.

The following three pictures show in turn the representations of the signals

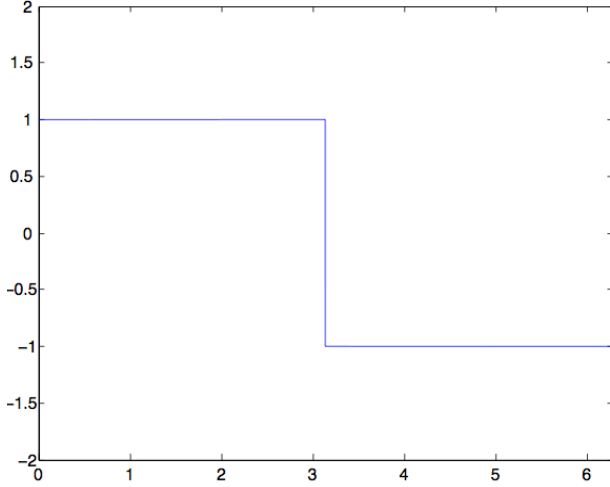


Figure A.2: step function

$$\begin{aligned}
f_1(t) &= \sin(t) + \frac{1}{3}\sin(3t), \\
f_2(t) &= \sin(t) + \frac{1}{3}\sin(3t) + \frac{1}{5}\sin(5t) + \frac{1}{7}\sin(7t) + \frac{1}{9}\sin(9t) \\
f_3(t) &= \sin(t) + \frac{1}{3}\sin(3t) + \frac{1}{5}\sin(5t) + \frac{1}{7}\sin(7t) + \frac{1}{9}\sin(9t) + \\
&\quad + \frac{1}{13}\sin(13t) + \frac{1}{15}\sin(15t) + \frac{1}{17}\sin(17t) + \frac{1}{19}\sin(19t) + \\
&\quad + \frac{1}{21}\sin(21t) + \frac{1}{23}\sin(23t)
\end{aligned}$$

We can think of the last three signals as composed of different subsignals each with a constant frequency, amplitude and phase (although in this example all have the same phase). For example, if t represents seconds, the signal $f_2(t)$ is composed of 5 “subsignals” with the frequencies $\frac{1}{2}\pi Hz$, $\frac{3}{2}\pi Hz$, $\frac{5}{2}\pi Hz$, $\frac{7}{2}\pi Hz$ and $\frac{9}{2}\pi Hz$ and with amplitudes $1, \frac{1}{3}, \frac{1}{5}, \frac{1}{7}$ and $\frac{1}{9}$. Notice that the more sines (i.e. subsignals) we add to the summation, the more accurate is the approximation to the signal illustrated in figure A.2.

In general the last intuition can be formalized as follows: A function $f(t)$ (sufficiently well behaved) can be expressed as:

$$F(f) = a_0 + a_1\cos(t) + a_1\sin(t) + a_2\cos(2t) + b_2\sin(2t) + \dots \quad (\text{A.1})$$

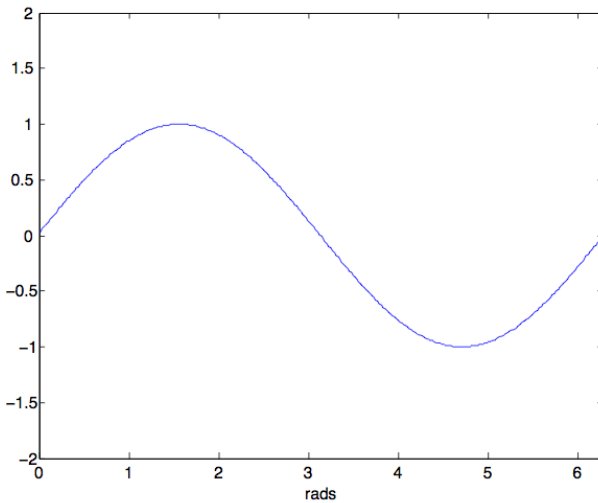


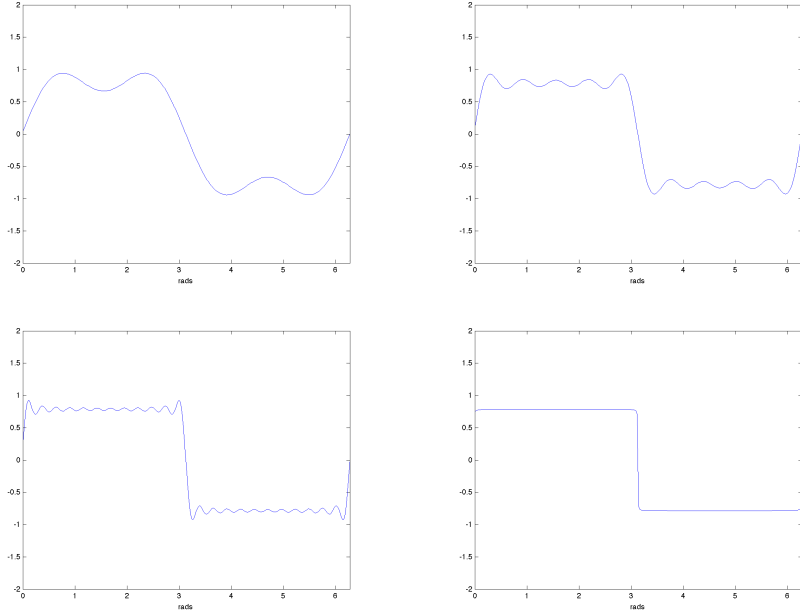
Figure A.3: sine function

Mathematicians are not very happy with approximations, so they will approximate the first signal by the infinite serie:

$$F(f) = a_0 + \sum_{n=1}^{\infty} a_n \cos nt + \sum_{n=1}^{\infty} b_n \sin nt \quad (\text{A.2})$$

In general, it can be formally proved that the serie F converges to the original signal f . The proof will not be provided here (even Fourier was not able to prove it). In any practical application, we must choose a finite value of n .

The question we pose now is: given a signal that represents a physical quantity, for example, a fragment of sound, how do we get the amplitude and phase of each “frequency” present in the signal? This is an important question since the energy of a wave is a magnitude that depends both on the frequency and the amplitude of the wave. So the energy carried by a signal is equal to the sum of the energy of each “subsignal” (this result is derived from the Parseval Theorem found in advanced texts in this topic). Therefore, we could obtain how much energy is carried in the signal due to the presence of a given frequency. We wish an algorithm that given a signal and a frequency returns the amplitude of that frequency in the signal. If the frequency is not present in the signal, the amplitude should be 0.



A.2 Approximation by the minimum mean square error

As we said, our intention is to approximate a function by means of other function which is more useful to the problem at hand. But, let's be more formalists about what approximation means in the context of Fourier Analysis. When approximating a function we want to reduce the mean square error between the original and approximated function. Intuitively, we want the graphs of both function to be as close as possible. For the sake of simplicity, before seeing the mean quadratic error for sinusoids, let's put it forward with polynomials.

Let $f(t) : [a, b] \rightarrow \mathbb{R}$ be some function we want to approximate. Let $P(x) = a_n x^n + \cdots + a_2 x^2 + a_1 x + a_0$ be an n -degree polynomial. The mean square error (thereinafter called E) is a function of the coefficients a_n, \dots, a_1, a_0 . That is, we have to find the values a_i that minimize E . By the way, E is defined as

$$E(f, P(a_n, \dots, a_0)) = \int_a^b (f(t) - P(t))^2 dt. \quad (\text{A.3})$$

To minimize E for each a_i we take partial derivatives for each a_i

$$\frac{\partial E(f, P(a_n, \dots, a_0))}{\partial a_i} = 0 \quad (\text{A.4})$$

From last two equations it follows

$$E(f, P(a_n, \dots, a_0)) = -2 \int_a^b x^j f(x) dx + 2 \sum_{k=0}^n a_k \int_a^b x^{j+k} dx \quad (\text{A.5})$$

So, we have to solve the following system of $n + 1$ equations:

$$\sum_{k=0}^n a_k \int_a^b x^{j+k} dx = \int_a^b x^j f(x) dx \quad j = 0, 1, \dots, n \quad (\text{A.6})$$

As an example, we apply the last algorithm for approximating the function $f(t) = \sin(\pi t)$ by the polynomial $P(t) = a_2 t^2 + a_1 t + a_0$ so we obtain:

$$a_2 = -4.12251, a_1 = 4.12251, a_0 = -0.050465$$

The following graph represents the functions f and P in blue and red respectively. Notice how close they are even for a polynomial of such low degree.

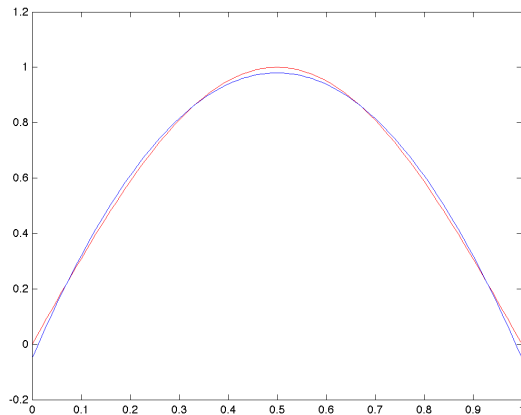


Figure A.4: $\sin(\pi t)$ approximated by a polynom

A.3 Orthogonality

Recall from elemental geometry that two vectors are orthogonal if the dot product between them is 0. In a two-dimensional euclidean space, a vector is an “arrow” from the origin to a given point on the plane, and two vectors are orthogonal if the form 90 degrees between them. Analytically if $v_1 = (x_1, y_1)$ and $v_2 = (x_2, y_2)$ are two vectors in \mathbb{R}^2 , then they are orthogonal if and only if $x_1x_2 + y_1y_2 = 0$. More general, two vectors $v = (x_1, x_2, \dots, x_n)$, $v' = (x'_1, x'_2, \dots, x'_n) \in \mathbb{R}^n$ are orthogonal if :

$$\sum_{i=1}^n x_i x'_i = 0 \quad (\text{A.7})$$

The notion of vector in mathematics is actually much more general than the usual concept of vector in geometry. In fact, it can be found in any text of linear algebra that functions from and to $\mathbb{N}, \mathbb{R}, \mathbb{C}$ belong to a vectorial space, and so are vectors too.

Let $f, g : I \subset \mathbb{R} \rightarrow \mathbb{R}$. f, g are orthogonal in the interval I if,

$$\int_{t \in I} f(t)g(t)dt = 0 \quad (\text{A.8})$$

Note the parallelism between the notion of orthogonality of vectors in a Euclidean space and that of two functions in a functional space.

From the paragraph above, we can extend the concept of orthogonality to a set of functions $\{f_1, f_2, \dots, f_n\}$. This set orthogonal in I if

$$\int_I f_i(t)f_j(t)dt = 0, i \neq j \quad (\text{A.9})$$

Recall we are looking for a procedure that given a signal composed of many frequencies, it returns the amplitude of each frequency component (i.e. The coefficients a_i, b_i of the Fourier Serie)

Now, we show that two sinusoids of the same phase are orthogonal in an interval multiple of 2π if and only if the frequency of one of them is an integer multiple of the frequency of the other and the respective frequencies are different. Let f, g be two signals defined as $f(t) = \sin(mt)$ and $g(t) = \sin(nt)$. Hence

$$f(t)g(t) = \sin(mt)\sin(nt) = \frac{[\cos(mt - nt) - \cos(mt + nt)]}{2}$$

Firstly assume $m = n$. Thus,

$$\int_k^{2\pi k} f(t)g(t)dt = \int_k^{2\pi k} \frac{1 - \cos(2nt)}{2} dt = \pi$$

Therefore, according to the definition they are not orthogonal.

On the other hand, assume now that $m \neq n$ then

$$\begin{aligned} & \int_k^{2\pi k} \sin(nt)\sin(mt)dt \\ &= \frac{1}{2} \int_k^{2\pi k} (\cos((m-n)t) - \cos((m+n)t))dt \\ &= \frac{1}{2} \left[\frac{\sin((m-n)t)}{m-n} - \frac{\sin((m+n)t)}{m+n} \right]_k^{2\pi k} = 0, (m \neq n) \end{aligned}$$

$$\begin{aligned} & \int_k^{2\pi k} \cos(nt)\cos(mt)dt \\ &= \frac{1}{2} \int_k^{2\pi k} (\cos((m+n)t) + \cos((m-n)t))dt \\ &= \frac{1}{2} \left[\frac{\sin((m+n)t)}{m+n} + \frac{\sin((m-n)t)}{m-n} \right]_k^{2\pi k} = 0, (m \neq n) \end{aligned}$$

We almost have all the ingredients for computing the amplitudes of all the components in the Fourier Serie. Finally we show under what conditions both a sine and a cosine are orthogonal. Without loss of generality let $f(t) = \sin(mt)$ and $g(t) = \cos(nt)$.

$$\begin{aligned} & \int_k^{2\pi k} \cos(nt)\sin(mt)dt \\ &= \frac{1}{2} \int_k^{2\pi k} (\sin((m+n)t) + \sin((m-n)t))dt \\ &= \frac{1}{2} \left[\frac{\cos((m+n)t)}{m+n} - \frac{\cos((m-n)t)}{m-n} \right]_k^{2\pi k} = 0, (m \neq n) \end{aligned}$$

Here we are, we are ready to obtain the coefficients a_i, b_i . For commodity, I rewrite here the Fourier Serie:

$$F(f) = a_0 + a_1 \cos(t) + a_1 \sin(t) + \dots + a_n \cos(nt) + b_n \sin(nt) \quad (\text{A.10})$$

As n approaches infinity $F(f)$ will be equal to $f(t)$

$$\lim_{n \rightarrow \infty} f(t) = F(f) \quad (\text{A.11})$$

Therefore, to obtain a_0 we integrate both sides of (A.10).

$$\int_0^{2\pi} F(f) dt = a_0 2\pi \quad (\text{A.12})$$

therefore

$$a_0 = \frac{1}{2\pi} \int_0^{2\pi} f(t) dt$$

To compute a_1 just multiply both sides of (A.10) by $\cos(t)$ and integrate. From orthogonality, the only factor that is not 0 is $a_1 \cos(t) \cos(t)$, hence

$$\int_0^{2\pi} F(f) \cos(t) dt = \int_0^{2\pi} f(t) \cos(t) dt = \int_0^{2\pi} a_1 \cos^2(t) dt = \pi a_1$$

hence,

$$a_1 = \frac{1}{\pi} \int_0^{2\pi} f(t) \cos(t) dt$$

Following the same argument we arrive to the general formula to compute the a_i 's:

$$a_k = \frac{1}{\pi} \int_0^{2\pi} f(t) \cos(kt) dt$$

Following an analogous argument, the coefficients b_i 's can be computed as:

$$b_k = \frac{1}{\pi} \int_0^{2\pi} f(t) \sin(kt) dt$$

A.4 Fourier Transform in Periodic Complex Functions

So far we have discussed how a real function can be approximated by the Fourier serie (A.1). However, we can extend the same argument to complex valued functions. This might seem a mathematical nicety because, after all, who cares about complex numbers? Well, it is not the objective of this course to convince the reader of the usefulness of complex numbers. Many physical facts are best modeled with complex numbers. In the field signal modulation, a QPSK signal carries two bits in each baud. The first and second bits are coded in the real and imaginary parts of a complex number respectively. Then the complex number is modulated into the carrier signal and launched “through the air”. In signal processing, the Fourier Transform is surely the most performed operation. If we had not the Fourier Transform for complex signals, we could not process the information contained within the QPSK signal.

There is a tight and mysterious relation between sinusoids, the number $e = 2.7183\dots$ and the imaginary number i . To understand this, let's introduce another serie reminiscent to that of Taylor for approximating a real function. This is called the Maclaurin's Serie and says that a function $f(t)$ can be approximated as follows:

$$f(t) = f(0) + \frac{1}{1!}f'(0)t + \frac{1}{2!}f''(0)t^2 + \frac{1}{3!}f'''(0)t^3 + \dots \quad (\text{A.13})$$

We know from our childhood that the derivative of e^t is equal to itself. We can write e^t as a Maclaurin's serie:

$$e^t = 1 + t + \frac{1}{2}t^2 + \frac{1}{6}t^3 + \frac{1}{24}t^4 + \dots + \frac{1}{n!}t^n$$

We know also that the derivative of $\sin(t)$ and $\cos(t)$ are “almost” equal to themselves. The derivative of $\sin(t)$ is $\cos(t)$ whose derivative is in turn $-\sin(t)$ and so on. Next we expand the Maclaurin's series for both functions:

$$\sin(t) = x - \frac{1}{6}x^3 + \frac{1}{120}x^5 + \dots$$

$$\cos(t) = 1 - \frac{1}{2}x^2 + \frac{1}{24}x^4 - \dots$$

Finally we unfold the function e^{-it} :

$$f(t) = e^{it} = t + ix - \frac{1}{2}x - \frac{1}{6}ix^3 + \frac{1}{24}x^4 + \frac{1}{120}ix^5 + \dots$$

We are now in position to see that cosines, sines, e , π and i are all together related in the following well-known equality:

$$e^{it} = \cos(t) + i\sin(t)$$

It follows that:

$$\begin{aligned}\cos(t) &= \frac{e^{it} + e^{-it}}{2} \\ \sin(t) &= \frac{e^{it} - e^{-it}}{2i}\end{aligned}$$

Our original Fourier serie (A.1) becomes now:

$$\begin{aligned}f(t) &= a_0 + \sum_{n=1}^{\infty} a_n \cos nt + \sum_{n=1}^{\infty} b_n \sin nt = \\ &= a_0 + \sum_{n=1}^{\infty} a_n \frac{e^{int} + e^{-int}}{2} + \sum_{n=1}^{\infty} b_n \frac{e^{int} - e^{-int}}{2i}.\end{aligned}$$

Since $\frac{1}{i} = -i$:

$$\begin{aligned}f(t) &= c_0 + \sum_{n=1}^{\infty} (c_n e^{int} + c_{-n} e^{-int}) = \\ &= c_0 + \sum_{n=1}^{\infty} c_n e^{int} + \sum_{n=-1}^{-\infty} c_n e^{int} = \sum_{n=-\infty}^{+\infty} c_n e^{int}\end{aligned}\tag{A.14}$$

where

$$c_0 = \frac{1}{2}a_0, \quad c_n = \frac{1}{2}(a_n - ib_n), \quad c_{-n} = \frac{1}{2}(a_n + ib_n).$$

So far we talked about orthogonality of vectors in \mathbb{R}^n and with a little effort we extended

the definition to functions from $\mathbb{R} \rightarrow \mathbb{R}$. We recapitulate here the definition of orthogonality of vectors in a vectorial space by defining it in its most abstract form. Let \mathbb{V} a vectorial space with inner product denoted by $\langle , \rangle : \mathbb{V}^2 \rightarrow \mathbb{V}$. Two vectors $v, v' \in \mathbb{V}$ are orthogonal if $\langle v, v' \rangle = 0$.

The inner product in \mathbb{C}^2 is defined as follows:

Let $z, z' \in \mathbb{C}$ then $\langle z, z' \rangle = z\bar{z}'$ where \bar{z}' is the complex conjugate of z' .

With these definitions at hand we are now ready to define orthogonality of functions $\mathbb{C} \rightarrow \mathbb{C}$. Let $f, g : C \subset \mathbb{C} \rightarrow \mathbb{C}$. f, g are orthogonal in I if,

$$\int_{t \in I} f(t)\overline{g(t)} dt = 0. \quad (\text{A.15})$$

From this, it follows that the set of functions $\{e^{int}\}_{n \in \mathbb{Z}}$ is orthogonal in the interval $[0, 2\pi]$:

Assume $n \neq m$

$$\begin{aligned} \int_0^{2\pi} e^{int} \overline{e^{imt}} dt &= \int_0^{2\pi} e^{int} e^{-imt} dt = \\ \int_0^{2\pi} (\cos(nt) + i \sin(nt))(\cos(mt) - i \sin(mt)) dt &= 0 \end{aligned}$$

On the other hand if $n = m$

$$\int_0^{2\pi} (\cos(nt) + i \sin(nt))(\cos(nt) - i \sin(nt)) dt = 2\pi \neq 0$$

The coefficients c_i can be calculated as we did in the case of real-valued functions. Recall that

$$\begin{aligned} f(t) &= \sum_{n=-\infty}^{\infty} c_n e^{int} \\ \langle f(t), e^{imt} \rangle &= \int_0^{2\pi} \left(\sum_{n=-\infty}^{\infty} c_n e^{int} \right) e^{-imt} dt = \\ &= \sum_{n=-\infty}^{\infty} c_n \int_0^{2\pi} e^{i(n-m)t} dt = \end{aligned}$$

$$\begin{aligned}
 &= \sum_{n=-\infty}^{\infty} c_n \int_0^{2\pi} \cos[(n-m)t] + i \sin[(n-m)t] dt = \\
 &\quad = 2\pi c_n
 \end{aligned}$$

so

$$c_n = \frac{1}{2\pi} \int_0^{2\pi} f(t) e^{-int} dt \quad (\text{A.16})$$

By the way, the function $c : \mathbb{Z} \rightarrow \mathbb{C}$ defined as

$$c(n) = c_n$$

is called the spectrum of the function. Equivalently,

$$c(n) = \frac{1}{2\pi} \int_0^{2\pi} f(t) e^{-int} dt$$

A.5 Integral Fourier Transform

So far we have talked about periodic signals and how to obtain the frequency components (that is, the Fourier Coefficients). We made the implicit assumption that the period was 2π . First we redefine the Fourier Serie for a signal of an arbitrary period. After that, we will deduce the Integral Fourier Transform that will allow us to deal with aperiodic functions.

It is not at all difficult to see that the Fourier Serie of a signal f of period T is:

$$f(t) = \frac{1}{T} \sum_{n=-\infty}^{\infty} c(n) e^{\frac{-2\pi i n t}{T}} = \frac{1}{T} \sum_{n=-\infty}^{\infty} c(n) e^{\frac{-2\pi i n t}{T}} \quad (\text{A.17})$$

hence,

$$c(n) = c_n = \int_{-\frac{T}{2}}^{\frac{T}{2}} f(t) e^{\frac{-2\pi i n t}{T}} dt \quad (\text{A.18})$$

Note that for convenience, instead of taking the interval $[0, T]$ we took $[-\frac{T}{2}, \frac{T}{2}]$. This is legitimate, and even though the Fourier coefficients will be different to those of the original serie, the latter form still converges to f .

You might have studied the Reimann's integral in elemental calculus. Let $h : [a, b] \rightarrow \mathbb{R}$ an integrable function. We split up the interval $[a, b]$ in subintervals with the same length (ω_0) , so $[a, b] = [a = x_0, x_1, \dots, x_n = b]$ and $x_i - x_{i-1} = \omega_0$. Then,

$$\lim_{\omega_0 \rightarrow 0} \sum_{n=1}^k h(a + n\omega_0)\omega_0 = \int_a^b h(t) dt. \quad (\text{A.19})$$

By taking $\xi_n = \frac{n}{T}$ and $\Delta\xi = \frac{n+1}{T} - \frac{n}{T} = \frac{1}{T}$ we transform the Fourier serie in a Riemann sum:

$$f(t) = \sum_{n=-\infty}^{\infty} c(\xi_n) e^{-i\xi_n t} \Delta\xi \quad (\text{A.20})$$

If $T \rightarrow \infty$ the Riemann sum tends to the Fourier transform, given by:

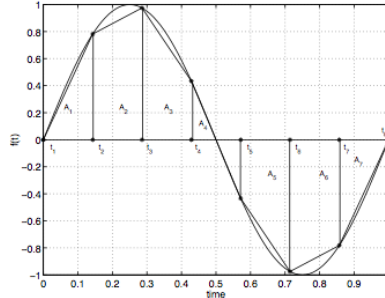
$$\mathcal{F}(\xi) = \int_{-\infty}^{\infty} f(t) e^{-i\xi t} dt, \quad t \in \mathbb{R} \quad (\text{A.21})$$

On the other hand, the inverse Fourier transform is given by:

$$f(t) = \int_{-\infty}^{\infty} \mathcal{F}(\xi) e^{i\xi t} d\xi \quad (\text{A.22})$$

The intuition behind this is that we consider a non-periodic serie as a periodic function with infinite period.

Up until now we have presented a lot of integrals and assume that they can be calculated using symbolic calculus. We might well use numerical methods to evaluate the integrals. For example, the Fourier Coefficients $a_0, a_1, b_1, \dots, a_n, b_n$ can be approximated by calculating the integral by means of the trapezoidal rule: To obtain the area under a curve, divide that area in trapezoids, calculate the area of each trapezoid and then sum them all together.



An multitude of methods exist for approximating integrals. But the aim of this work is not how to approximate integrals, rather it is how to approximate a function by sinusoids. How the Fourier Transform is applied in computers and DSPs depends upon the Discrete Fourier Transform and the Nyquist Theorem which will be presented in a moment.

A.6 DFT

So far we have presented the essential ideas of Fourier Analysis for continuous functions. However, the ideas already introduced of the Fourier Transform implies calculus, integrals (infinite sums) and so on. An integral is a summation of infinite rectangles of infinitesimal base and infinitesimal area. Thanks to the Fundamental Theorem of Calculus, we find that there is a tight connection between derivatives and integrals. In most cases, we can analytically calculate the integral of a function by knowing that integral and derivation are inverse operations. However, the continuum does not exist in the real world. Quantum mechanics, the paradigm that best describes the known Universe in its most microscopic scale teaches us that the magnitudes we measure are discrete rather than continuous. Moreover computers handle discrete numbers in discrete steps of time. Any integral is substituted by a finite sum in order to be computed by a machine. This translates the Fourier Transform into the Discrete Fourier Transform (DFT). The integral in the Fourier Transform becomes the summation

$$\mathcal{X}(k) = \sum_{n=0}^{N-1} x(n)e^{-ink}, \quad n = 0, 1, \dots, N-1 \quad (\text{A.23})$$

whereas the inverse DFT is

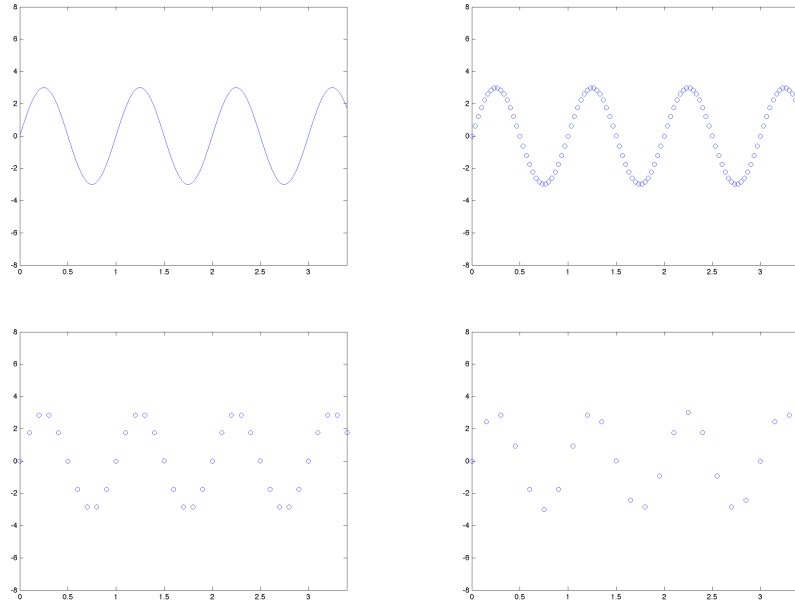
$$x(n) = \frac{1}{N} \sum_{k=0}^{N-1} \mathcal{X}(k)e^{ink} \quad (\text{A.24})$$

x is the vector of samples $x = [x_0, x_1, \dots, x_{N-1}]$. This vector is obtained by discretizing the continuous signal f in equally spaced points. The process of sampling is usually done by a device called Analog to Digital Converter (ACD). A note about sampling. There is a theorem due to Nyquist and Shannon that says that the sampling frequency must be at least the double of the maximum frequency present in the continuous periodic signal in order to recover the continuous signal from the discretized signal. If this criterion is not satisfied, we cannot recover the information contained within the original signal f from the sampled one, a phenomenon known as aliasing.

Note that the frequency domain of a sampled version cannot have an infinite range

of frequencies. If fact, if we sample the signal according to the Nyquist's criterion (to a rate double that the maximum frequency of the continuos signal), we shall not encounter frequencies bigger than half the sampling rate in the frequency domain.

Next, I show the continuos signal $f(t) = 3 * \sin(2\pi t)$ and three sampled version with less and less sampling rate. Note that in the case of the last one, the information of the original signal is almost unrecoverable.



Everything said in the case of the continuos Fourier Transform applies equally well to the Discrete Fourier Transform. For example,

Let $f, g : R \rightarrow \mathbb{R}$. f, g are orthogonal if,

$$\sum_{t \in T} f(t)g(t) = 0 \quad (\text{A.25})$$

where $T = \{t_0, t_1, \dots, t_{N-1}\}$

It can be shown that $f(t) = \sin(mt)$ and $g(t) = \sin(nt)$ where $t \in \{t_0, t_1, \dots, t_{N-1}\}$ are orthogonal if and only if $m = n$. The orthogonality test is the same as that of continuous functions. Finally, for discrete complex-valued signals, f, g are orthogonal if,

$$\sum_{t \in T} f(t)\overline{g(t)} = 0 \quad (\text{A.26})$$

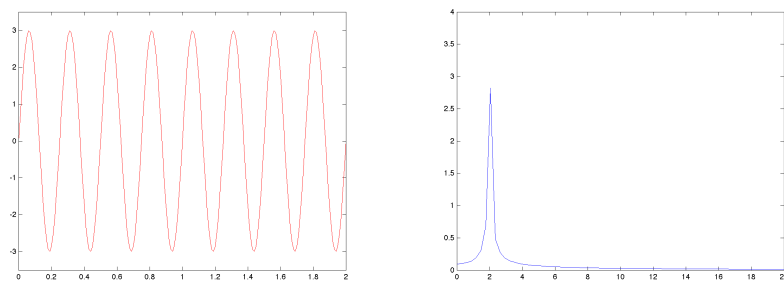
where $T = \{t_0, t_1, \dots, t_{N-1}\}$

To conclude with the theory, I should say that this work is only an intuitive introduction to the Fourier Transform in one dimension. The Fourier Analysis is in itself a vast discipline in which a lot of research is done even in present days. I do not pretend to cover everything with this work. For example, we have explained functions $\mathbb{R} \rightarrow \mathbb{R}$ and $\mathbb{R} \rightarrow \mathbb{C}$. However, in the field of Digital Signal Processing, it is very usual to work with functions $\mathbb{C} \rightarrow \mathbb{C}$. The intuition behind these functions is the same (studying the variability of the dependent variable with respect the independent variable), but explaining them requires knowledge in complex variable and it might not be so intuitive. Fourier Analysis can even be extended to multidimensional domains $\mathbb{C}^n \rightarrow \mathbb{C}^m$. This is useful for example, for dealing with image processing from which I borrow some practical examples for the next chapter.

A.7 Spectral Analysis

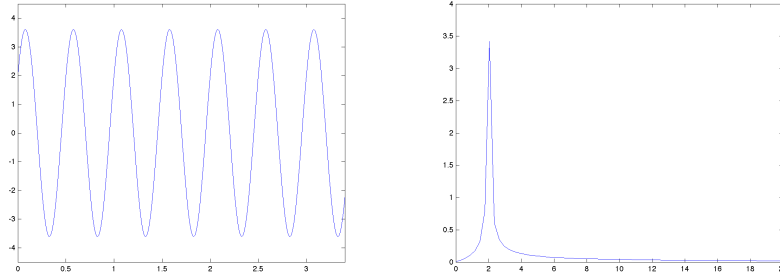
We have talked about the time domain and the frequency domain of a function (periodic or aperiodic), however we have not represented graphically a function in the frequency domain. Whereas in the x -axis in the time domain we plot the variable t , in the frequency domain we shall plot the frequency f . We will make a distinction here from the rest of this text. So far we have dealt with orthogonal functions in the form $f(t) = \sin(kt)$ and $f(t) = \cos(kt)$ with $k \in \mathbb{Z}$. That representation ignores physical units, like seconds and Hertz. We will normalize the functions by multiplying the arguments in the sinusoids by $2\pi f$, where f is the frequency of the sinusoid. In this way, if we convey that time is measured in seconds, then the units of f are in Hz. So for example, the voltage in AC between two points can be given by $V(t) = 3\sin(2\pi 4t)$. In this case, the voltage will oscillate 4 times per second with a maximum peak value of 3 Volts. Everything explained in earlier chapters applies equally well to the normalized representation. If we have the function $g(t) = \sin(3t)$ we can normalize it just by calculating $f = \frac{3}{2\pi}$ and substituting f into $g(t) = \sin(2\pi ft)$.

The following pictures show on the left the function $v(t) = 3\sin(2\pi 2t)$. In this case, $f = 2\text{Hz}$. As expected, we see a peak of amplitude 3 at the point 2 in the x -axis in the frequency domain. You might wonder why we do not obtain a perfect peak, but there appears some residual frequencies around the point 2 in the x -axis. Presumably, this is because we are dealing with discrete signals, made up of little steps. These steps seem to introduce such undesirable frequencies.

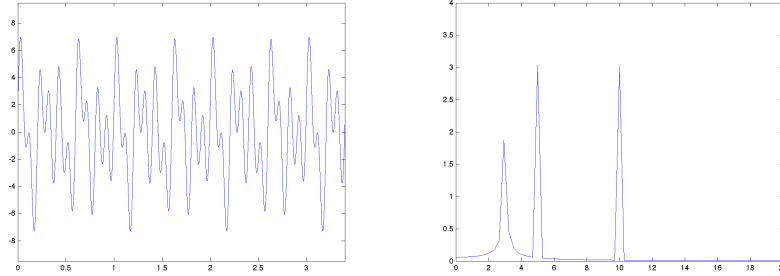


The frequency domain graph does not represent whether the frequency was due to a sine or a cosine component in the time domain. This is because both sine and cosine do

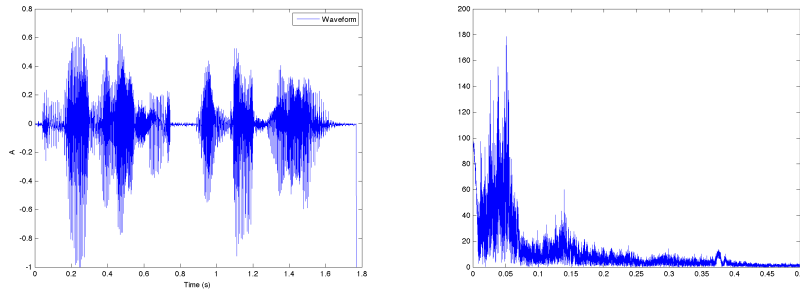
not differ in frequency, they do in phase. In order to see this, the following pictures shows the function $v(t) = 3\sin(2\pi 2t) + 2\cos(2\pi 2t)$. Notice that only the amplitude has changed with respect to the last graph, but the frequency remains the same. i.e. the peak in the frequency domain is still in 2Hz.



Let's see what happens with a slightly more complex signal made up of 3 different frequencies, for example $v(t) = 3 * \sin(2\pi 5t) + 2 * \cos(2\pi 3t) + 8 * \cos(2\pi 10t)$. We should see in the frequency domain three peaks at points 3, 5, 10 in the x -axis.



We have just analyzed some quite nice signals made up of at most 3 different frequencies, but they do not contain any interesting amount of information. Just to show a real example, I have loaded into MATLAB an audio file from the Internet and plot it both in the time and frequency domain. Even incredible it might seem, the signal in the time domain is made up of sinusoids just as were the signals we examined so far. See that most of the information is contained within the frequencies between 0 (DC) and 0.15 Hz.



Now that we have seen how to pass from the time domain to the frequency domain, we will see how to do that in MATLAB. In MATLAB there exists a function that calculates the Fourier Transform from discretized input signal. This function can be called by typing `fft(inputdata)`. Recall that the Fourier Transform returns a list of complex numbers. Therefore we cannot plot the amplitude versus frequency directly in a two-dimensional plane. In order to obtain the amplitude within each frequency present in the signal, we must take the module of the complex numbers in the output list. So, by calling `abs(fft(input data))` we obtain the last graphs. I exhibit here the code in MATLAB to generate both the time and frequency domain functions.

```

clear all;
N = 100;
T = 3.4;
P = 10000000;
t = [0 : N - 1]/N;
t = t * T;
f = 3 * sin(2 * pi * 10 * t);
p = abs(fft(f))/(N/2);
p = p(1 : N/2);
freq = [0 : N/2 - 1]/T;
subplot(2, 1, 1)
plot(f, t), axis([-5 5 0 3.4])
subplot(2, 1, 2)
plot(freq, p), axis([0 20 0 4])

```

A.8 Applications of the Fourier Transform

A.8.1 Noise Filter

As a first example, we will apply the Fourier Transform to one dimensional waves like sound.

I will show how to restore signal affected by gaussian white noise.

Let's plot a wave together with its spectra.

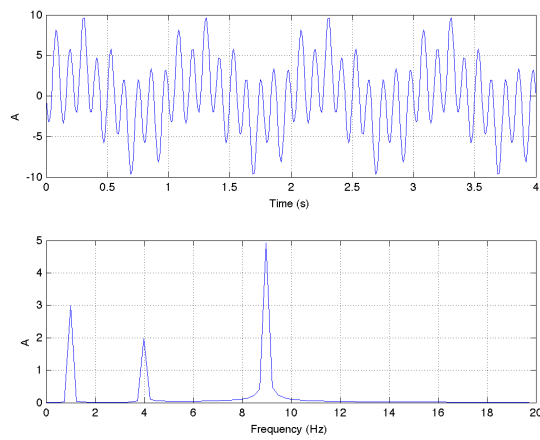


Figure A.5: Noiseless signal example and its spectrum

The following code generates the last function:

```

dt = 1/100;
et = 4;
t = 0 : dt : et;
y = 3 * sin(1 * 2 * pi * t) - 5 * sin(9 * 2 * pi * t) + 2 * sin(4 * 2 * pi * t);

subplot(2, 1, 1);
plot(t, y); grid on
axis([0 et -10 10]);
xlabel('Time(s)');
ylabel('Amplitude');

Y = fft(y);
n = size(y, 2)/2;
amp_spec = abs(Y)/n;

subplot(2, 1, 2);
freq = (0 : 79)/(2 * n * dt);
plot(freq, amp_spec(1 : 80)); grid on
xlabel('Frequency(Hz)');
ylabel('Amplitude');

```

We can simulate noise interference by calling the function randn().

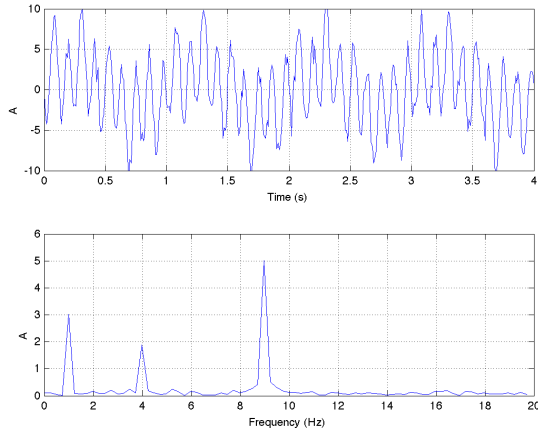


Figure A.6: Noisy signal and its spectrum

See that in addition to the three peaks of the original signal, there appears residual frequencies with low amplitudes that were not present earlier. Therefore, if we are to filter the noise, we must reduce to 0 such low amplitudes in the frequency domain. Look carefully at the next code.

```

noise = randn(1, size(y, 2));
ey = y + noise;

eY = fft(ey);
n = size(ey, 2)/2;
amp_spec = abs(eY)/n;

figure
subplot(2, 1, 1);
plot(t, ey); grid on
axis([0 et -10 10]);
xlabel('Time(s)');
ylabel('Amplitude');

subplot(2, 1, 2);
freq = (0 : 79)/(2 * n * dt);
plot(freq, amp_spec(1 : 80)); grid on
xlabel('Frequency(Hz)');
ylabel('Amplitude');

```

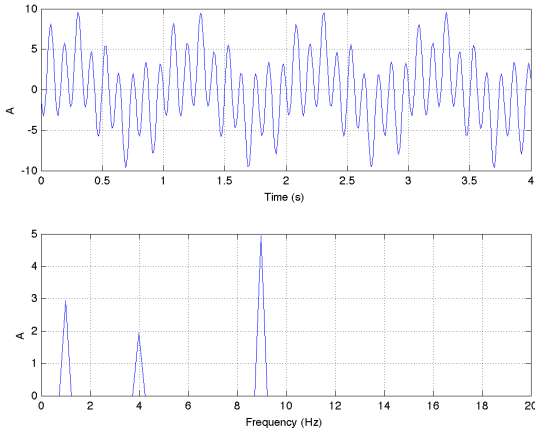


Figure A.7: noisy signal restored

In the last picture we see the original signal restored.

A.8.2 Image Compression

So far we have dealt with one dimensional signals, in which the independent variable was the time. An image is just a two dimensional signal, where the independent variables are the coordinates measured in pixels from the top-right corner of the picture. The dependent variable is a three dimensional vector indicating the color components of the pixel. Each

```
fY = zeros(size(eY));  
[A B] = size(eY);  
for i = 1 to B do  
    if abs(eY(i))/n < 1 then  
        fY(i) = 0;  
    else  
        fY(i) = eY(i);  
    end if  
end for  
ifY = ifft(fY);  
cy = ifY;  
  
subplot(2, 1, 1);  
plot(t, cy); grid on  
axis([0 et - 10 10]);  
xlabel('Time(s)');  
ylabel('Amplitude');  
  
Y = fft(cy);  
n = size(cy, 2)/2;  
amp_spec = abs(Y)/n;  
  
subplot(2, 1, 2);  
freq = (0 : 79)/(2 * n * dt);  
plot(freq, amp_spec(1 : 80)); grid on  
xlabel('Frequency(Hz)');  
ylabel('Amplitude');
```

pixel is colored by mixing different quantities of Red, Green and Blue (RGB Model). Everything explained so far for one dimensional signals applies here too. Think again of sound. The sound received in your ear is a variation of the air pressure with respect to time. An image is a variation of intensity of light in a two dimensional plane. Therefore we might extrapolate Fourier Analysis to image processing.

It happens that the range of frequencies that the human brain can process is limited. Psychoacoustics is the study of subjective human perception of sounds. The same holds for colors. We cannot perceive very high changes in color in a small space. Recall that more frequencies implies more Fourier Coefficients to represent the information. If we cannot perceive some frequencies, why should we waste space to store them? As we are about to see, by applying the FFT to an image, removing the unperceived frequencies and then going back to the spatial domain we can considerably reduce the size of a picture.

The next MATLAB script traverses all colors and for each color all rows. In the first block of loops, each row is transformed using the DCT, then high-order samples are discarded, and the low-order samples are reverse-transformed using IDCT. The same is done for columns, which results in a higher compression ratio.

```

clear all;
foto = imread('f22.jpg');
ancho = size(foto, 2);
mitadSuperior = floor(ancho/2);
cuartoSuperior = floor(ancho/4);
octavoSuperiorh = floor(ancho/8);
fotoComprimida2 = [];
fotoComprimida4 = [];
fotoComprimida8 = [];
for k = 1 : 3 do
    for i = 1 : size(foto, 1) do
        filaDCT = dct(double(foto(i, :, k)));
        fotoComprimida2(i, :, k) = idct(filaDCT(1...mitadSuperior), ancho);
        fotoComprimida4(i, :, k) = idct(filaDCT(1...cuartoSuperior), ancho);
        fotoComprimida8(i, :, k) = idct(filaDCT(1...octavoSuperiorh), ancho);
    end for
end for
{Now, do it for columns}
altura = size(foto, 1);
mitadSuperior = floor(ancho/2);
cuartoSuperior = floor(ancho/4);
octavoSuperior = floor(ancho/8);
fotoComprimida2full = [];
fotoComprimida4full = [];
fotoComprimida8full = [];
for for k = 1 : 3 do
    for i = 1 : size(foto, 2) do
        colsDCT2 = dct(double(fotoComprimida2(:, i, k)));
        colsDCT4 = dct(double(fotoComprimida4(:, i, k)));
        colsDCT8 = dct(double(fotoComprimida8(:, i, k)));
        fotoComprimida2full(:, i, k) = idct(filaDCT(1...mitadSuperior), altura);
        fotoComprimida4full(:, i, k) = idct(filaDCT(1...cuartoSuperior), altura);
        fotoComprimida8full(:, i, k) = idct(filaDCT(1...octavoSuperiorh), altura);
    end for
end for

```

Finally, we save the compressed pictures.

```
imwrite(uint8(fotoComprimida2full),'/Desktop/pict2x.jpg')
imwrite(uint8(fotoComprimida4full),'/Desktop/pict4x.jpg')
imwrite(uint8(fotoComprimida8full),'/Desktop/pict8x.jpg')
```

Whereas the original image occupied 253 KBytes, we have reduced the size to 167 KBytes and 57 KBytes respectively.



Appendix B

Resumen en español del proyecto

B.1 Implementación software de DAB sobre la arquitectura CoolFlux BSP

En este capítulo explicaremos el proceso de demodulación de DAB junto a su implementación en CoolFlux BSP.

Desde un punto de vista abstracto, la entrada del demodulador DAB consiste en una señal modulada OFDM-DQPSK, representada numéricamente por un conjunto de números complejos. Generalmente, la salida resultante del proceso de demodulación es el sonido real, aunque también es posible obtener otros tipos de datos como información textual sobre predicciones del tiempo, el tráfico, etc.

La demodulación DAB está dividida en una cadena de módulos, cada uno de los cuales tiene una funcionalidad diferente. El objetivo de este capítulo es explicar la funcionalidad de cada uno de los módulos junto a su implementación en la arquitectura CoolFlux BSP.

La siguiente figura ilustra la concatenación de los diferentes módulos.

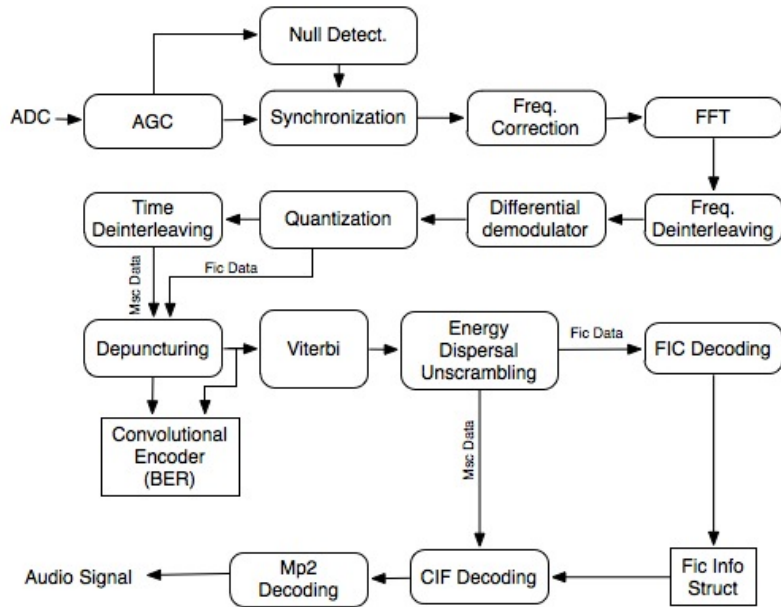


Figure B.1: Cadena de demodulación.

B.2 Control Automático de Ganancia

Este sistema, conocido en inglés por las siglas AGC (Automatic Gain Control) lo podemos encontrar en muchos dispositivos electrónicos. Su función es ajustar el nivel de potencia de la señal de entrada para aprovechar la máxima resolución que ofrece la arquitectura (24 bits de precisión simple y 48 bits de precisión doble). Es decir, este módulo reduce la potencia de la señal de entrada si ésta es muy fuerte y la aumenta si es muy débil.

Inicialmente, la señal de entrada se multiplica por un factor de 1. La potencia media se calcula durante un periodo fijo de muestras IQ. Después de esto, la ganancia aumenta o disminuye dependiendo de si la potencia media de la ventana de muestras es mayor o menor que la potencia de referencia (-12 dB en el caso del CoolFlux).

Se necesita un filtro paso baja para evitar que el ajuste de la ganancia sea demasiado sensible a cambios bruscos en la señal de entrada. Como ejemplo de un cambio brusco en la potencia de la señal de entrada tenemos el Símbolo Nulo, cuyo propósito es la sincronización

temporal del receptor. Dicho símbolo se caracteriza por tener una baja potencia en relación al resto de símbolos que conforman la señal de radio. Sin este filtro, dicho símbolo sería amplificado (perdiendo la propiedad de ser un símbolo de potencia nula) haciendo imposible su detección.

Una implementación software de un filtro paso baja puede ser como sigue:

$$AvgPwr = Tav * IQpwr + (1 - Tav) * AvgPwr$$

donde $IQpwr$ es la potencia de la muestra IQ actual. $AvgPwr$ es la potencia media recibida en la ventana actual. Tav es el parámetro con el valor que queremos filtrar.

La siguiente gráfica muestra cómo la señal de entrada es amplificada progresivamente hasta que finalmente se estabiliza. Nótese la presencia del símbolo nulo cerca del punto 3 en el eje de abscisas y cómo el AGC ignora su amplificación.

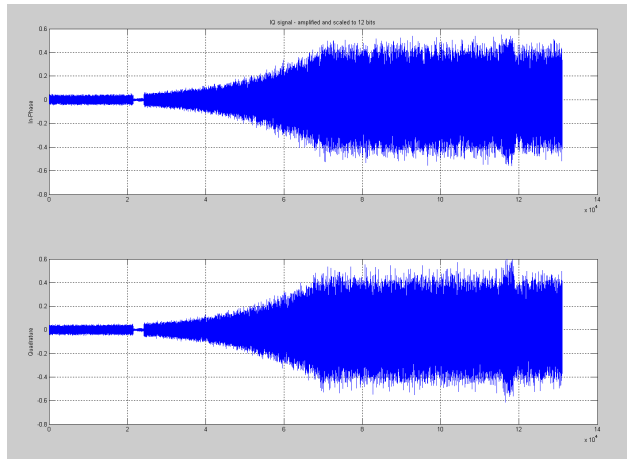


Figure B.2: AGC amplificando una señal real

B.3 FFT

La transformada rápida de Fourier es un algoritmo fundamental en cualquier sistema de procesamiento de señales. No es el objetivo de este resumen en español explicar para qué se utiliza la FFT en la demodulación de una señal OFDM. Consúltese el documento en inglés para una exposición detallada de la aplicación de la FFT a DAB. Para el desarrollo del

demodulador de DAB se probaron dos implementaciones de la FFT, a saber la radix 2 y la radix 4. Nuestro trabajo consistió en analizar el número de MIPS empleados por cada una de ellas y comparar el error de precisión que se obtiene en dichas implementaciones en punto fijo (cuya precisión es menor) con distintas implementaciones en coma flotante que existen en la comunidad de software libre.

Para permitir una computación eficiente de la FFT el tamaño del buffer de entrada debe ser una potencia de 2. La señal de DAB modo 1 es transportada por medio de 1536 portadoras, por lo que el número de puntos de la FFT que se debe utilizar es de 2048. Los restantes puntos no se utilizan.

B.4 Demodulación diferencial

La señal de radio DAB utiliza un esquema de modulación conocido como DQPSK. En una señal QPSK se utilizan distintas fases de la onda portadora para convenir los bits de información. La modulación DQPSK es esencialmente igual excepto que no se utilizan fases absolutas para convenir la información, sino que ésta es codificada en la diferencia de fases entre el símbolo actual y el previo.

B.5 Frecuency de-interleaving

Además del símbolo de referencia de fase, un marco completo de transmisión o frame se compone de 75 símbolos OFDM. En DAB se utilizan 1536 portadoras en paralelo, cada una de las cuales transporta 2 bits de información en cada periodo. Una estrategia naive para la transmisión de la señal sería dividir la cadena de bits en 75 bloques de 3072 bits y asociar el primer par de bits con la primera portadora, el segundo par de bits con la segunda portadora y así sucesivamente. Sin embargo dicha estrategia es propensa a errores de tipo burst. El frequency de-interleaver reordena la asignación de cada par de bits a cada portadora de una forma pseudoaleatoria, convenida en el estándar de DAB.

B.6 Cuantización

Una vez que se ha llevado a cabo la demodulación diferencial, el número complejo resultante de la resta tiene que ser convertido a bits reales. La cuantización es el proceso mediante el cual se reconstruye el díbit codificado en cada símbolo IQ y enviado en la transmisión. Para resolver este problema se implementaron dos soluciones, a saber la hard-decision y la soft-decision. La entrada al cuantizador se puede representar en los ejes cartesianos en lo que se conoce como diagramas de constelación, como muestra la siguiente figura.

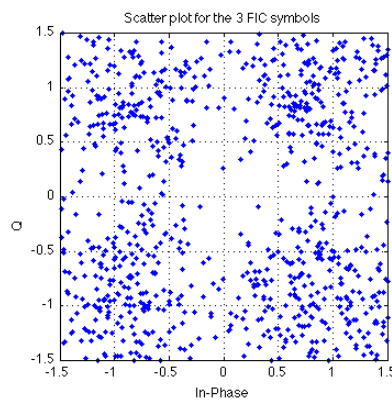


Figure B.3: Diagrama de constelación.

B.6.1 Hard Decision

Conceptualmente, este método es el más sencillo. Sea $a + bi$ un número complejo. Cada componente a, b se asocia a uno de los valores del par binario $\{1, -1\}$ según a, b sean positivos o negativos respectivamente. A continuación presentamos el pseudo-código:

```
for i = 0 to 1535 do
    r = real(input[i]);
    i = imag(input[i]);
    if (r > 0) then
        output[i] = 1;
    else
        output[i] = -1;
    end if
    if (i > 0) then
        output[i + 1536] = 1;
    else
        output[i + 1536] = -1;
    end if
end for
```

Todos los puntos que caen en el primer, segundo, tercer y cuarto cuadrante corresponden respectivamente a los díbits $\{1, 1\}$, $\{1, -1\}$, $\{-1, -1\}$, $\{-1, 1\}$.

B.6.2 Soft Decision

Mientras un decodificador con hard-decision opera con datos de un conjunto fijo de valores (-1 ó 1), las entradas al soft-decision pueden tomar más valores dentro de ese rango, típicamente 16 valores diferentes. Esta información extra indica con mayor fiabilidad cada punto de entrada con los datos originales. De esta manera este decodificador se comportará mejor en presencia de ruido que su equivalente hard-decision.

B.7 Time De-Interleaving

Este método de entrelazado de datos se implementa para mayor tolerancia al ruido. En lugar de enviar los datos en el orden temporal en el que se generan en el emisor, se introduce una retraso en cada bit conforme a unas reglas precisadas en el estándar. De este modo hacemos

que bits que estén próximos en la cadena de bits original estén más dispersos cuando viajan a través del canal. El mismo retraso se aplica siempre a los bits que ocupan la misma posición en distintos frames.

El algoritmo de Viterbi, como será explicado más adelante es capaz de recuperar errores en la cadena de bits recibida, aunque la longitud de la cadena corrupta no debe superar un cierto límite para que el algoritmo sea capaz de restaurar la cadena original.

Si alguna fuente de ruido afecta al canal durante un periodo de tiempo en la transmisión de un frame, sólo se verá afectado un grupo de bits no relacionados entre sí. Retrasando algunos bits en el emisor y reordenándolos en el receptor evitamos que en el canal haya segmentos dañados mayores que la duración crítica. Más adelante, el algoritmo de Viterbi será capaz de recuperar los bits perdidos.

El time de-interleaving sólo se lleva a cabo para los bits del MSC, ya que los bits del FIC necesitan ser procesados más rápidamente.

B.8 Energy Dispersal Unscrambling

Para asegurar una dispersión apropiada de la energía de la señal transmitida y evitar de este modo que patrones sistemáticos den como resultado una regularidad no deseada en la señal transmitida del módulo, los bits de entrada son transformados mediante una suma modulo-2 cuyos parámetros son los propios bits de entrada y una secuencia binaria pseudo-aleatoria, llamada PRBS (Pseudo-Random Binary Sequence). Por consiguiente, es necesario hacer alguna operación para reconstruir la señal original. Esta operación es la misma que se realiza en el transmisor: sumar módulo-2 los bits aleatorizados y la secuencia PRBS. La adición modulo-2 equivale a una XOR a nivel de bit.

B.9 Canal de Sincronización

Debido a condiciones adversas del canal es posible que la frecuencia y fase de los distintas portadoras se vean perturbadas. Dichas perturbaciones provocan que el receptor no de-

module correctamente la señal. Para evitar este tipo de errores se introducen dos símbolos especiales de sincronización en el frame de DAB.

B.9.1 Símbolo Nulo

En el frame de radio, existe un símbolo especial llamado “Null-symbol” con el que se realiza la sincronización del frame. Su detección se realiza gracias a que su potencia es cero. Para detectar este símbolo se utiliza una ventana de decisión de 512 palabras, para la que se calcula la potencia media de la señal entrante. El símbolo nulo se detecta cuando hay una caída por debajo de cierto umbral de la potencia media de la señal de entrada.

En la siguiente figura se muestra el valor medio de una señal DAB real en modo I. Obsérvense las abruptas caídas de potencia correspondientes a la llegada de un símbolo nulo, el cual es recibido una vez cada 96ms.

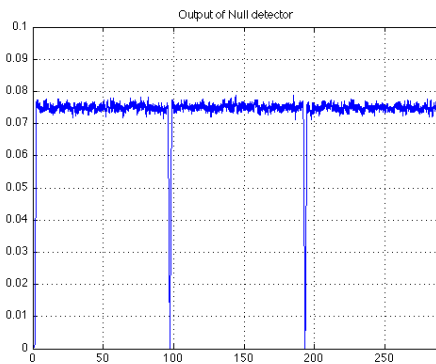


Figure B.4: Detección del símbolo nulo.

Para evitar el caso de que se confunda por error una caída accidental de la potencia con un símbolo nulo, se realiza un filtro paso baja con el fin de atenuar cambios espúreos.

B.9.2 TFPR symbol

El símbolo TFPR esta compuesto siempre por un patrón fijo de muestras. Durante la transmisión del símbolo TFPR todas las portadoras son transmitidas a una potencia normal. Dicho patrón se analiza en el receptor una vez la señal ha sido procesada por la FFT. No obstante, la posición del patrón dentro del array de salida de la FFT depende de la frecuencia

de la señal recibida y del oscilador RF del receptor. El objetivo es localizar el patrón en una determinada posición para que las portadoras puedan ser identificadas de forma unívoca en el siguiente frame. El mismo patrón es almacenado en el receptor. De esta forma el error en frecuencia se puede determinar midiendo la desviación entre los patrones recibidos y almacenados.

El símbolo TFPR también facilita medidas de la respuesta al impulso del canal de transmisión, tiene la longitud de un símbolo normal y toda su capacidad es utilizada para funciones de sincronización.

B.10 Implementación hardware del demodulador DAB

La implementación de nuestra aplicación se ha realizado en la arquitectura CoolFlux BSP versión 2.0, un procesador de señal baseband de ultra-bajo consumo especialmente diseñado para aplicaciones de audio por la compañía NXP Semiconductors, donde se realizó este proyecto.

Una de las grandes dificultades encontradas en este proyecto fue la de poder realizar la demodulación de la señal al mismo tiempo que ésta es transmitida. A este tipo de sistemas se les conoce por sistemas en tiempo real. Si el demodulador no fuera lo suficientemente rápido para procesar todos los símbolos OFDM dentro de un frame de duración muchos datos podrían llegar a perderse.

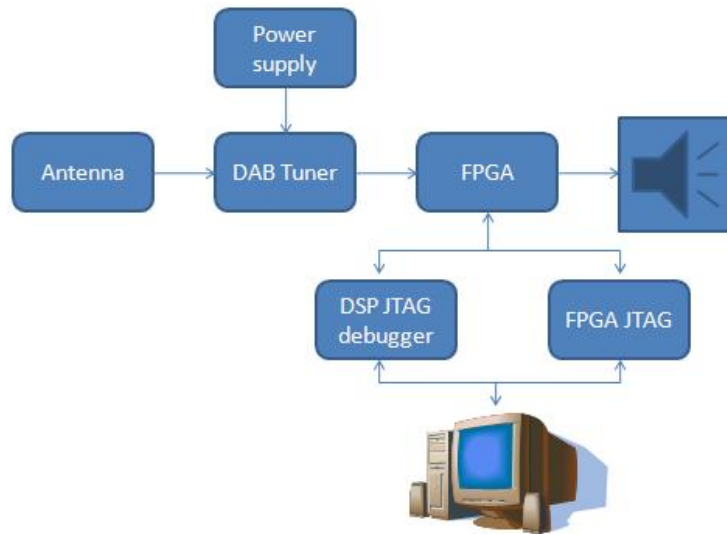


Figure B.5: Conexión de los componentes

El primer paso para las pruebas fue generar el código VHDL para la FPGA con la especificación de la ruta de datos y crear la estructura del sistema y los dispositivos periféricos (osciloscopio, sintonizador, depurador, etc) en MATLAB/Simulink.

Mientras un BSP es capaz de funcionar a 300MHz en una implementación real, la FPGA utilizada (Virtex XC4VLX100) sólo es capaz de funcionar a 50MHz. CoolFlux BSP tiene un CPI (Cycles per Instruction) de 1, por lo que cada BSP mapeado en la FPGA no puede procesar más de 50 MIPS. La cantidad total de MIPS requeridos para la demodulación resultó ser de 80 después de varias optimizaciones. En teoría se podría modular la señal con tan sólo 2 BSPs. Sin embargo, la adición de más núcleos aumenta el número de MIPS debido a las transferencias de datos que se llevan a cabo entre ellos. Por ello, la implementación del demodulador se ha realizado con 3 BSPs. De ahora en adelante nos referiremos a ellos como BSP_0 , BSP_1 y BSP_2 . En la imagen siguiente (B.6) observamos las conexiones entre los distintos BSPs. La separación de la funcionalidad en 3 DSP no fue una simple división del código en tres módulos transmitiendo los datos de uno a otro. Los requerimientos de memoria y MIPS fueron factores a tener en cuenta.

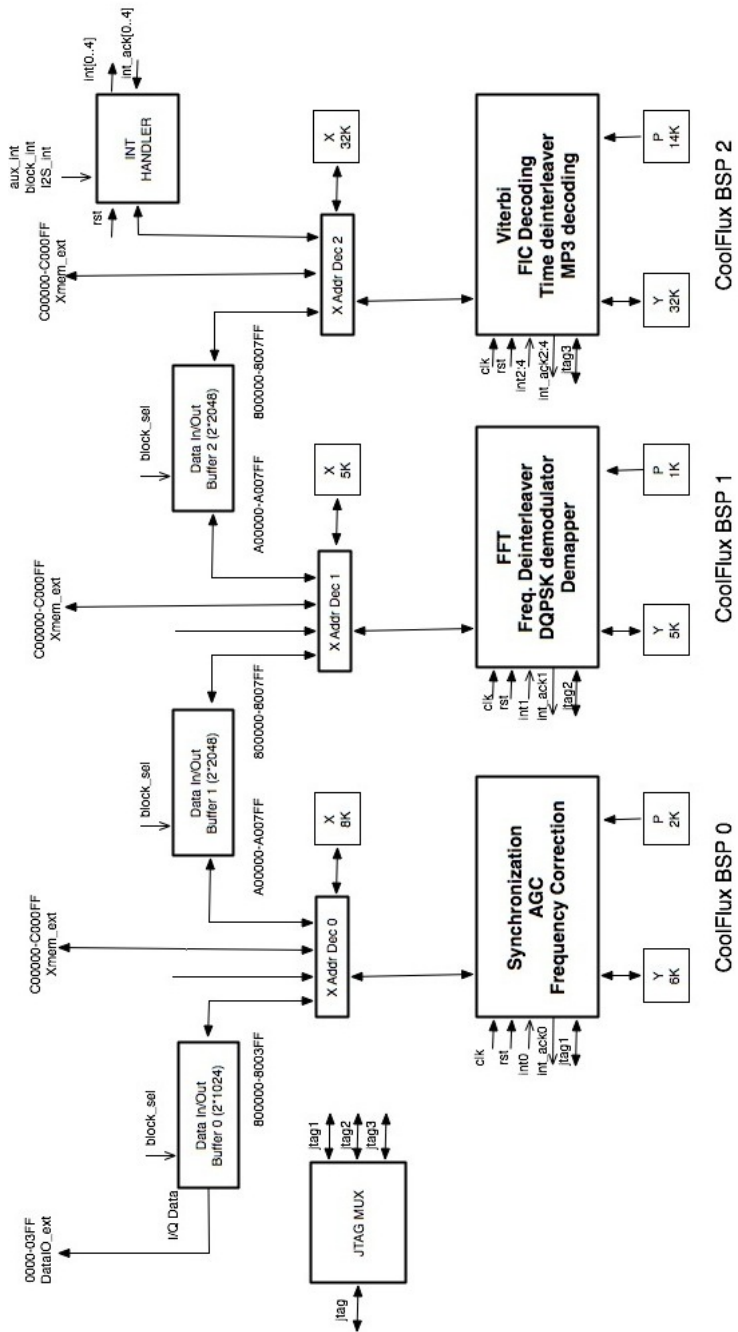


Figure B.6: DAB Architecture.

B.10.1 DAB datapath

Alrededor de las tres instancias BSP existen varios módulos que aseguran el flujo de datos desde la entrada a la salida y entre los diferentes BSP's. Los datos IQ de entrada deben ser almacenados en el buffer 0. Entre cada par de núcleos se encuentra un par de buffers alternos.

Cada BSP tiene su propia memoria local y una dirección en memoria X. Además cada uno tiene su controlador de interrupciones. Cuando todos los datos han sido procesados, el último núcleo escribe los datos de salida en un buffer de intercambio. El flujo de datos realizado en hardware es unidireccional. En las siguientes secciones se explicará la interconexión de los módulos.

B.10.2 Memorias locales

Cada instancia BSP tiene tres memorias locales (X, Y y P). Los tamaños utilizados en el diseño se muestran en la siguiente tabla(B.7):

Instance	Memory	Size
CoolFlux BSP instance 0	P Memory	2 Kwords (0x000000-0x0007FF)
	X Memory	8 Kwords (0x000000-0x001FFF)
	Y Memory	6 Kwords (0x000000-0x0017FF)
CoolFlux BSP instance 1	P Memory	1 Kwords (0x000000-0x0003FF)
	X Memory	5 Kwords (0x000000-0x0013FF)
	Y Memory	5 Kwords (0x000000-0x00013FF)
CoolFlux BSP instance 2	P Memory	14 Kwords (0x000000-0x0037FF)
	X Memory	32 Kwords (0x000000-0x007FFF)
	Y Memory	32 Kwords (0x000000-0x007FFF)

Figure B.7: Memorias CoolFlux DAB

B.10.3 Interfaz de depuración

Cada uno de los núcleos BSP tiene una unidad de depuración y una interfaz JTAG que permite comunicarse con cada uno de ellos. Para hacer esta depuración multi-núcleo, fue necesario un depurador multi-núcleo proporcionado por NXP. Cada Coolflux BSP tiene cuatro posibles breakpoints, siendo posible detener todos los núcleos cuando alguno de ellos alcanza este punto. En el depurador multi-núcleo, es posible exportar un breakpoint de uno a otro, lo que permite depurar los núcleos de una forma relativamente simple.

B.10.4 Interfaz de interrupciones

Todas las interrupciones van directamente al controlador de interrupciones y éste es el encargado de manejarlas en orden de prioridad.

Cada BSP puede generar una interrupción al BSP contiguo escribiendo en una determinada dirección Input/Output. La interrupción se genera independientemente del valor que se haya escrito.

B.10.5 Buffers Compartidos

Para la comunicación entre los BSP se utilizan buffers intermedios entre ellos. En total existen tres buffers compartidos en la ruta de datos. El diseño de cada buffer intermedio se muestra en la figura B.8:

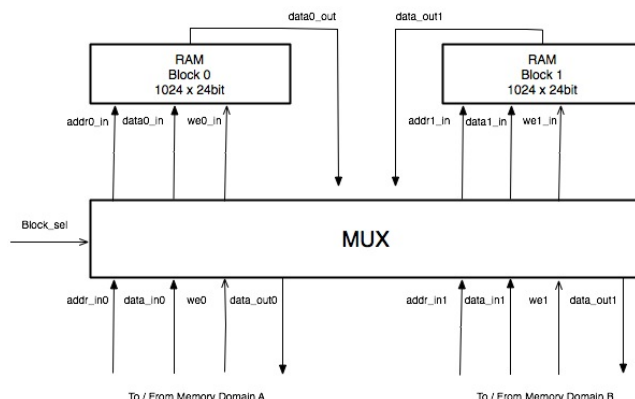


Figure B.8: Arquitectura de los buffers intermedios

Cada uno de los buffers conecta 2 módulos hardware en el diseño. Mientras una memoria está siendo accedida por un módulo hardware en el dominio de la memoria A, la segunda memoria puede ser accedida por el segundo módulo en el dominio de la memoria B. En algún momento de la ejecución, este orden cambia, accediendo por el primer módulo hardware a la segunda memoria y viceversa.

Este cambio se debe a la señal *block_sel*. Cuando ésta señal cambia su valor, las conexiones entre las dos memorias y las dos interfaces cambian, por lo que nunca habrá un conflicto entre las memorias. El estado de los bloques de memoria es oculto al software.

El primer BSP comienza recibiendo los datos IQ de la memoria de entrada. Las palabras impares almacenarán datos imaginarios y las pares guardarán valores reales de la señal. Esto da lugar a 512 valores complejos. Una vez cada 512 muestras IQ tiene lugar una interrupción que realiza el cambio entre los dos buffers. Cuando el primer BSP ha terminado, se envía una señal al siguiente BSP para que comience su ejecución.

Cada BSP comienza a ejecutar cuando recibe una interrupción del anterior o bien una interrupción hardware (sólo en el primero de ellos).

Obsérvese que la memoria total de la FPGA era próxima a 45KB, de modo que el espacio utilizado tuvo que ser reducido, ya que todo la memoria tenía que ser dividida y compartida por los tres módulos.

B.11 Descripción de los módulos BSP

B.11.1 BSP_0 : Sincronización y buffering de muestras

Este es el módulo responsable de la tarea más compleja en términos de procesamiento de señales: la sincronización de la señal de entrada.

La entrada de este BSP proviene de la señal de radio y los datos resultantes son enviados al siguiente BSP. Lo primero de todo es inicializar la estructura del demodulador y después se habilitar las interrupciones. Si se ejecuta una interrupción antes de inicializar apropiadamente los parámetros del sistema pueden surgir datos incorrectos.

Al comienzo de las pruebas del sistema en tiempo real, surgieron algunos problemas debido a que nuevos símbolos de entrada sobreescribían a los anteriores sin que éstos hayan sido procesados. Para evitar esto la primera solución propuesta fue incrementar el tamaño del buffer de entrada a 16KWords, pero debido a las restricciones de memoria de la FPGA éste era un tamaño intolerable. Una solución mas eficiente fue crear una máquina de estados. De este modo, en lugar de trabajar con un buffer auxiliar, se utiliza el propio buffer de entrada al sistema para reescribir los datos de salida del AGC y como entrada al algoritmo que implementa la detección del símbolo nulo.

La funcionalidad de este DSP se divide principalmente en dos bucles, uno de ellos es lanzado durante la interrupción emitida por el conversor analógico digital y ejecuta el AGC

y la máquina de estados que analiza la señal y prepara los datos para almacenarlos en el buffer intermedio. El otro bucle se encarga de corregir los errores de frecuencia y de fase.

Cuando un BSP no tiene trabajo útil que realizar se “duerme” (llamada a la función `sleep()`), lo que permite un mayor ahorro de energía que la solución clásica de esperar en un bucle que ejecuta NOPs. El BSP_0 está “dormido” hasta que recibe una interrupción. Entonces realiza los cálculos correspondientes y vuelve al estado “dormido”. Una vez el BSP_0 recibe el símbolo TFPR comienza a calcular el error de fase y frecuencia.

Una vez se recibe una interrupción se procesan 512 muestras. El motivo de ello es que utilizamos un buffer de entrada de 1024 palabras donde se sitúan consecutivamente las partes reales y imaginarias de las muestras. Por este motivo, si fuera necesario procesar un símbolo de más de 512 muestras, por ejemplo el Null Symbol de 2656 muestras, serían necesarias varias vueltas en el bucle de ese mismo estado: ($2656/512 = 5.18$, o sea, 6 vueltas). Las posiciones restantes se analizan en el siguiente estado.

B.11.2 BSP_1 : FFT, Deinterleaving, Demapping

Una vez que la señal ha sido sincronizada en el primer BSP, el segundo BSP comienza con la demodulación de ésta. Se utiliza el centinela (es decir, un valor que no se encuentra entre los posibles de la emisión de la señal) 0000FFFF FFFF0000 como entrada a BSP_1 para indicarle que empiece a trabajar.

Este módulo consiste en una cadena de algoritmos como se explica en la figura:

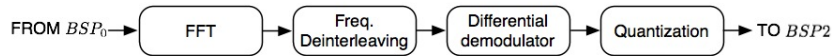


Figure B.9: BSP_1 modules

Para asegurarse de que el último BSP (BSP_2) recibe los datos en el orden correcto, es necesario escribir en el buffer compartido el número del símbolo enviado. Es importante resaltar que tras la cuantización solamente usamos 1536 palabras de las 2048 disponibles en el buffer intermedio. Utilizamos este espacio libre para escribir este número. En este módulo es muy importante la reutilización de la memoria, ya que sin ello hubiera sido imposible la implementación.

Después de esto se enviará la interrupción correspondiente al BSP_2 .

B.11.3 BSP_2 : FIC and CIF Decoding, Audio decoding

Este es el BSP del final del pipeline, y como tal tiene que ser capaz de obtener los bytes del audio que se reproducirá con circuitería específica del cliente del sistema CoolFlux BSP/DAB.

Para decodificar la información del FIC es necesario almacenar en un buffer todos los símbolos que lo conforman. Una vez éstos han sido recibidos, la cadena de bits resultante se hace pasar por los módulos del depuncturing, viterbi y dispersión de energía. Al finalizar este proceso se debe extraer la información del FIC (número de subcanales, direcciones de comienzo y final de éstos, etc) para poder proceder con la demodulación de un subcanal (el audio) elegido por el usuario.

El usuario entonces selecciona el canal que desea escuchar y se procede a procesar el MSC. Éste contiene el audio de la emisora seleccionada. La demodulación del MSC difiere ligeramente de la del FIC en que ahora además del depuncturing, viterbi y dispersión de energía tenemos que realizar un deinterleaving temporal de los bits. Este proceso es costoso en términos de memoria y tiempo. Finalmente introducimos la cadena de bits resultante al decodificador de MP2. Este último almacenara en un buffer de salida del sistema los bytes de audio que deberá reproducir el cliente del CoolFlux.

B.12 Conclusiones

El mercado de los receptores ha estado hasta el momento dominado por receptores estáticos o destinados a su integración como accesorios de automóviles. Los receptores portátiles son los que presentan un mayor problema de diseño debido a la limitación que han de presentar tanto de tamaño como de consumo eléctrico. Una de las motivaciones que llevaron a cabo la planificación de este proyecto por parte de la compañía, fue la ausencia de receptores portátiles de bajo consumo actualmente en el mercado. La proliferación y popularidad de dispositivos móviles hace que el bajo consumo unido a la alta productividad se haya vuelto imprescindible.

El imparable avance en el campo de la electrónica, particularmente en las técnicas de fabricación de circuitos integrados, ha tenido un gran impacto en la industria de las comunicaciones. El rápido desarrollo de la tecnología de integración a gran escala (VLSI, Very Large Scale Integration) de circuitos electrónicos ha estimulado el desarrollo de computadores digitales más potentes, pequeños, rápidos y baratos, cuyo hardware responde a propósitos específicos. Esta tecnología ha hecho posible construir sistemas digitales altamente sofisticados, capaces de realizar funciones y tareas del procesado de señal digital que normalmente eran demasiado difíciles y/o caras con circuitería o sistemas de procesado de señales analógicas.

Dentro del procesamiento de señal digital, en los últimos años se ha experimentado un direccionamiento de las tendencias del mercado tecnológico hacia las telecomunicaciones móviles de altas prestaciones, lo que ha provocado un creciente interés por arquitecturas empotradas de bajo consumo. La proliferación y popularidad de dispositivos portátiles hace que el bajo consumo unido a la alta productividad se haya vuelto imprescindible. Además, como consecuencia de la complejidad creciente de los protocolos de comunicación y del advenimiento de la era multimedia, se ha producido un espectacular aumento de los requerimientos computacionales para abordar funcionalidades cada día más demandadas. Por otro lado, cabe comentar que el ciclo de vida de los dispositivos móviles y multimedia se está reduciendo considerablemente debido a la presión del mercado, lo que provoca a su vez una reducción del tiempo de desarrollo de los procesadores. Esto significa que lograr la máxima eficiencia computacional con el mínimo consumo de energía y en el menor tiempo posible se ha convertido en la meta de varias compañías de desarrollo de DSPs.

B.12.1 Punto de partida

El desarrollo de este proyecto ha supuesto un gran esfuerzo por parte de los integrantes del grupo debido al amplio rango de conceptos que éste engloba. Previamente a su implementación, fue necesario un estudio a fondo tanto de procesamiento de señales digitales (no cubiertos en el plan de estudios de la Ingeniería en Informática), como del estándar DAB y de la arquitectura CoolFlux BSP. No obstante, gracias a la ayuda de profesionales dentro

de este ámbito hemos realizado un desarrollo del mismo que cumple ampliamente con las expectativas iniciales.

En los siguientes apartados exploraremos los resultados obtenidos en la implementación y concluiremos con los motivos por los cuales pensamos que los objetivos del proyecto han sido cubiertos.

B.12.2 Objetivos propuestos y cumplidos

El objetivo principal de nuestro proyecto era diseñar un demodulador completo de radio digital, orientado especialmente a dispositivos móviles, siguiendo el estándar europeo Digital Audio Broadcasting. Para ello utilizaríamos el procesador CoolFlux BSP, propiedad de la empresa en la que este proyecto se llevó a cabo, aprovechando su alta capacidad de procesamiento de bajo consumo.

El objetivo final de nuestro proyecto consistiría en conseguir una señal de audio libre de errores y un demodulador lo más optimizado posible en cuanto a espacio de memoria y tiempo de ejecución. Estos dos últimos aspectos juegan un papel muy importante en el consumo de energía del receptor.

Actualmente, el sistema es capaz de demodular una señal de radio captada directamente del medio y procesarla hasta concluir toda la cadena de demodulación que nos llevará a la obtención del audio. Las complicaciones surgidas durante el desarrollo del proyecto no nos han permitido implementar el modelo más óptimo deseado, no obstante se han realizado mejoras notables en términos de memoria y ciclos de computación durante el transcurso del mismo.

B.12.3 Aspectos futuros

Gracias a las ventajas que CoolFlux BSP nos ofrece, sería posible reducir de forma notable tanto las dimensiones (utilización de memoria) del diseño actual, como su consumo. El objetivo principal del proyecto no englobaba reducir al máximo estos términos, pero incluso para una primera implementación han sido necesarios considerables pasos de optimización.

Una vez finalizados todos los procesos de optimización y posibles mejoras del proyecto, el paso siguiente sería la implementación en un chip dedicado con el diseño del demodulador

para su posterior comercialización. Actualmente, son varias las empresas interesadas en su compra para la instalación en equipos portátiles tales como reproductores MP3, teléfonos móviles y radios para automóviles.

B.12.4 Dificultades encontradas

Una dificultad añadida ha sido el hecho de lidiar con un sistema en tiempo real, con las complicaciones que ello conlleva, ya que la señal tiene que ser procesada dentro de unas restricciones de tiempo muy exigentes. Durante la especificación se calculaba que para demodular la señal en tiempo real sería posible utilizar un sólo DSP. Durante el prototipado del mismo en una FPGA, algunas restricciones del hardware, principalmente la frecuencia de reloj de ésta, nos obligaron a implementarlo con tres módulos DSP.

Con respecto al procesamiento de señal digital, es importante recalcar la importancia de los códigos de corrección de errores, ya que sin ellos no sería posible la recepción de una señal limpia y sin perturbaciones, y tal vez ni siquiera audio, ya que algunos frames contienen información importante de cabeceras. Estos métodos de corrección han supuesto gran parte de la implementación del sistema.

Por razones de eficiencia energética en el diseño del procesador éste no incluye una unidad para realizar cálculos en punto flotante. Dicha limitación dificulta más el proceso de desarrollo, ya que ahora es el programador el que debe escalar los números para que estos no desborden y saturen la señal.

Además de todo esto, es importante recalcar que contábamos con módulos genéricos de software ya implementados por la compañía, como el decodificador MP2. Sin duda, esto supuso una ventaja para alcanzar más rápidamente nuestros objetivos. Sin embargo, la adaptación e inclusión de dichos módulos a nuestros demodulador supuso una dificultad añadida.

Bibliography

- [1] *ETSI EN 300 401 v1.4.1; Radio Broadcasting Systems; Digital Audio Broadcasting (DAB) to mobile, portable and fixed receivers; European Broadcasting Union* June, 2006
- [2] Wikipedia. *Frequency Modulation*. Last Updated 7 June, 2010
http://en.wikipedia.org/wiki/Frequency_modulation
- [3] Wikipedia. *Phase Shift Keying*. Last Updated 24 mar, 2010
http://en.wikipedia.org/wiki/Phase-shift_keying
- [4] Wikipedia. *Analog Digital Converter*. Last Updated 17 June, 2010
http://en.wikipedia.org/wiki/Analog-to-digital_converter
- [5] Wikipedia. *Multipath propagation*. Last Updated 10 June, 2010
http://en.wikipedia.org/wiki/Multipath_propagation
- [6] BBC *R&D White Paper*. June 2003
- [7] Wikipedia. *Quadrature Phase Shift Keying*. Last Updated 24 mar, 2010
http://en.wikipedia.org/wiki/Phase-shift_keying
- [8] Wikipedia. *Time-division multiplexing*. Last Updated 27 April, 2010
http://en.wikipedia.org/wiki/Time-division_multiplexing
- [9] Wikipedia. *Frequency-division multiplexing*. Last Updated 23 June, 2010
http://en.wikipedia.org/wiki/Frequency-division_multiplexing

- [10] Wikipedia. *Puncturing* Last Updated 17 December, 2009
<http://en.wikipedia.org/wiki/Puncturing>
- [11] Jen-Ming Wu. Associate Professor, Dept. of E.E./Inst. of Comm. Eng., National Tsing Hua Univ., Hsinchu, Taiwan *Example: Viterbi algorithm*
http://my.com.nthu.edu.tw/~jmwu/com5195/viterbi_example.pdf
- [12] Wikipedia. *Digital Signal Processors* Last Updated 8 June, 2010
http://en.wikipedia.org/wiki/Digital_signal_processor
- [13] Wikipedia. *Finite impulse response*. Last Updated May 16, 2010
http://en.wikipedia.org/wiki/Finite_\impulse_\response
- [14] Wikipedia. *Bit Error Ratio*. Last Updated May 20, 2010
http://en.wikipedia.org/wiki/Bit_error_rate
- [15] <http://www.insidedsp.com/>
<http://www.insidedsp.com/tabid/64/articleType/ArticleView/articleId/319/New-Details-Emerge-on-NXPs-CoolFlux-BSP-Core.aspx>
- [16] <http://www.insidedsp.com/>
<http://www.insidedsp.com/tabid/64/articleType/ArticleView/articleId/319/New-Details-Emerge-on-NXPs-CoolFlux-BSP-Core.aspx>
- [17] NXP Semiconductors *CoolFlux BSP Interrupt Controller version 1.6* January 2010
- [18] NXP Semiconductors *CoolFlux BSP Assembly Programmer's Manual version 1.4* November 2008
- [19] NXP Semiconductors *CoolFlux BSP: C Programmer's Manual version 0.3* November 2008
- [20] Target. The ASIP company.
<http://www.retarget.com/resources/pdfs/IPDesignerIPProgrammer.pdf>
- [21] Maxim 2172 datasheet.
<http://www.maxim-ic.com/datasheet/index.mvp/id/5883>

- [22] Xilinx.
<http://www.xilinx.com/support/documentation/index.htm>.
- [23] Philips PE 1542/00 Operating manual.
- [24] Wikipedia. *Baseband*. Last Updated Abr, 2010
<http://en.wikipedia.org/wiki/Baseband>
- [25] Tektronix Datasheets, Digital Storage Oscilloscopes
<http://www2.tek.com/cmswpt/psdetails.lotr?ct=PS&cs=psu&ci=14408&lc=EN>
- [26] Target. The ASIP company *Bridge Linker User Manual* November 2008
- [27] F. van de Laar, N. Philips, et. al 'General-purpose and application-specific design of a DAB channel decoder' Winter 1993
- [28] P. Kabal and B. Sayar *Rounding and Scaling in Fixed-Point FFT Implementation* June 12, 1985
- [29] Matteo Frigo and Steven G. Johnson *FFTW version 3.2.2*
<http://www.fftw.org>
- [30] Wikipedia. *NICAM* 26 June, 2009
<http://en.wikipedia.org/wiki/NICAM>
- [31] Agilent Technologies, Product description.
<http://www.ome.agilent.com/agilent>.
- [32] NXP Semiconductors *Software Way of Working. CoolFlux DSP Software Development* Junary, 2008
- [33] NXP Semiconductors *CoolFlux DSP Self-explanatory. Training Manual* May, 2009
- [34] Target. The ASIP company. *Chess Compiler User Manual. IP Programmer for CoolFlux BSP* November, 2008
- [35] Wikipedia. *JTAG* 26 June, 2010
<http://en.wikipedia.org/wiki/JTAG>

- [36] Wikipedia. Automatic gain control
http://en.wikipedia.org/wiki/Automatic_gain_control
- [37] Wolfgang Hoeg et. ál *Digital Audio Broadcasting. Principles and Applications of Digital Radio. Second Edition*, Wiley Press 2003.
- [38] Zonst, Anders E. *Understanding the FFT : a tutorial on the algorithm and software for laymen, students, technicians and working engineers*, Citrus Press 2000.
- [39] Zonst, Anders E. *Understanding FFT applications : a tutorial for students and working engineers*, Citrus Press 2004.
- [40] Villanueva Diez, Ignacio *Apuntes de Ampliacion de Calculo*, Universidad Complutense de Madrid.
- [41] Rafael C. González, Richard E. Woods *Digital image processing*, Prentice-Hall 2007
- [42] Richard Burden, J. Douglas Faires *Análisis numérico*, International Thomson Editores 1998
- [43] Luis Vázquez Martínez et ál. *Métodos numéricos para la Física y la Ingeniería*, McGraw Hill 2009
- [44] Stein, E.M., and G. Weiss . *Introduction to Fourier Analysis on Euclidean Spaces*. Princeton University Press
- [45] Smith, Steven W. *Chapter 8: The Discrete Fourier Transform". The Scientist and Engineer's Guide to Digital Signal Processing (Second ed.)*. San Diego, Calif.: California Technical Publishing. (1999)

